Università degli Studi di Ferrara

DOTTORATO DI RICERCA IN
"SCIENZE e TECNOLOGIE per l'ARCHEOLOGIA e i BENI CULTURALI"

CICLO XXVI

COORDINATORE Prof. Carlo Peretto

Study on Modern and Contemporary works of art through non invasive integrated physical techniques

Settore Scientifico Disciplinare FIS/07

Dottorando
Dott. Tisato Flavia

Tutore
Prof. Petrucci Ferruccio C.

Anni 2011/2014

Corso di Dottorato in convenzione con

UNIVERSITA' DEGLI STUDI DI SIENA

UNIVERSITÀ DEGLI STUDI DI MODENA E REGGIO EMILIA

Study on Modern and Contemporary works of art through non invasive integrated physical techniques

Table of contents

Introduction

Every work of art, regardless whether ancient or modern, is not eternal and is thus subject to unavoidable alterations over time.
In the recent decades, the study of contemporary painting materials, used both for realization and for restoration of works of art, has acquired great importance. Many of those materials were originally created for different purposes than for the artistic and conservative aims, and designed for different needs than those asked by Cultural Heritage. Therefore, they may – or may not – had to be adapted to new demands.

The study presented in this thesis has been articulated around two themes.
The first one is focused on works of art, contemporary in particular but also but not exclusively, the second one relates to materials, used for realization and restoration of such objects.
The study of works of art, discussed in Chapters 1 and 2, was carried out by making use of different diagnostic techniques available in the Archaeometry laboratory, taking advantage of a variety of methodologies. In particular, frequently used image techniques include photography and macro photography in diffuse light and specular and raking light, ultraviolet fluorescence, wide band infrared reflectography, digital radiography and K-edge radiography. To get as much information as possible, to be properly integrated with other data, other, specific diagnostic techniques have been used, such as reflectance spectrophotometry, colorimetry and X Ray fluorescence (XRF).
All these techniques were exploited in a complementary way, in order to meet the different requirements, and to answer to the questions of knowledge requested, each time, by the various artifacts. Just this integrated mode in exploiting the diagnostic techniques, represents the innovative aspect of the research, being all the techniques already developed, and possibly already commercial.

The main goal of the study on art materials was, instead, to monitor their behaviour over time and, if possible, to predict their degradation in advance. This last objective has been achieved on materials applied on a support (Chapter 3). On the other hand, on materials *as they are*, investigations allowed their characterization, mainly from the visual point of view, and hence for some of their optical properties.

The same section also includes the experience carried out during a three-month internship at the *Centre for Fine Print Research*, University of the West of England (Bristol).
In this context, I've been working with an empirical approach to the realization of a prototype of dome, provided with an electrical circuit, with which to equip a stereo microscope. Constant conditions, relative to the illumination and observation geometry, was thus provided while examining artifacts (mainly on paper) in raking light, at different magnifications, allowing their qualitative characterization.

Finally, diagnostic instruments and techniques used to investigate both works of art and materials, are described in detail in Chapter 4.

Overall, this thesis presents the main results of diagnostic activities carried out on different works of art, mainly of contemporary art, but also from other times.
The main aspect of the work, that links all the artworks presented here, ancient and contemporary ones, is to detect the artistic technique used by artists, and their ways to proceed.
Conservation and valorisation of works of art and collections are the primary aspects of the whole work, and have been reached through the use of different diagnostic techniques. In all of the investigated case studies, the work of art decided, each time, the techniques to be used. Such methodologies, already developed and eventually commercial, have thus been significantly integrated together.
As a consequence of that, the part devoted to instruments is simply a description, taking on the task of obtaining a greater completeness of the whole thesis.

Chapter 1

Investigations on Contemporary art

Documentation and conservation are very important issues to deal with, as they can be the initial start point to embark on a restoration. But they are not end in themselves, as a close investigation on artworks is enlightening to go back to painting techniques. Moreover, the aspect of valorization plays an important role in the dissemination of knowledge about works of art, achieved by means of various diagnostic techniques.

1.1 Diagnostic survey (2011-2013) on six paintings at *Casa Museo Remo Brindisi*

In this section, results of a diagnostic survey performed at *Casa Museo Remo Brindisi* in Lido di Spina, Comacchio, Italy, are presented.
Six contemporary paintings, all belonging to the twentieth century and characterized by different pictorial techniques, were analyzed, to suggest the wide range of possible case studies. Results presented are proposed as examples of integrated image diagnostics, to study both the material characteristics of the works of art, and the artists' executive techniques. The activity was also conducted to try to develop a protocol, devoted to the study of the XX century paintings on the basis of materials and artistic techniques. The diagnostic curriculum, which is well known for ancient artworks, has never found an updated definition for contemporary artworks, because of the wide availability of artistic materials and the fragmentation of their use, limited to the individual artist. The definition of a sequence of non invasive investigations, in the near future, will have multiple purposes, such as the study and the conservation of the artwork. In this regard, *Casa Museo Remo Brindisi*, with its huge and diversified content of works of art and materials, is an ideal context where to start a systematic study by means of non invasive image diagnostics.

The building (fig. 1), which is the result of the collaboration between Remo Brindisi and the architect and designer Nanda Vigo, was created primarily to house the art collection of Brindisi. It is at the same time the summer house and the workshop of the artist, a place for exchange and comparison, where to express creativities and to discuss. The house consists of both a public and a private part. The first one includes an entrance hall, the living room on the ground floor and a large central cylinder, which develops along the entire height of

the building. Around it, private parts are arranged on four floors: the bedrooms and the study of the artist. Outside there is a big garden (fig. 2), an evocative place which poses serious problems of conservation to the metal sculptures, there erected.

Fig.1 Entrance of the *Casa Museo Remo Brindisi*.

Fig. 2 *Casa Museo Remo Brindisi*, the outdoor garden.

Fig. 3 Interior of the *Casa Museo*, with Remo Brindisi's profile.

Fig. 4 G. Pomodoro, *Radiale*. Fiberglass (1965), along the spiral staircase.

Overall, the *Casa Museo* was set up as a manifesto of the "integration of arts", an open space for everybody, without physical, conceptual interruptions between architecture and furniture, design and works of art. The space in here, goes beyond the division of the arts, according to the research of Nanda Vigo, and also fits in with the latest trends of the time (figs. 3, 4) (Piraccini, 2005).

During the collaboration with the *Casa Museo Remo Brindisi*, the use of image diagnostics to analyze six works of art from the collection, proved to be a useful and non invasive tool to document and study the paintings (figs. 5-8). On six of them, presented hereafter, different aspects concerning their study will be highlighted.

While diagnostics were in progress, such different issues, concerning the study of the artifacts, variously emerged, depending on the investigated work of art.

As an example, on the painting by Giulio Turcato, the materic appearance of the creation made his pictorial technique the predominant issue to deal with, giving the opportunity to speculate about his way to proceed.

The conservative issue was, instead, the starting point that moved the observation in raking light on Mario Sironi's painting, which was submitted to a conservative intervention after a first diagnostic survey.

Works such as those by Emilio Vedova and Joan Mirò gave good pretexts to highlight some technical issues, like the diversity of materials used.

On the painting by Giorgio De Chirico, again, the preparatory study was the starting point for deeper investigations by means of infrared radiations.

The surfaces of all the paintings were investigated by selecting appropriate spectral bands, allowing thus to get useful and various information about them. In particular, pictures taken in raking light revealed the morphological features of the surface, while infrared reflectography showed the presence of preparatory drawings and *pentimenti*, underneath. Trans-illumination proved to be helpful in order to get more information about the conservation of the support, and on the thickness and homogeneity of the paint layers. Finally, induced ultraviolet fluorescence emphasized both the varnish and the diversity of pictorial materials on the surface (Albertin, 2012 (a)).

Fig. 5 Image diagnostic survey at *Casa Muse Remo Brindisi*, 2011-2013.

Nonetheless, valorisation of works of art resulted to be one of the main aspects of the entire project developed at *Casa Museo*, as an issue that connected all the different aspects emphasized in each case. As a matter of fact, paintings and artworks in the *Casa Museo*, are nowadays not so well known, and should thus be more valorised.

During the exhibition *L'invito del Maestro*, held in the summer of 2011 at the *Casa Museo*, an educational exhibition, based on image diagnostics performed on the artworks, was prepared (fig. 6).

Fig. 6 Dissemination of the results obtained.
Realization of informative posters, dedicated to some of the works of art (2011).

An innovative museum itinerary was also inaugurated on October 5th 2013, with the aim to reveal new details on works of art, by means of devices for Augmented Reality. The project *Lo sguardo dentro l'opera - A look inside the work of art*, was originated by the synergy between two research groups focused on *Equipment, materials and techniques for museography and exhibition design* and *Diagnostics and preservation* (TekneHub Laboratory, University of Ferrara), just with the purpose to promote and enhance the collection at the *Casa Museo*.

In such a realization, some short videos, illustrating image diagnostics and other contents, are linked to works by Turcato, Boccioni, Vedova, Sironi and others. The painting technique of each artist was thus highlighted by image diagnostics, which becomes, in this context, a tool for enhancement and enjoyment (figs. 7, 8).

Fig. 7 Poster of the event *The look inside the work of art* (Opening: 5 October 2013).

Fig. 8 *The look inside the work of art.* Implementation of additional content through augmented reality.

1.1.1 G. De Chirico, *Ettore e Andromaca*. The underdrawing

The first investigated painting is an oil on canvas, by Giorgio De Chirico. The subject, typically painted in the metaphysical manner, depicts Hector and Andromache. In this case, the use of infrared radiation revealed itself as illuminating, in discovering invisible details under the paint layer.

Fig. 9 *Ettore e Andromaca*. Total in diffuse light, *recto*.

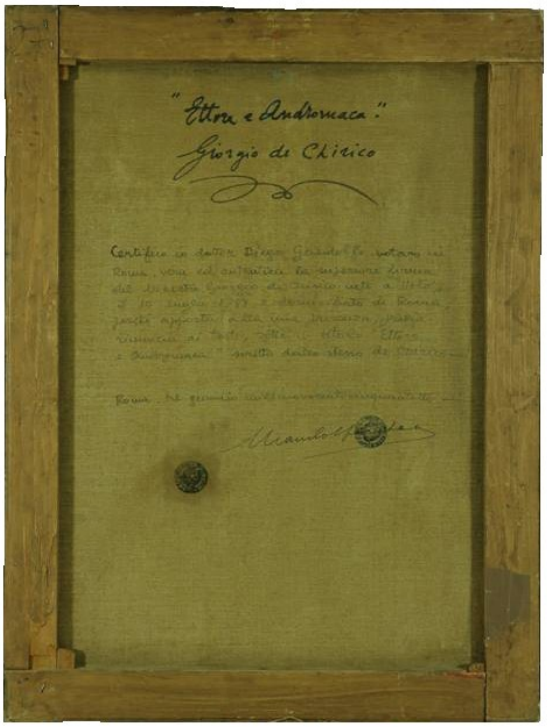

Fig. 10 *Ettore e Andromaca*. Total in diffuse light, verso.

First images acquired in raking light allowed to study the three dimensionality of the diversified surface. A diffuse *craquelure* was highlighted, due to a non homogeneous tension of the canvas (figs. 11, 12).

Thanks to infrared reflectography, traces of a preparatory drawing, made with a fine-tip tool, probably a pencil, were unveiled. It was also possible to observe some *pentimenti* between the preliminary drawings and the final painting, for instance in the decorations (twirls and swirls) on the chest of the dummy on the left, and in correspondence with its thigh, as well as on some elements that make up the scenography. Changes from the final version were also detected by trans-irradiation, that is, by collecting the transmitted infrared radiation through the canvas.

Such a technique allowed to better appreciate the underdrawing and the *pentimento*, referred to the mantle of the figure on the right (fig. 13), as well as the trend of *craquelure*.

Shadows and shades of colour were set by pencil during the execution of the preparatory drawing (fig. 14).

Fig. 11 Raking light photograph. Folds in corners and diffuse *craquelures*, due to uneven tension of the canvas.

Fig. 12 *Craquelure*, in raking light.

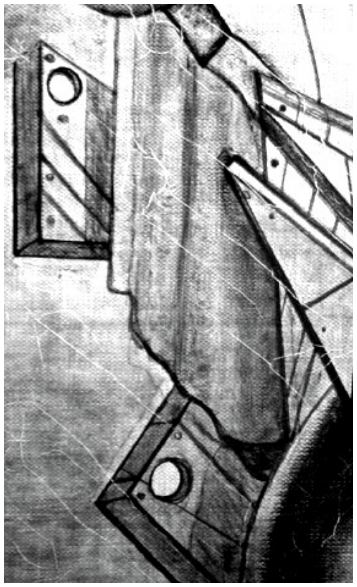

Fig. 13 *Pentimento* on the mantle of the figure on the right, in trans-irradiation.

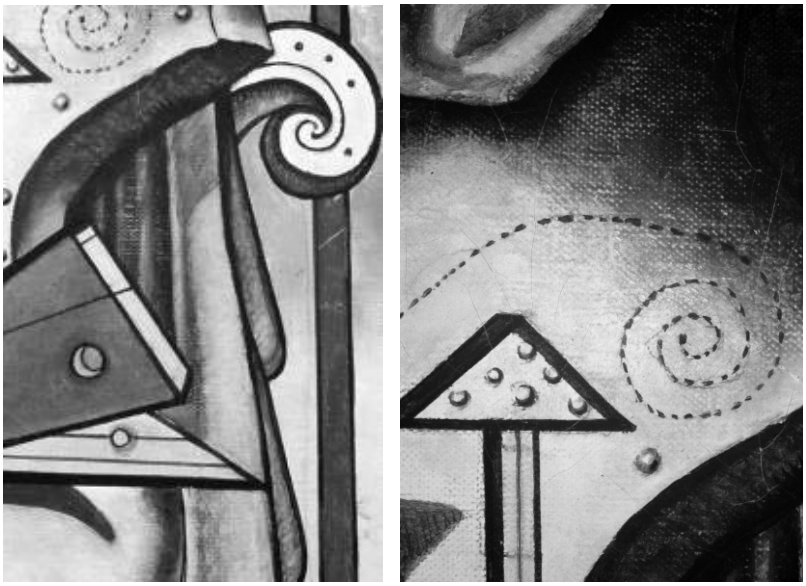

Fig. 14 Details of *pentimenti*, in infrared reflectography

1.1.2 J. Mirò, *Composition with figures*. Differentiation of materials

At a first sight, the choice of vivid colours and the contrast of complementary colours in the composition, stand out. What immediately emerges is the variety of hues used by Mirò (figs. 15, 16). In such a work, ultraviolet fluorescence was particularly functional in differentiating materials having the same hue at a simple visual inspection.

Fig. 15 *Composition of figures*. Total in diffuse light, *recto*.

Fig. 16 *Composition of figures.* Total in diffuse light, *verso*.

Afterwards, going more in depth, it is interesting to hypothesize how Mirò originally thought the composition. In this regard, infrared image of both whole and details of the painting, allowed to find out traces of a preparatory drawing, disappeared under the pictorial layer (figs. 17-19) and related to the creative phase of the drawing.
Ultraviolet fluorescence played an important role in the differentiation of materials, by returning the painting with different colours, depending on the pigment used (fig. 24).
Photographs in raking light emphasized the rough texture of the canvas support and the strokes of the secure boundaries. The author signature, observed in raking light, showed the roughness of the canvas, while the reproposal of the same signature in the infrared reflectography, at a close distance, allowed to fully appreciate the paint layer (figs. 20, 21).
The features of canvas, colour and brush strokes, are well appreciable in the photographs taken in raking light (figs. 22, 23).

On the *verso* of the painting, finally, the structure of the canvas was revealed, due to the white preparation passing through it, as well as some writings, which must still be interpreted.

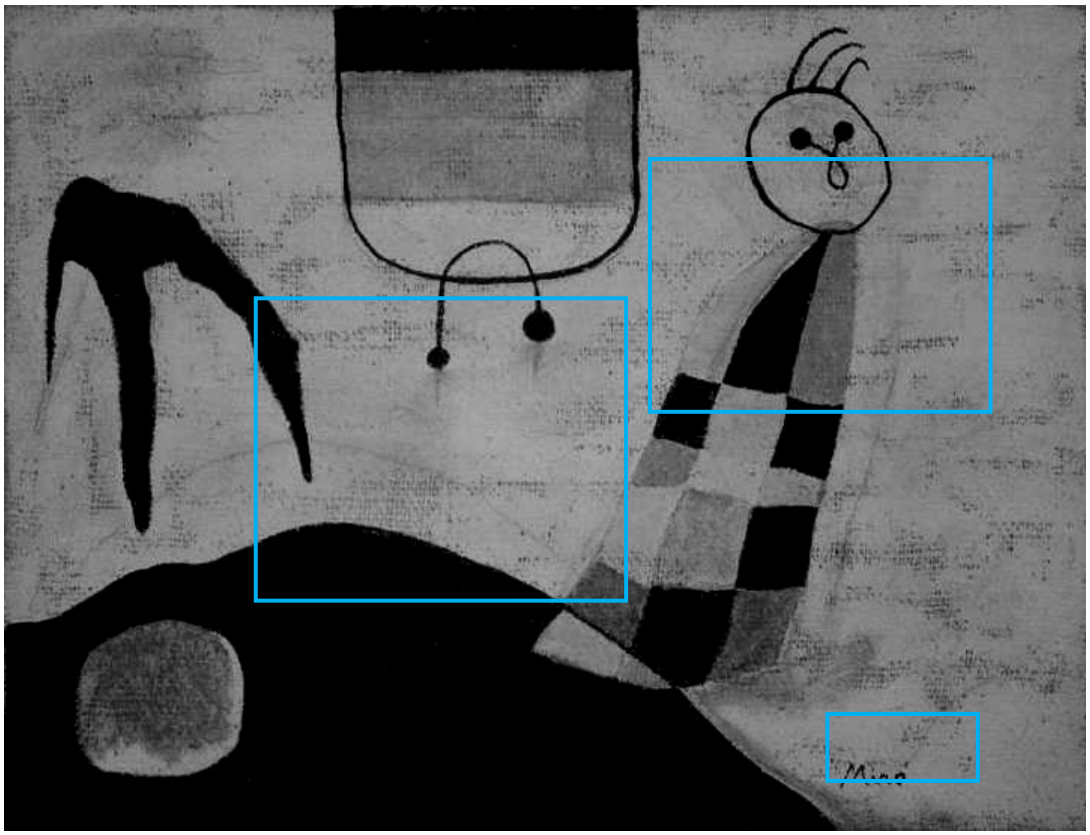

Fig. 17 Total in infrared reflectography, *recto*.
Blue frames individuate the following details in infrared reflectograhy.

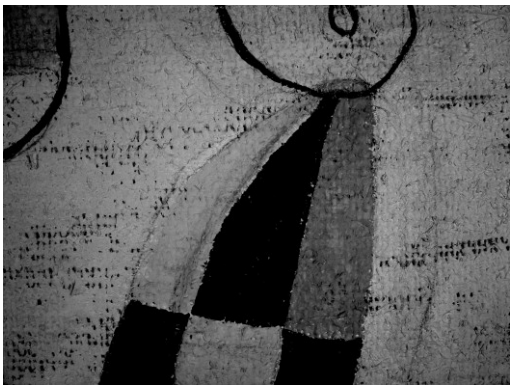

Fig. 18 Detail in infrared reflectography.
A *pentimento* pertains to the position of the dress.

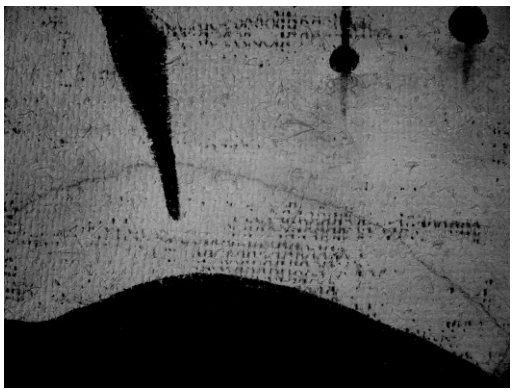

Fig. 19 Detail in infrared reflectography, emphasizing a different, previous version.

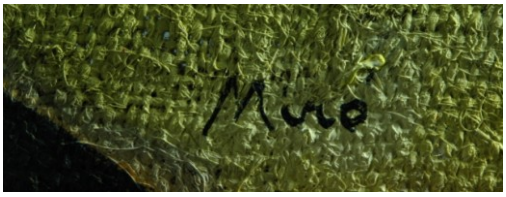

Fig. 20 Detail of the signature in raking light.

Fig. 21 Detail of the signature in infrared reflectography.

Fig. 22 Detail in raking light of the figure's head. Features of the rough canvas are well emphasized.

Fig. 23 Detail in raking light of the figure's dress. The colour, pretty liquid, has dampened the fibers of the canvas.

Fig. 24 Total in ultraviolet fluorescence, *recto*.
Different pictorial materials are distinguished, due to their fluorescence to ultraviolet radiation.

1.1.3 G. Turcato, *Senza titolo*. The polimatericity

While craft artistic materials are progressively replaced by equivalent commercial products and synthetic compounds, unusual pigment associations are also used, as well represented in the case of Turcato's creation (figs. 25, 26). In this "painting", raking light technique proved to be particularly useful in amplifying the three-dimensional components, and try to reconstruct the technique used by the artist.

Fig. 25 *Untitled*. Total in diffuse light, *recto*.

Fig. 26 *Untitled*. Total in diffuse light, *verso*. An inscription is present: "TURCATO. Autentico".

All the gathered observations on this particular work of art (fig. 27), made it possible to hypothesize the artist's way of painting. As shown in fig. 28, the artist probably firstly prepared the canvas surface (reasonably, a canvas with industrial preparation) with various colours. Some black, granular material (fig. 29) has thus been overlaid, in all likelihood after applying an adhesive substance. Then, he glued, in various agglomerations, a material of variable grain size (maybe sand), which he subsequently scraped in some places, to make room for strokes of full-bodied red-orange pigment (fig. 30).

The observation in raking light facilitates the study of the painting technique, enhancing in here the polimatericity of the work. The colour laids in a thick *impasto*, highlighting the features of the brush stroke: relief, direction, width and curvature. Sand and earthy material concurred to create suggestive and varied effects on the pictorial surface (figs. 29, 32).
Images obtained in trans-illumination provided information about the thickness of the paint layers and their homogeneity. The light selectively passed through the material, where the brush strokes were thinner (fig. 31).

The multi-material aspect of the work is also confirmed by the images obtained by ultraviolet fluorescence (fig. 33), which differentiated the various materials used by the artist.
On the background, dark in the inspection with ultraviolet radiation, the fluorescent pink and red portions stood out, presenting, respectively, purple and red-orange colours.

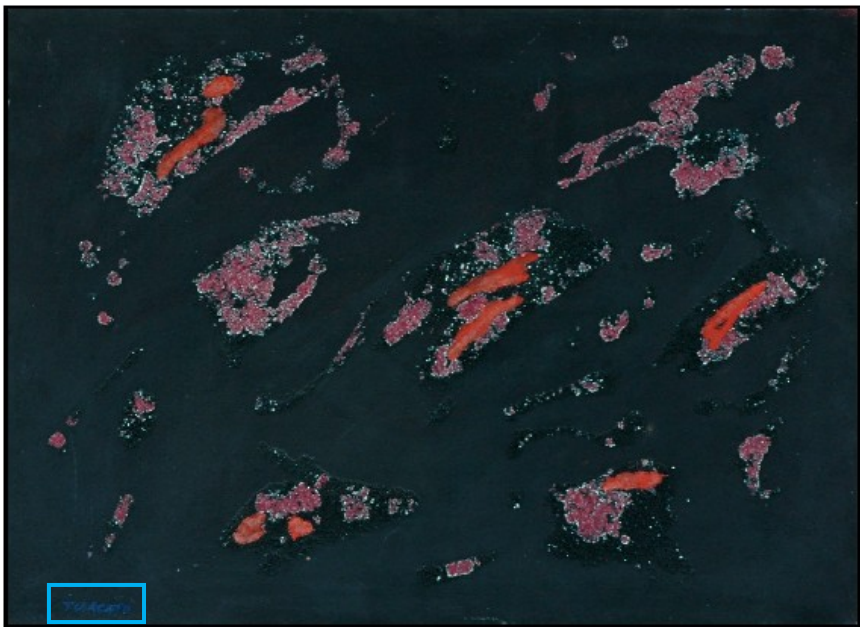

Fig. 27 Overall vision of the painting without frame. Picture taken in diffuse light does not highlight the three-dimensionality of the artwork. The signature is present at the bottom (in the frame).

Fig. 28 Detail in diffuse light, showing the presence of a coloured preparation, under the upper layers.

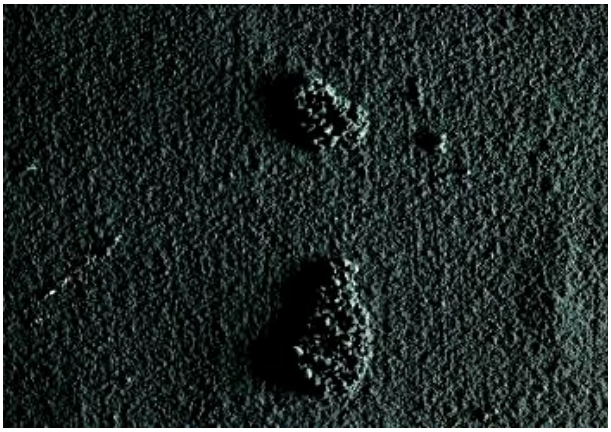

Fig. 29 Detail in raking light of the black, granular material, applied on some areas of the surface.

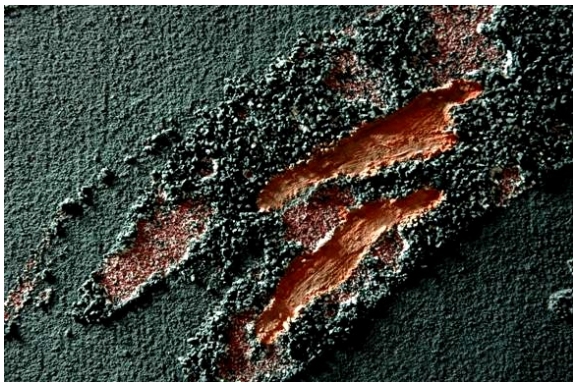

Fig. 30 Detail in raking light of a part where various layers followed one another.

Fig. 31 Detail in trans-illumination of the same detail. Light passes through the canvas where less material is present on the support.

Fig. 32 Detail in raking light, emphasizing the grainy nature of the black material.

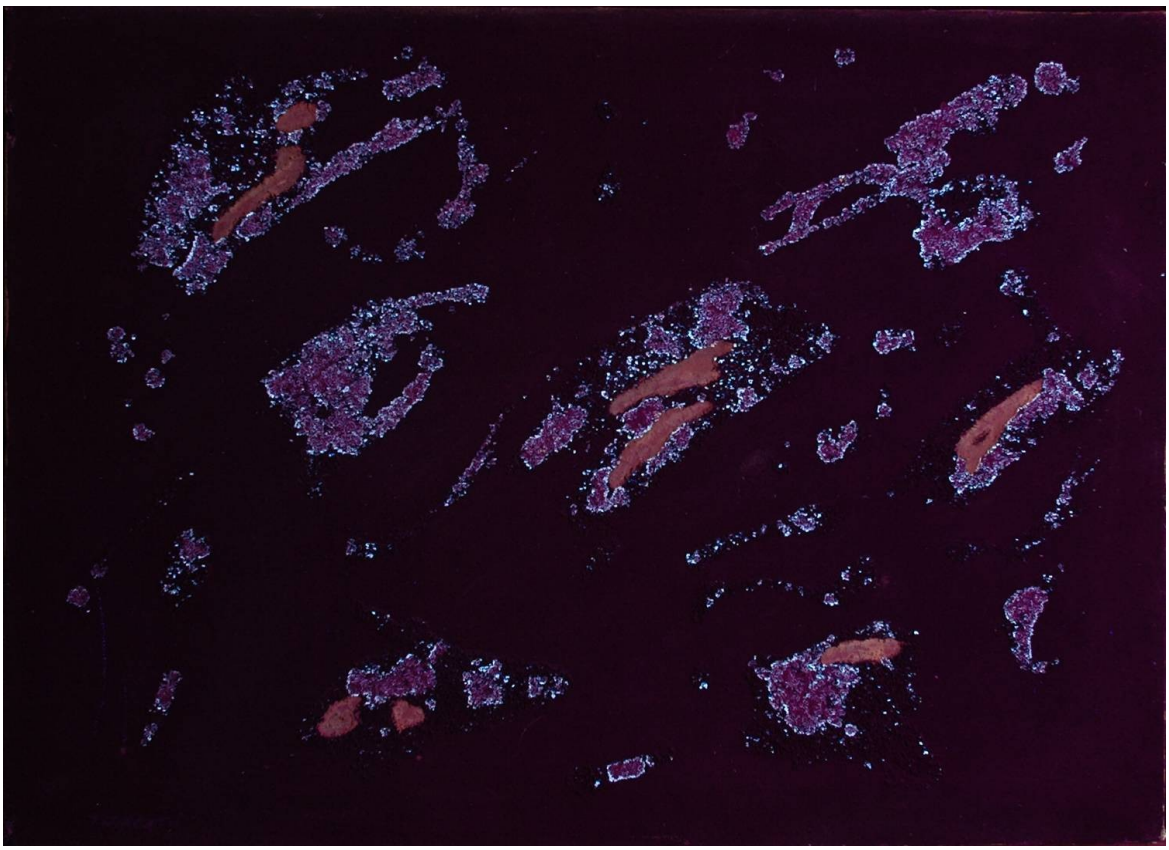

Fig. 33 Total in ultraviolet fluorescence, *verso*. Differentiation of pictorial materials is due to their behaviour to the radiation.

The painting by Turcato is a prime example of how it is possible to reconstruct the painting technique of an artist. Observations result from the application of image techniques and, therefore, do not provide the contact with the work of art.

1.1.4 E. Vedova, *Senza titolo*. The diversity of expressive media

The work by Emilio Vedova is a painting on paper, transferred to a canvas to give greater support to the paper itself (fig. 34). It appears to be quite significant as an example of the capability, by radiations different than visible light, to differentiate materials.

The painting by Vedova is characterized by spontaneity and immediacy of the artistic gesture. Rapid brush strokes were directly applied on the support, without an underlying preparation, and colours were chosen from a wide range of materials.

Diagnostic imaging was a valuable aid, both for analyzing the conservative state of the painting, as in the case of ultraviolet fluorescence, and to make preliminary investigations on the materials used by the artist, differentiating between them.

Fig. 34 *Untitled*. Total in diffuse light, *recto*.

Initial photographic documentation in diffuse and, particularly, in raking light, provided interesting information about the artist's way to proceed and the tools he used, highlighting the flatness of the stretch obtained with pastel, in contrast to the materic, protruding stroke, applied with brush (figs. 35, 36). Looking at the same details in raking light, it can also be

assumed the use of another tool, probably wax pastels, apart from brush. A first sketch was probably executed in pastel, while brush strokes in different colours were later applied.

Illumination with ultraviolet light stimulated fluorescence of the support, which appeared clear in the infrared image, contrasting whit the lack of fluorescence on the black pigment (fig. 37a-b).

The red pigment disappeared in the infrared image, being transparent to this radiation, whereas an evident red fluorescence resulted when observing the painting under ultraviolet light (fig. 38a-b). Yellow pigments presented, in some areas, a characteristic yellow fluorescence (fig. 39a-b).

Furthermore, particularly interesting is the comparison of the behavior of painting materials to the solicitation provided by ultraviolet and infrared radiations. Both the red and the yellow pigment, for example, disappear in the infrared image, being transparent to this type of radiation. Instead, when observed under ultraviolet radiation, the same materials exhibit fluorescence, red (for red pigment) and, only in some parts, yellow (for yellow pigment). The presence of fluorescence in the yellow pigment only in some parts of the painting is probably related to the use of the two materials (having the same yellow hue) used for the realization.

Figs. 35-36 Raking light pictures, showing both materic and thin brush strokes, and the different materials used.

Fig. 37a Detail of the painting, with a large portion of the paper support, uncovered by pictorial material.

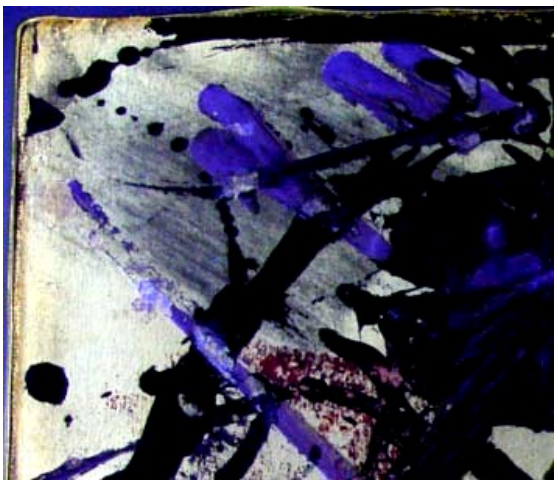

Fig. 37b The paper support appears white when inspected with ultraviolet radiation.

Fig. 38a Red pigments, detail in diffuse visible light.

Fig. 38b Red pigments, detail inspected with ultraviolet radiation.
The red material presents a dark red fluorescence.

Fig. 39a Yellow pigments, detail in diffuse visible light.

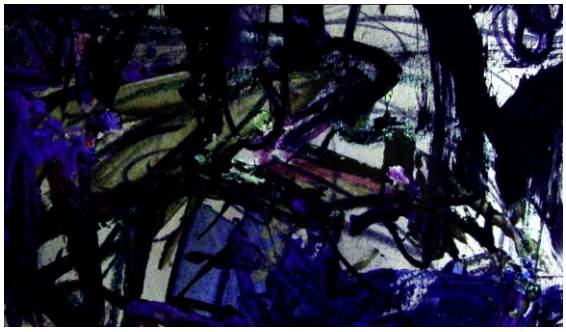

Fig. 39b Yellow pigments, detail inspected with ultraviolet radiation.
Yellow material presents, only in some areas, a characteristic yellow fluorescence.

1.1.5 U. Boccioni, *Senza titolo*. The brush stroke becomes a protagonist

The application of a simple and immediate technique, such as raking light, can sometimes result the most suitable, in highlighting the most important features of a work of art.
This is the case of the painting by U. Boccioni.

Fig 40 *Untitled*. Total in diffuse light, *recto*.

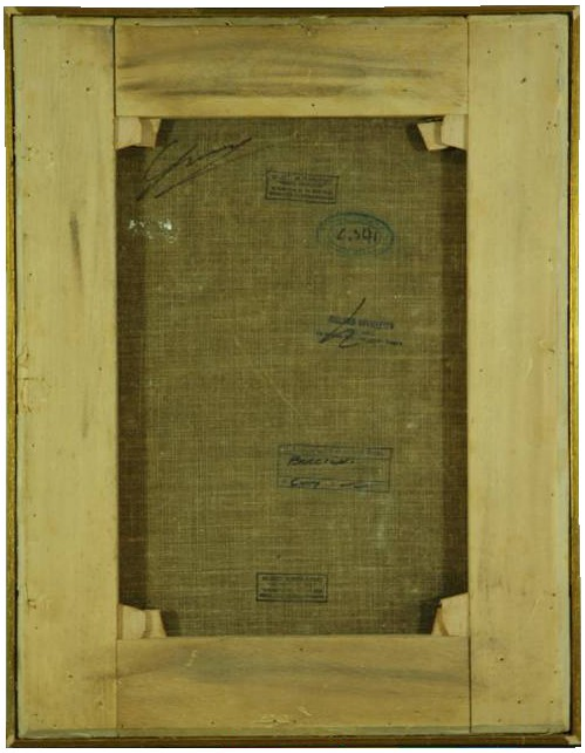

Fig 41 *Untitled*. Total in diffuse light, *verso*. Many ink stamps are present.

Through the painting technique, the futurist painter expressed the dynamism of the subject (figs. 40, 41), and the brush stroke became thus a protagonist when observing the painting in raking light.
Such a technique, as a matter of fact, highlighted the materiality of the brush stroke, in contrast to the black, flat signs, which separate the coloured areas (fig. 42). Some horizontal lines are due to irregularities on the edge of the canvas. The fluid brush strokes, sometimes more dense, were used to create highlights, concurring to the delineation of shapes. On the contrary, thinner glazes revealed the texture of the canvas (fig. 43). The dark contours, below the painting, determined the direction of the brush stroke.

Fig 42 Raking light photo highlighting the materiality of the brush stroke, in contrast to the black, flat signs, which separate the coloured areas.

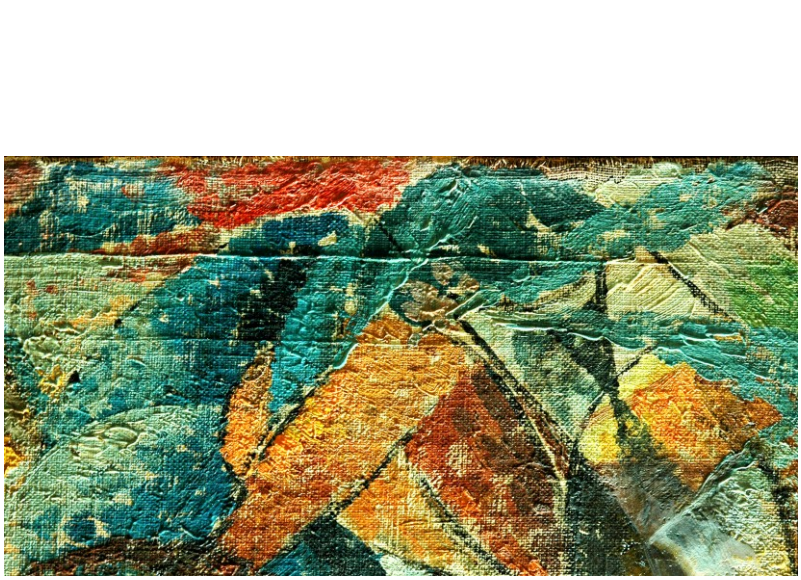

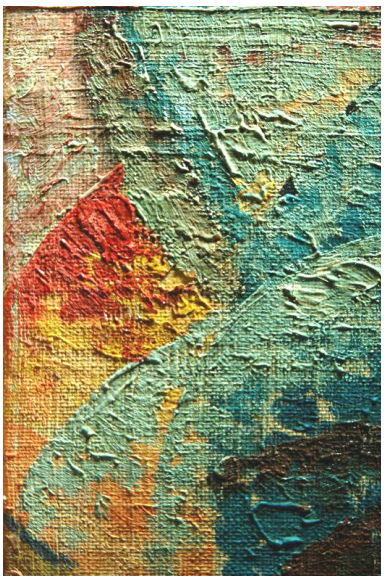

Fig 43 Raking light pictures, showing materic and thin brush strokes.

1.1.6 M. Sironi, *Composizione*. What the eye does not see

Imaging techniques, even when simple, like diffuse and semi-raking light, can be useful for conservation purposes, as shown in the case of Mario Sironi's painting (figs. 44, 45).
On this work, first applied documentation techniques, revealed adhesion problems on the pictorial film, on the yellow background field.

Fig 44 *Composition*. Total in diffuse light, *recto*.

Fig 45 *Composition*. Total in diffuse light, *verso*.
Several inscriptions and labels are visible, regarding the title of the painting, the date of its execution and its conservative history.

On the verso of the artwork, several inscriptions are documented, giving the opportunity to trace back to vicissitudes, changes in ownership, and exhibition venues.

Photographic documentation in visible light, both on the *recto* and on the *verso* of the painting, enabled to gain more information about its lifetime. On the *recto*, a raising of the pictorial film was documented before and after the restoration (fig. 46), aimed at its levelling, while on the *verso* some inscriptions relate to its conservative history (fig. 47).

Fig 46 Detail in raking light of a detachment of the pictorial layer.

Fig 47 The same detail in raking light, after the conservative intervention, aimed at ensure that the paint film re-adhered to the support.

Conclusions

Overall, the main contribution to an enhanced knowledge about techniques and artistic methods adopted by various artists, has been achieved by means of different techniques. Such techniques, considering the uniqueness of every artwork, were differently adopted and mixed, allowing in many case to speculate about the succession of work phases.

The most evident case is represented by the work of Turcato, where raking light transillumination, and UV fluorescence altogether, played a crucial role in recognizing and differentiating the various materials used, according to their different materiality and appearances.

On the artwork by Sironi, the aspect that most emerges, is the conservative one, as a simple observation of the painting in raking light allowed to recognize a lift in the pictorial film, which therefore could be conveniently cured with a minimum intervention.

On the artwork by De Chirico, instead, the discovery of the underdrawing under the pictorial film, traced back to the different phases of the work, highlighting the value of diagnostic techniques in studying the creative processes.

1.2 Artworks from private collections

Diagnostic techniques were carried out on contemporary works of art from other private collections, aimed at understanding the painting techniques and at identifying their constituent materials for authentication purposes. Information obtained were also helpful to a deepening of the peculiarities in the artists' way to proceed, outlining a richer cognitive framework, about materials used in contemporary times and on their methods of use. Considering the wide variety of pigments available since the nineteenth century, it is not surprising the large number of elements identified. Moreover, it makes it difficult to distinguish and recognize such materials.

1.2.1 G. Boldini, *Donna in lettura sul letto e anziano*

The painting, part of a private collection (figs. 48, 49), was firstly submitted to image diagnostics, to better understand the general behaviour of the surface, and to address subsequent deeper and punctual analysis, such as X Ray fluorescence. On this artwork, data collected were aimed to find out more information, in order to support or not, the assumption that materials and techniques used were actually compatible with a painting by Boldini. Data obtained were subject of study for a bachelor thesis (D'Avossa, 2012).

As a first approach, photographs in raking light were acquired, hightlighting the diffuse *craquelures*, mainly caused by contraction of the different constituents of the painting: support, preparation and pictorial layers (fig. 50).

Image obtained in ultraviolet fluorescence let guess that no interventions have been performed on the painting after its execution, as no trace of alterations, fillings, re-varnishings or new added elements were visible. A general, homogeneous behaviour is shown on the entire surface. The varnish showed a greenish fluorescence, which increased where tiny droplets of material resulted spread on the whole surface of the work.
Also the figure of the elderly seemed to be coeval with the rest of the work. Such a finding could help in solving some doubts about the addition of the man in a second version of the work. As a matter of fact, a particular issue pertains to this figure, that appears in other attested works by Boldini. On the other hand, the overall workmanship raises some doubts about the authenticity of the painting, still not solved.

Fig 48 *Donna in lettura sul letto e anziano*. Total in diffuse light, r*ecto*.

Fig 49 *Donna in lettura sul letto e anziano*. Total in diffuse light, *verso*.

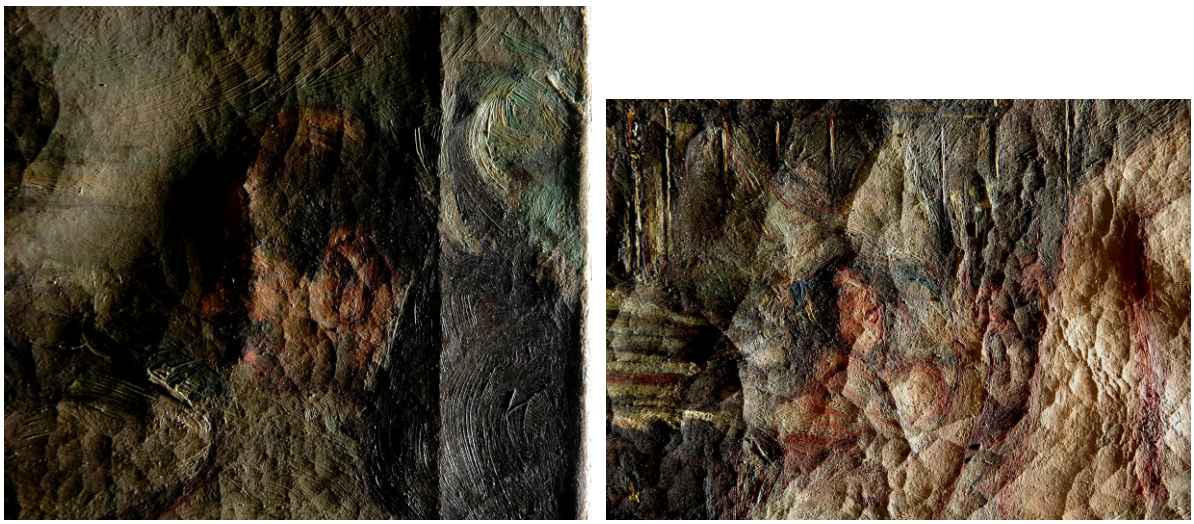

Fig 50 Raking light, details. The old man, on the left edge of the painting, near the frame (left), and the young woman on the bed (right). Both dense brush strokes and *craquelures* are well emphasized.

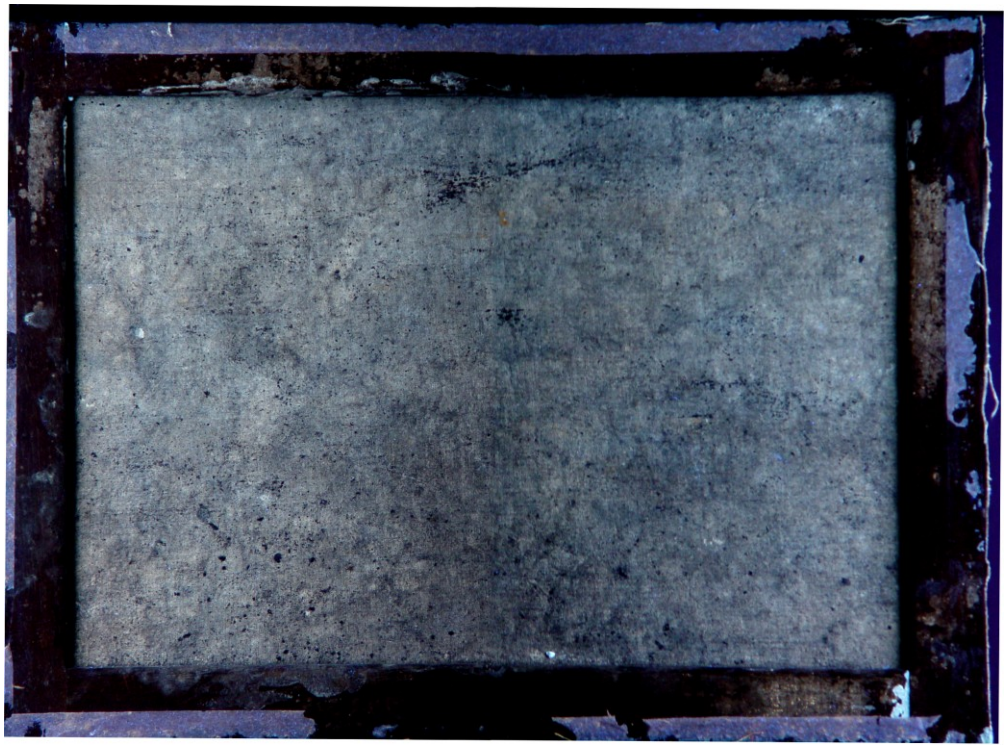

Fig 51 Ultraviolet fluorescence, total of the *verso*. Differentiation of materials due to their behaviour: bluish fluorescence of paper, pale blue light related to the glue, and no fluorescence of the coloured preparation passed through the canvas.

As well as on the front, UV fluorescence distinguished different materials also on the back of the painting. As an example, the paper presented a bluish fluorescence (fig. 51), while the pale blue fluorescence related to the glue. Halos due to moisture, and a coloured preparation with no fluorescence, passed through the canvas, are also observed (D'Avossa, 2012).

Infrared reflectography showed no preparatory drawing (fig. 52), but the thick paint layers could also have a role in the difficulty to detect anything below. The signature disappeared, only leaving a trace of its presence (fig. 53a-b). An additional element explaining the obstacle in detecting any preparatory drawings, is the hypothesis of a dark pigmentation of the background layer, that appeared to be confirmed by X Ray fluorescence analysis. On the edge of the painting, a red coloration was observed under the green-brown pictorial film, in correspondence with the background of the painting. This was analyzed by X Ray fluorescence (fig. 55), showing a strong presence of mercury. The distribution of such a coloration, on the whole surface, although not uniformly, is confirmed by the presence of white spots in digital radiography (fig. 54).

Fig 52 Infrared reflectography, total of the *recto* (contrasted image).
Differentiation of materials due to their behaviour: bluish fluorescence of paper, pale blue light related to the glue and no fluorescence of the coloured preparation passed through the canvas.

Fig 53a Diffuse light, detail of the signature, on the left, low corner of the painting.

Fig 53b Infrared reflectography, detail of the signature. Only the capital letter (B) can slightly be distinguished.

Fig 54 Digital radiography, total of the *recto*. On the edges, white portions correspond to the nails. White spots, diffused on the whole surface of the painting, are related to the presence of mercury and lead, respectively contained in *Cinnabar* and *Lead white*.

XRF data in the table below present results as peak integrals.

On some points on the back of the painting, in correspondence with points on the front, XRF detected increased counts of mercury and, sometimes, lead. Higher counts of calcium on the front were thus probably due to a preparation based on *gypsum*, animal glue and earths (due to the presence of iron). The presence on the back of mercury and lead, highly radiopaque elements, could instead justify the white spots in radiography. It can also be assumed that the canvas used for the painting is a reused painting, roughly cleaned from a preparation based on lead and mercury.

In all the other points, XRF investigation did not allow to clarify the composition in terms of pigments used on the painting. Spectra of the investigated points showed the presence of the same elements in many areas. The large amount of chemical elements found, and their coexistence (often likely to be indistinguishable), did thus not allow to attribute only one pigment to specific areas. Such a finding confirmed the non-use of pure colours as directly released from the tube, but more likely mixed together, to modulate colour tones.

The most frequently found elements are: lead, zinc, iron, calcium, followed by barium,

copper, cobalt, manganese, chrome, cadmium, tungsten and, probably, sulfur, potassium, silicon, aluminum and sodium (fig. 56). According to the hues that characterize the different areas, such elements can be related to lots of pigments, as indicated below for each different colour.

On points 9 and 26, there is a lot of calcium, as these areas are in correspondence with the preparation of the painting, probably constituted by *gypsum* (hydrated calcium sulfate). In addition, the coexistence of iron together with calcium, zinc, lead and barium, explained the dark coloration of the preparation.

On white points, elements such as lead, zinc and calcium are present in high amounts, suggesting *Lead white*, *Zinc white*, *Lithopone* and *Gypsum* as the most probable pigments.

In correspondence with the yellow points, elements found (cadmium, strontium, chrome, barium, iron, zinc, potassium and silicon) left several possibilities open, regarding the pigments used. These include: *Cadmium Yellow*, *Strontium yellow*, *Chromium yellow*, *Barium yellow*, *Mars yellow*, *Litharge*, *Zinc yellow*, *Yellow ochre*, *Burnt Siena earth*, *Smalt yellow*. It is also not possible to exclude the presence of organic pigments, such as *Spincervino yellow*.

For red pigments, instead, *Cadmium Red*, *Minium*, *Chrome Red*, *Natural red ocher*, *Mars red*, *Red earth*, *Ultramarine red*, *Vermilion* and *Garanza lake* were hypothesised, based on the detected elements (cadmium, selenium, sulphur, lead, iron, chrome, mercury, sodium).

Among the hypothesized blue pigments, according to the elements found in the related areas (tungsten, iron, sodium, aluminum, manganese), there are: *Wolfram blue*, *Prussian blue*, *Manganese Blue*, *Ultramarine artificial blue*, *Artificial Indigo*.

The most probable green pigments were *Transparent green Chrome oxide*, *Lamoriniere green*, *Chrome green*, *Malachite*, *Verdigris*, *Verditer*, *Smalt Green*, *Ultramarine green*, due to the relative amounts of chrome, copper, iron, chloride, silicon, aluminium and sodium.

Finally, among the possible browns, *Natural Siena earth*, *Burnt Siena earth*, *Natural umber*, *Burnt umber*, *Green burnt earth*, *Iron brown*, *Mars brown*, *Prussian brown*, *Cassel brown*, *Bistro* and *Bitumen brown* were suggested, being iron, manganese, aluminium and silicon the majoritarian elements (Moioli, 2002).

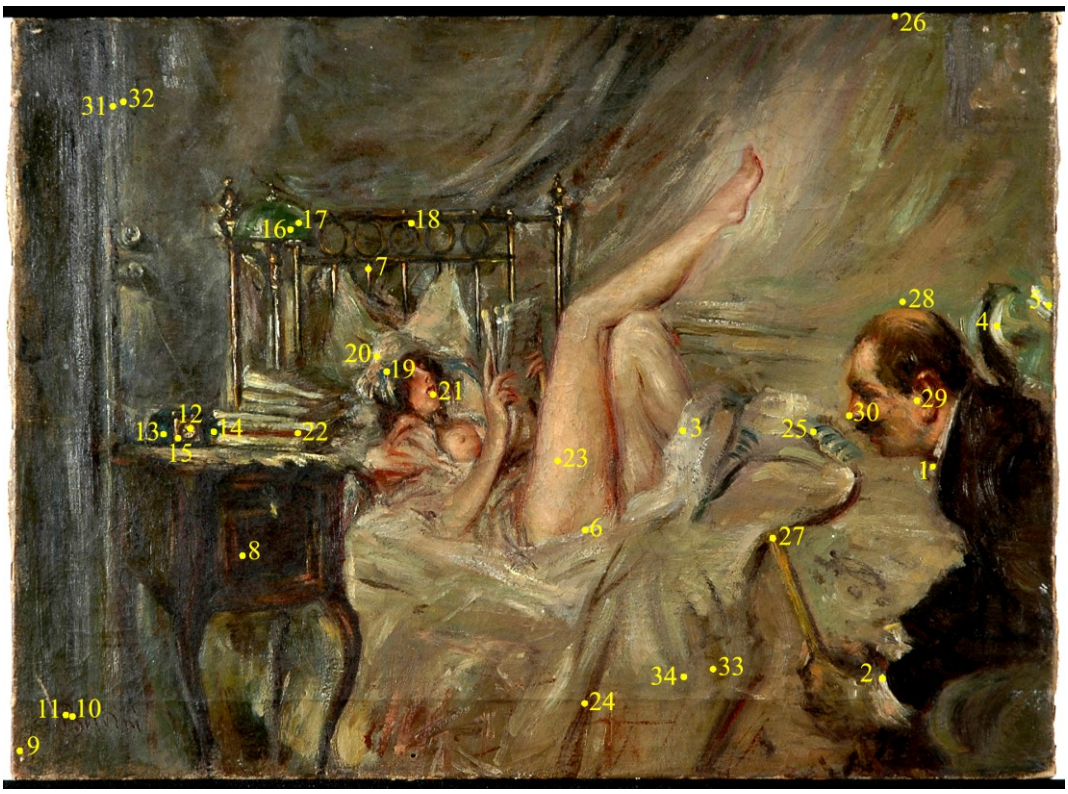

Fig 55 Measuring points analyzed by XRF.

Point / cps	Si	S	K	Ca	Cr	Mn	Fe	Co	Ni	Cu	Zn	As	Se	Sr	Cd	Sn	Ba	W (*)	Hg	Pb (*)	Bi
1	0	0	0	32	8	3	163	0	0	0	8826	0	12	22	19	0	3	0	0	267	0
2	0	0	0	8	28	3	43	0	0	0	17566	0	9	14	20	0	4	0	0	337	0
3	0	0	0	39	59	4	78	0	0	0	15689	0	10	14	16	0	2	0	0	339	0
4	0	3	0	7	5	1	16	0	0	0	19699	0	13	9	41	1	6	0	0	364	0
5	0	5	0	18	2	1	56	0	0	0	14265	0	6	7	14	0	3	0	0	248	0
6	0	4	0	41	13	2	198	8	0	0	13476	0	13	16	14	0	2	0	0	327	0
7	0	0	0	25	28	4	62	0	0	0	11410	0	31	46	33	0	10	0	0	465	0
12	0	0	0	51	60	6	97	0	0	0	9875	0	25	39	42	0	9	0	0	411	0
20	0	0	4	23	44	4	107	0	0	0	13153	0	21	45	27	0	4	0	0	346	0
10	1	0	0	205	30	9	428	3	0	6	1152	0	42	57	10	0	2	0	0	471	0
11	0	0	0	258	29	10	452	8	0	4	957	0	6	57	3	0	2	0	0	405	0
8	0	0	0	290	20	13	413	4	0	4	380	0	6	40	5	0	2	0	0	175	0
9	1	7	0	409	1	21	639	11	0	0	1276	0	16	34	2	0	1	0	0	1114	0
13	0	0	0	127	118	10	345	3	0	0	1571	0	11	84	11	2	6	16	0	475	0
14	0	0	16	124	132	5	354	4	0	0	1568	0	7	98	12	1	8	17	0	512	0
19	0	0	5	36	28	5	296	5	0	0	8495	0	9	72	17	2	8	83	0	475	0
26	0	0	0	327	0	6	309	4	0	6	402	0	5	20	1	1	1	5	0	269	0
25	0	0	0	64	20	7	397	4	0	0	4376	0	17	67	21	1	8	46	0	295	1
16	0	0	0	88	39	6	324	3	0	6	1334	0	7	60	28	1	6	10	0	457	0
17	0	0	0	61	37	7	265	6	0	7	2939	0	20	52	34	1	6	27	0	342	0
28	0	0	0	78	16	8	284	6	0	12	6888	0	13	36	28	1	5	70	20	634	0
18	0	0	0	46	106	8	144	0	0	0	1894	0	27	95	37	2	10	0	0	988	0
15	0	0	0	144	66	7	420	0	0	0	914	0	15	78	11	2	4	0	0	565	0
27	0	0	0	76	166	7	174	0	0	5	1199	0	28	137	6	1	12	0	0	1842	0
22	0	0	0	168	38	7	412	0	0	0	1389	4	63	62	15	1	3	0	0	311	0
30	0	0	0	78	26	6	278	0	0	20	3644	25	189	44	58	1	5	0	0	988	3
23	0	0	0	27	45	3	125	0	0	0	13699	0	19	19	20	1	3	0	0	329	0
29	0	0	0	94	187	6	120	0	3	0	10093	0	22	19	23	1	3	60	0	322	0
21	0	12	0	60	42	8	86	0	0	0	4686	0	758	43	172	2	5	0	0	442	0
24	0	0	0	89	32	4	243	0	0	0	5081	30	38	57	25	1	4	0	0	346	0
31	0	0	0	213	34	8	471	0	0	5	2740	0	0	51	5	0	4	0	0	777	18
32	0	0	0	82	25	5	245	0	1	15	8710	0	0	38	7	0	4	0	0	988	14
33	0	7	0	349	0	20	615	0	0	0	1060	0	3	50	5	0	2	0	0	105	12
34	0	0	0	141	15	5	352	0	1	0	5573	0	7	48	11	0	3	0	4	257	1
35_32	0	0	0	127	2	7	273	0	0	18	2129	0	0	41	4	0	3	22	0	1655	10
36_33	0	0	0	165	0	6	324	0	0	2	242	0	0	49	1	0	2	0	26	141	0
37_34	0	0	0	178	0	8	294	0	0	3	258	0	0	35	2	0	2	0	25	112	0

Fig 56 Table with XRF results (cps: counts per second). Points 35, 36 and 37 correspond, on the back of the painting, to points 32, 33 and 34. (*): indicates counts per second referred to L lines. If not specified, cps refer to K lines.

Conclusions

The X ray fluorescence is a non invasive technique, which did not need to take any sample from the painting surface. It detected many possible pigments, despite not being able to identify the single formulations. Regarding the investigated painting, the advantageous use of not absolutely invasive techniques, did not detect any anachronism in found elements. However, it proved impossible to determine most of the pigments.

Radiography allowed to obtain a map relating to the distribution areas of the elements, according to their different densities. In correspondence of many bright areas, the although slight presence of mercury, identified by XRF, led to hypothesize the widespread presence, perhaps in preparation level, of a pigment such as *Cinnabar*. Such a finding would lead back to the particularity of a dark preparation.

Overall, scientific investigations performed on the painting did not dispel the doubts about the figure of the elderly. Whether it can be attributed - or not - to Boldini, remains a stylistic issue, still not solved.

1.2.2 F. De Pisis, *Natura morta* and *Fiori*

Both paintings, signed *De Pisis*, come from private collections, and represent a floreal subject. What differs, is the support and the pictorial technique: *Natura morta* (figs. 57, 58) is a oil on a (thin) wood panel, while the other artwork, representing a flowerpot, is made by watercolours. Despite different materials have been used, some common features emerge, constituting a peculiarity.

As a matter of fact, De Pisis painting technique is considered to be full of pathos and emotivity. In this perspective, the choice of the palette, to the materiality and density of the brush strokes, is dictated by the artist's emotions. Moods that De Pisis blocks on the canvas with a few, instantaneous and immediate gestures (Briganti, 1991).

Fig 57 *Natura morta*. Total in diffuse light, *recto*.

Fig 58 *Natura morta*. Total in diffuse light, *verso*.

The conservative history of the artworks did not probably know any problematic moment, as their conservative state appears to be quite good. A different amount of information, instead, was obtained from the two works of art, according to the painting technique and the materials used. Just due to the greater complexity and richness in terms of materials, the oil on wood returned the most interesting data.

On this (latter) painting, as usual, investigations started with a general photographic documentation in visible light.

In particular, raking light highlighted the different thicknesses that characterize the pictorial layer. Thin brush strokes are present on the background, where the support, without any preparation, often emerges. Protruding, more materic brush strokes are evident, instead, on some details, as shown in figs. 59 and 60.

Investigations with specular reflected light was also useful, facilitating the observation of the most reflective areas of the painting, although the lack of varnish (fig. 61). On the contrary, the support (with its matt appearance) emerges on non-painted areas.

Images of the ultraviolet fluorescence returned diversified colours, occasionally even in similar backgrounds (in visible light). A low, general fluorescence, also pertaining to the lack of paint or protective materials, is evident (fig. 62).

Reflectographic images brought to light, instead, some traces underlying the final version of the painting. Lines related to a preparatory drawing, about setting up, emerge, as well as some details, designed in an earlier version and later covered by overlying pictorial layers (figs. 63, 64). Composition sketches delineate the lines of the table and of a book above it, subsequently hidden by brush strokes. Rounded lines seem instead to trace the outline of some grapes, also disappeared in the final version.

Fig 59 Detail in raking light.
Materic brush strokes characterize some details.

Fig 60 Macrophotographs in diffuse light.
Detail of a protruding brush stroke.

Fig 61 Detail in specular reflected light. Highlighting of the most reflective areas of the painting.

Fig 62 Total of the painting in ultraviolet fluorescence. Differentiation of pictorial materials. Stronger UV fluorescence of white pigments.

Fig 63 Detail in infrared reflectograhy. Composition sketches refer to a preparatory drawing, highlighting some details, later covered by overlying pictorial layers.

Fig 64 Detail of signature in infrared reflectograhy.

X Ray fluorescence was performed on several points on the surface, to deepen the knowledge about pigments used. Hypothesis about artist's palette include some modern pigments such as *Prussian blue*, *Ultramarine blue*, *Zinc white*, *Cadmium red*, *Lead and tin yellow*, *Chrome green* and *Iron brown*. For all of them, the compatibility with the period of use can be asserted.

Points investigated by XRF analysis are variously located on the pictorial surface, concentrated in areas where colour is more saturated (fig. 65). The majority of them is characterized by thick and full-bodied brush strokes. Only three points (12, 13, 14) are distinguished for the absence or the thinness of the pictorial layers.

Overall, the pigments used would appear to be modern materials, compatible with the period of use and of the work's realization (first half of 1900).

In particular, on all the investigated points, the presence of zinc is constant, followed by others elements such as barium, lead, and calcium associated with strontium.

As an example, the two white points investigated (1, 6) are certainly based on a zinc compound, due to the important presence of this element.

For the other points, it is difficult to identify the various pigments used by the artist. As a matter of fact, a simultaneous presence, in the same small area, of elements attributable to different hues, was found. It seems therefore probable that, in the realization of the painting (characterized by spontaneous and impulsive strokes), the artist applied more layers of different colours, also in mixture between them.

Nevertheless, it is still possible to distinguish some of the pigments primarily responsible for the various colorations. As an example, the simultaneous presence on both the red points (3, 8) of cadmium and selenium, leads back to the use of *Cadmium red* (*Cadmium sulphoselenide*), probably one of the red pigments most commonly used at the time. That is also for the availability of various shades of the hue (from light red to reddish brown), depending on the proportion between sulphur and selenium present in it (Adrover Gracia, 2010).

The presence of lead, tin, barium, chromium and cadmium on the yellow point (5) suggested a mixture of *Tin and Lead yellow*, or *Cadmium Yellow*, *Barium Yellow* , *Chrome Yellow*, *Strontium yellow*.

The greenish yellow coloration on point 4, where the only element potentially responsible for the pigmentation is iron, can be attributed to many pigments containing this element, possibly in combination with an organic pigment.

Also with regard to the green points (2, 9), the presence of chromium suggested the use of *Chromium oxide green*, *Guignet Green*, or *Lamoriniere Green*. The additional presence of

iron betrayed, however, the mixture with one or more of the following pigments: *Green lake*, *Cinnabar Green*, *Zinc Green*.

The coexistence, on the blue point (7), of iron and cobalt, is not foreseen in any pigment. If *Cobalt Blue* and *Prussian Blue* (which contains iron) are the most probable candidates, just the presence of iron and cobalt leaned toward the hypothesis that it is a mixture.

The violet point (11), because of the presence of cadmium, selenium and iron, would be likely to have been obtained by mixing the same pigments used for the red and blue points.

On the brown point (10), the detection of iron left open a wide range of possible pigments. These include: *Mars Brown*, *Iron Brown*, *Prussia Brown*, *Caput Mortum*, *Sepia Brown*, *Earth of Kassel*, *Burnt Umber*, *Burnt Sienna Earth*, *Green Earth*. There is also the possibility of an organic brown pigment.

On the points at the bottom of the painting (12, 13, 14), characterized by the almost total absence of pictorial material, the elements zinc, lead, calcium, barium are present in varying amounts. On the same points, the lighter elements detected could be linked instead to the organic nature of the support (Moioli, 2002).

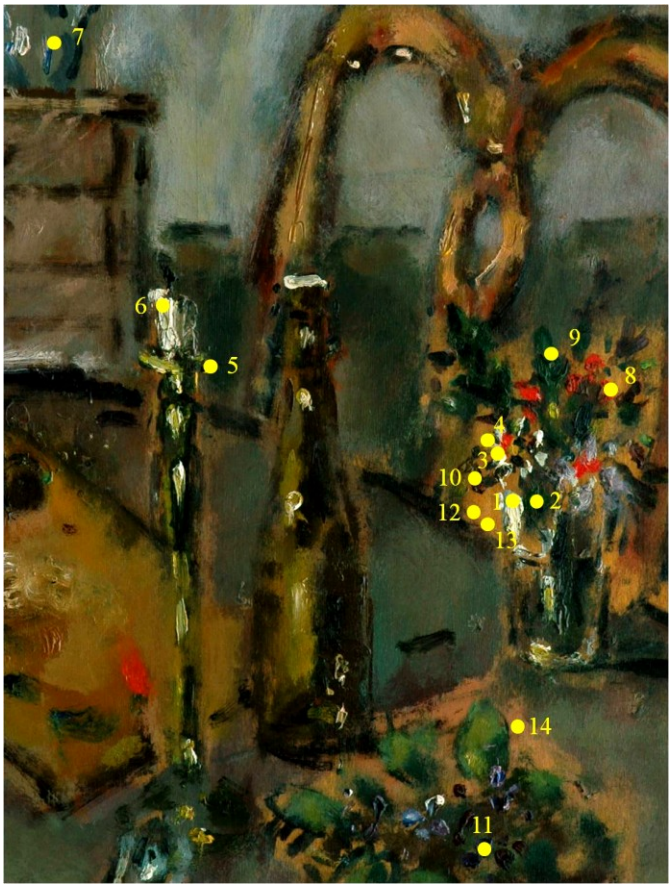

Fig 65 Measuring points analyzed by XRF.

On the other painting (a watercolour on paper) whose title could be *Fiori* (fig. 66), imaging techniques did not allow to reach significative information, only enabling to distinguish its different materials, as in the case of ultraviolet fluorescence (fig. 67), or to emphasize, by means of infrared reflectography, the squaring lines, evidently stretched with a pencil (fig. 68).

Fig 66 *Fiori*. Total of the painting in diffuse light.

Fig 67 Ultraviolet florescence, highlighting the strong fluorescence of the paper support.

Fig 68 Infrared reflectography, emphasizing the squaring lines of the composition.

Conclusions

In the case of the oil on panel, the material is thick and full-bodied, laid in rather materic layers.

The main observations are therefore related to the work realized with oil colours, which is more interesting for the painting technique used. In particular, this presents a strong contrast between full bodied and materic brush strokes, and areas where the color is lying in very thin layers.

The extreme variety of pigments, chosen from those available during the twentieth century, is perhaps the main feature of the oil painting. Here, moreover, the distinction and the recognition of the materials, are complicated by the presence of many of these pigments, on various points of the surface.

This way of painting can be considered usual for many artists of the twentieth century.

Another example of the variety of pigments available for contemporary artists is reported for the next painting.

1.2.3 F. Patruno, *Omaggio a De Pisis*

The painting was realized by F. Patruno with pastel and acrylic colours on canvassed cardboard, during a restoration course, held at the University of Ferrara (figs. 69, 70). The work of art was never restored, and the results of the diagnostics performed certified the good general condition of the painting. Nevertheless, the entire painting results extremely warped.

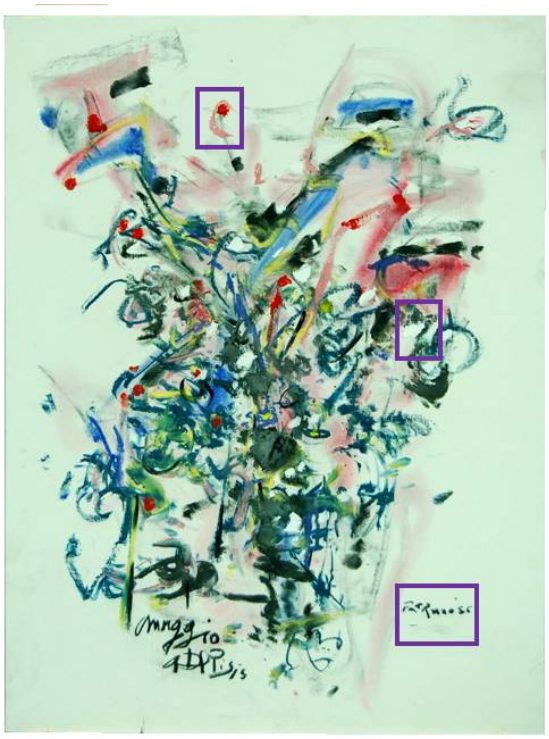

Fig 69 *Omaggio a De Pisis*. Total of the painting (*recto*) in diffuse light. Violet frames refer to details shown in following figures.

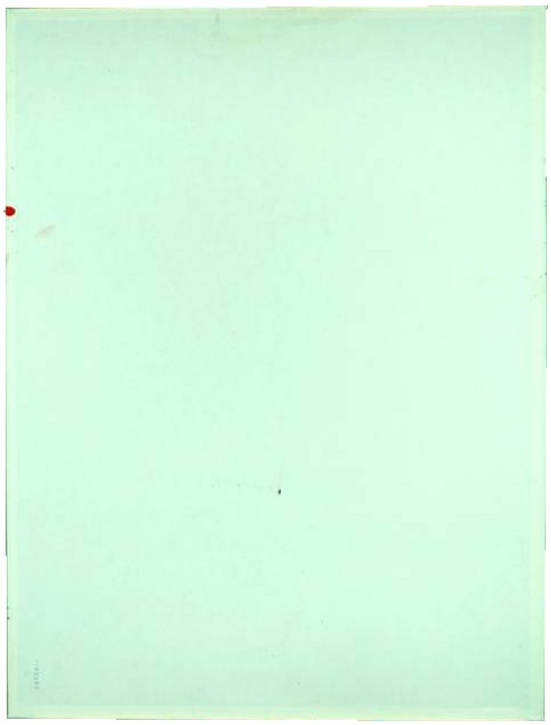

Fig 70 *Omaggio a De Pisis*. Total of the painting (*verso*) in diffuse light.

To a first simple visual inspection, the paint film presents a certain heterogeneity of colours (in terms of hues) and thicknesses, as shown by raking light photos (figs. 71, 72). To achieve this effect, the unconventional choice to side at the brush other work instruments such as pastels and fingers, as a tool of execution, gives a contribution. On the back, there are a red spot, a fingerprint of the artist and an ink stamp, showing the dimensions of the support (fig. 73-75) (Petitta, 2012).

If images in raking light showed the materiality of the brush strokes and the realization of layers with various tools and mediums, infrared reflectography did not show any preparatory drawing below. The painting was thus probably realized directly on the canvas. Nonetheless, the same reflectography clearly emphasized the diversity of materials used, showing different properties of transparency, absorption and reflectance of the pictorial materials to infrared radiation (fig. 76a-b). In particular, white and yellow appear opaque and reflective, blacks and dark blue are opaque but absorbent, while red, pink and blue light are transparent to infrared radiation.

A solicitation with ultraviolet radiation, finally, differentiates non fluorescent pastels from acrylic colours, which present some fluorescence (figs. 77, 78), which is obviously different according to the materials. As an example, thick brush strokes of white acrylic pigment returned a very weak fluorescence, while red and yellow fluorescence characterized red and yellow pigment. Just the yellows, showed two different behaviours to the radiation, probably due to the use of two kinds of pigments.

X-Rays fluorescence analysis was also performed, in order to better understand the compositional nature of pigments used, assuming that they were contemporary pigments.
As a start point, the presence of zinc on the canvas, and not on white points, was found, suggesting an industrially prepared canvas based on zinc, probably *Zinc White*.
On white points, instead, titanium, strontium and barium were the predominant elements, suggesting the presence of *Titanium white*.
Iron detected on yellow points can only be justified by pigments such as *yellow ocher* and *Mars yellow*.
Similarly, due to the presence of iron, *red ocher* and *Mars red* appear to be the pigments used with greater probability. However, the use of organic materials, such as *red lake*, can not be excluded.
Furthermore, in one of the pink points, the presence of lead (at least unusual for that period) suggested the use of *Lead white*, in mixture with an iron-based red (*Red ocher* or *Mars red*).
Iron would also appear the element responsible for coloration of blue points, which could thus be obtained with a *Prussian blue* or *Ultramarine blue*.
Finally, more difficult was to identify the pigment present used for black point, where the coexistence of several elements lets open (too) many possibilities.

Fig 71a Detail, in diffuse light.

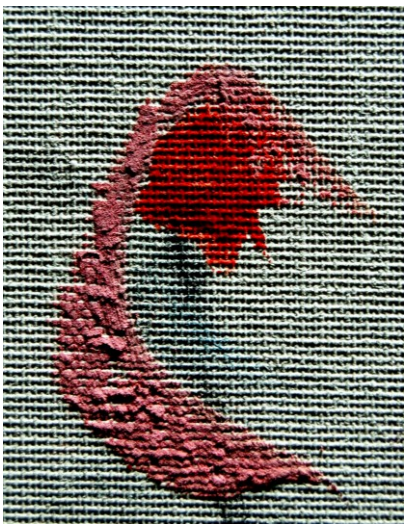

Fig 71b The same detail, in raking light, highlighting the cracking and detachment of the pictorial material.

Fig 72a Diffuse light, detail of a white brush stroke.

Fig 72b The same detail, in raking light, emphasizing the thickness of the materic brush stroke.

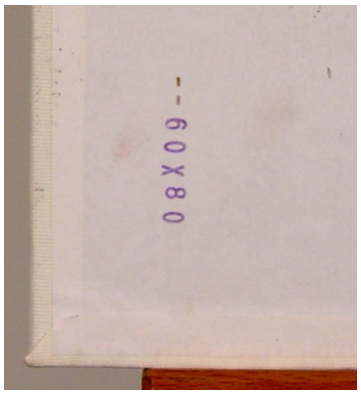

Fig 73 *Verso*, diffuse light. Detail of the ink stamp showing the dimensions of the support.

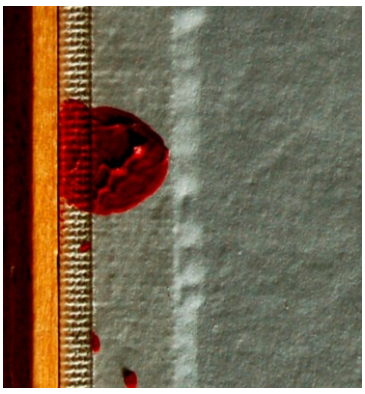

Fig 74 *Verso*, diffuse light. Detail of the red spot.

Fig 75 *Verso*, diffuse light. Detail of the fingerprint.

Fig 76a Diffuse light, detail of the central part. The green frame refers to the following detail in ultraviolet fluorescence.

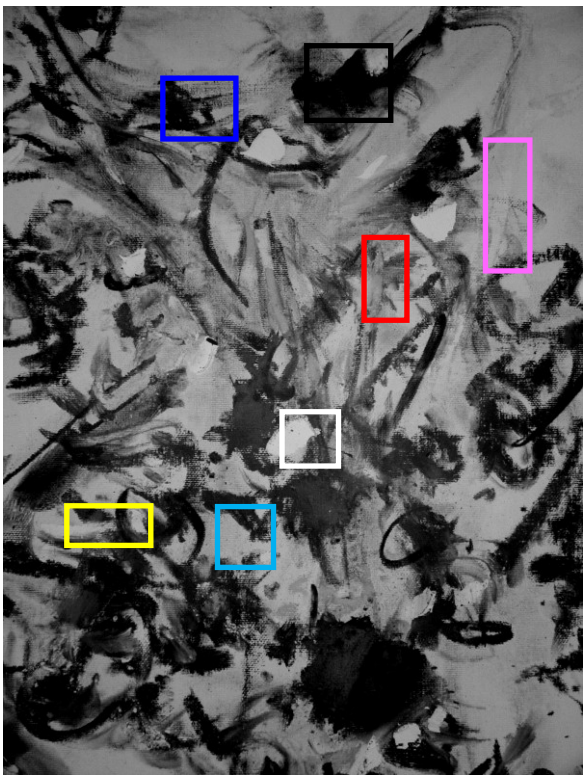

Fig 76b Infrared reflectography, detail of the central part showing the differentiation of materials and colours, according to their behaviour to near infrared radiation. Coloured frames individuate the different hues.

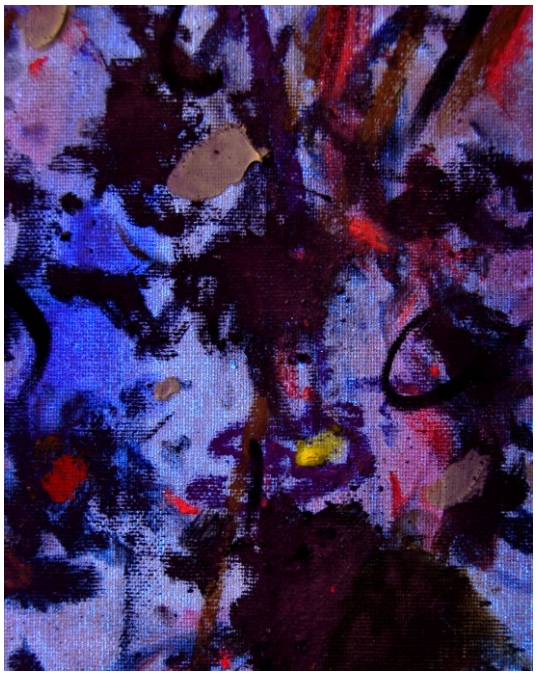

Fig 77 Ultraviolet fluorescence, detail of the previous picture (in the green frame).
Differentiation between non fluorescent pastels (dark appearance) and fluorescent red and yellow acrylic colours.

(a)

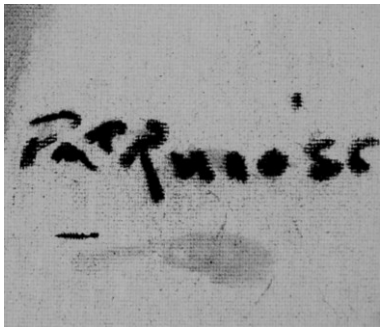

(b)

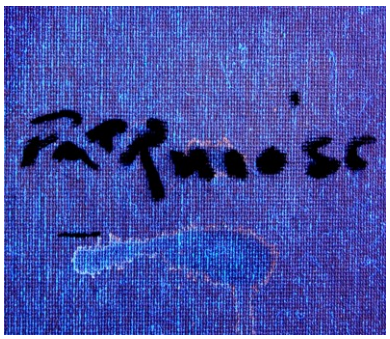

Fig 78 (a) Infrared reflectography, detail of the signature.
(b) Ultraviolet florescence, detail of the signature. A flack of different material, beneath, is emphasized.

Conclusions

The painting, on the whole, shows a variety of painting techniques and ways to use the paint materials, included by fingers. Colours were applied on canvas just as they came out of the tube, that is, without mixing them. Such a features made it easier to recognize some of the pigments used, by means of XRF.

In addition, image diagnostics applied, like ultraviolet fluorescence and infrared reflectography, emphasized the different characteristics of contemporary materials, differentiating them according to their hue and type (acrylic or pastel).

To sum up, the study of this work of art represents a typical example of how contemporary materials behave.

It can thus be a valuable reference for subsequent investigations of contemporary works of art, both regarding materials and pictorial technique.

1.2.4 E. Pazzini

Edoardo Pazzini was a painter from Romagna (Verucchio (Rimini) 1897- Rimini 1967). His production, focused on reproducing landscapes around his birthplace, includes various types of support and painting techniques. In order to better understand these latter, wide band infrared reflectography acted, in this case, as a useful tool in the detection of underdrawing and, even more, to deepen the executive technique. Some features about his way to proceed can thus be followed over time, outlining some peculiarities in the style and pictorial habits.

As an example, *Lungo la strada a Padulli con donna e anitre* (1943) is an oil on cardboard (fig. 79). On the front of the painting, surely due to the thickness of the brush strokes, infrared reflectography couldn't notice any trace of a preparatory drawing. On the back of the artwork, instead, reflectography clearly showed numerous inscriptions. These contribute to reconstruct part of the history of the painting, referring to the title, the outdoor stages, noted with sharp precision (12/11 "*terminato prima seduta*" – 12/12/1943), type of paper used (Fabriano) and the squaring lines under the framing tape (fig. 80).
The study of painting materials, takes advantage of results arising from the use of many diagnostic techniques, both imaging and punctual, integrated with each other. The inspection with ultraviolet radiation, for instance, showed a strong red fluorescence in correspondence with the yellow brush strokes (fig. 81). These are present on the sky, distributed in the *foliage*, and in correspondence with the human figures on the path. X Ray fluorescence analysis, performed on the yellow point in the sky, revealed the presence of cadmium, suggesting *Cadmium Yellow*, as a pigment used.
On another work of art, *Paesaggio di San Marino* (1926), realized on paper with pastels, the painter chose to create a preparatory drawing by setting the essential lines of the composition before applying the colour (figs. 82, 83). As a proof of this assertion, infrared reflectography performed with a InGaAs scanner (Section 4.1.1) returned decisive and dark lines of the drawing below in the image (fig. 84), moreover already visible to the naked eye. In particular, on the left side of the painting, various signs are clearly noticeable, conducted with a rather rough stretch and, moreover, not always well correlated to the final version. Also the date of realization (1926) is more clearly visible, thanks to the solicitation with infrared radiation.

In the case of *San Leo*, an oil on plywood attributable to the 50s of the twentieth century (fig. 85), the detection of a possible underdrawing was not possible, due to the superimposition of a fluid and materic brush stroke, whose trend and direction was well highlighted by infrared reflectography (fig. 86). On the contrary, the same technique emphasized a different kind of stroke, short and "dry", that characterizes another oil on cardboard, entitled *Buoi*, also attributable to the same years (figs. 87, 88). In both cases, a notation about the painting technique of the artist can be highlighted, like the practice of tracing the squaring lines, constantly maintained even in the years of his maturity. Such a habit is well shown on the painting *Buoi*, whose upper edge is interested by the presence of some sketches, delineating the scene of the landscape. The same outlines, to setup the scene, are shown in *L'azzurra vision di S. Marino* (figs. 89, 90), where tiny strokes just sketched, are visible on the bottom of the painting, through the use of infrared radiation.

X Ray fluorescence was also applied on both *San Leo* and on *Buoi*, in order to gain some more information about pigments used by the artist. On *San Leo*, detection of both selenium and cadmium on some yellow and red points, suggested the presence of Cadmium yellow and of Cadmium red (*Cadmium solphoselenide*), which were common material in the twentieth century and, thus, compatible with the artist's palette. Such a finding was already encountered in the painting *Lungo la strada a Padulli con donna e anitre*, but although suggesting certain use of this pigment, does not exclude the use of other materials and techniques. As an example, on the painting entitled *Buoi*, the low amount of cadmium detected was strangely not related to a red point, but to a green one. In general, the co-presence, on the same points, of several elements, relatable with a variety of different pigments (and different hues), made it impossible to proceed to a precise characterization of the pigments used. Just their simultaneous presence on various points of different hues, represented an indication about the artist's painting technique, consisting in mixing a variety of colours on his palette.

Conclusions

Overall, all these findings reveal the utility of imaging techniques, such as wide band infrared reflectography, sometimes with the support of punctual techniques like XRF, in deepening the painting technique of the artist. This becomes particularly important when considering several works of art of the same artist, regarding different periods of his production.

Fig 79 *Lungo la strada a Padulli con donna e anitre*, oil on cardboard, 1943. Total in diffuse light (*recto*).

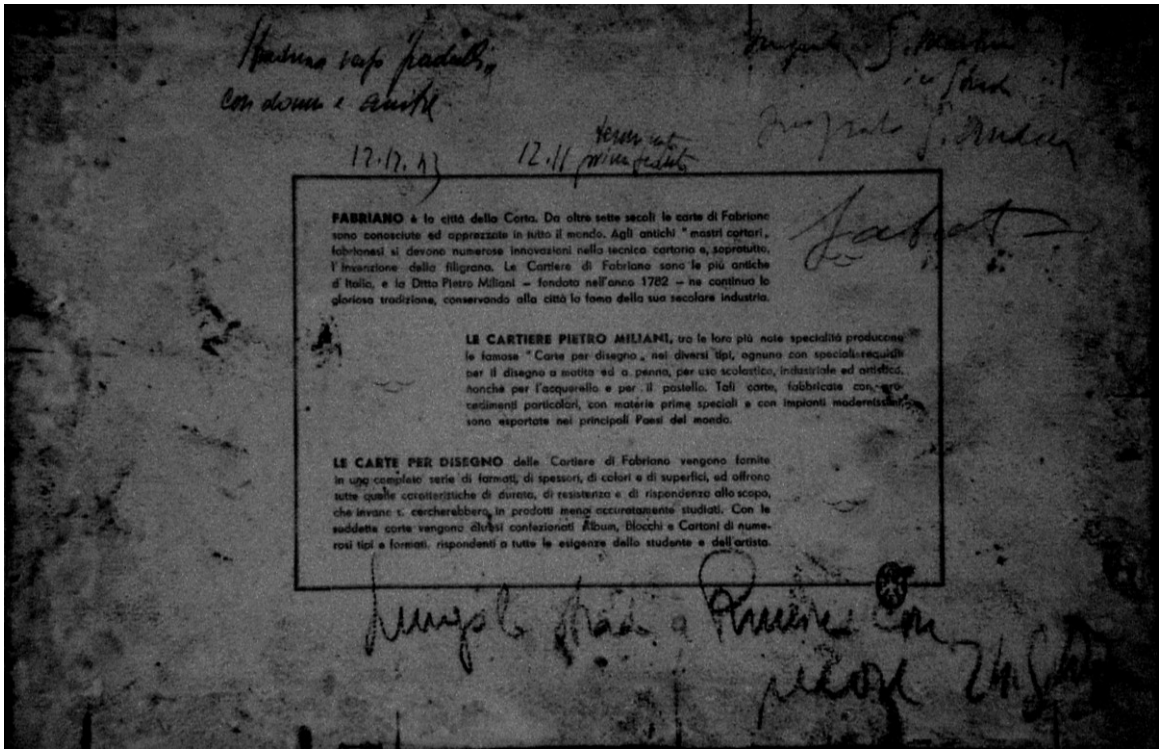

Fig 80 *Lungo la strada a Padulli con donna e anitre*, *verso*.
Infrared reflectography (strongly contrasted image), showing various inscriptions and, at the bottom, vertical traces of squaring lines.

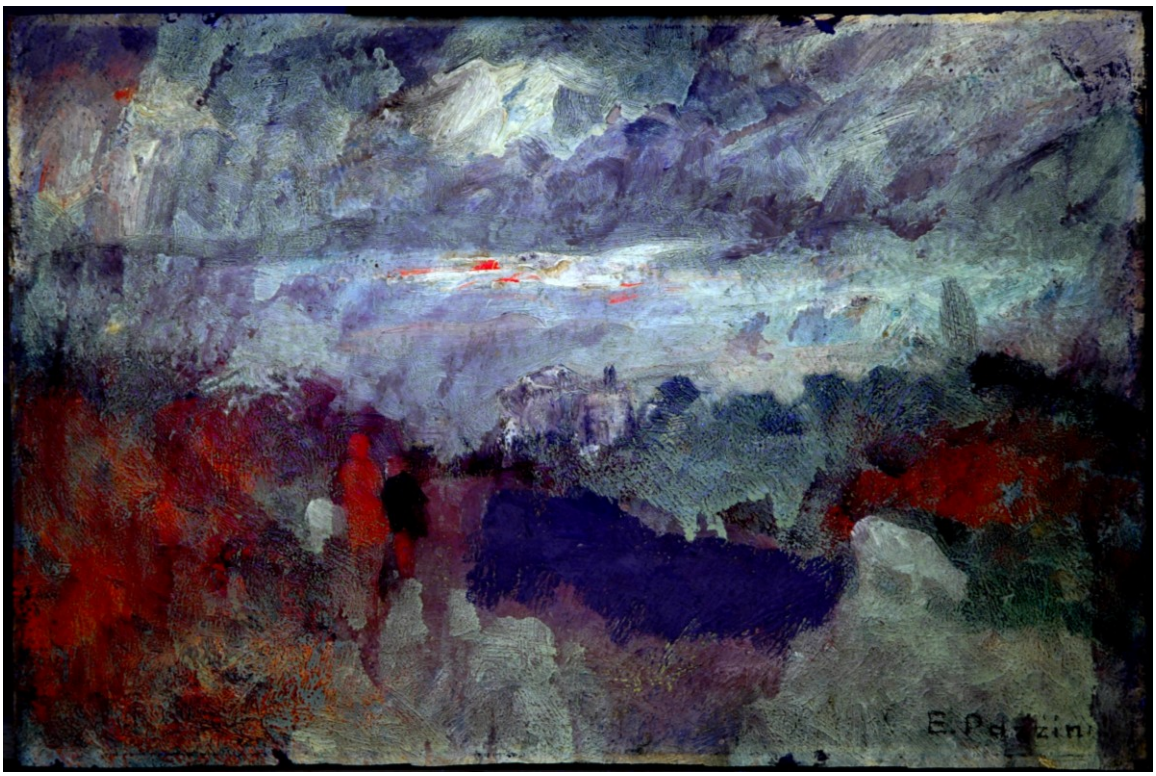

Fig 81 *Paesaggio di S. Marino* (*recto*). Total in visible light, inside the frame and with the glass.

Fig 82 *Paesaggio di S. Marino*. Total in visible light, inside the frame and with the glass (*recto*).

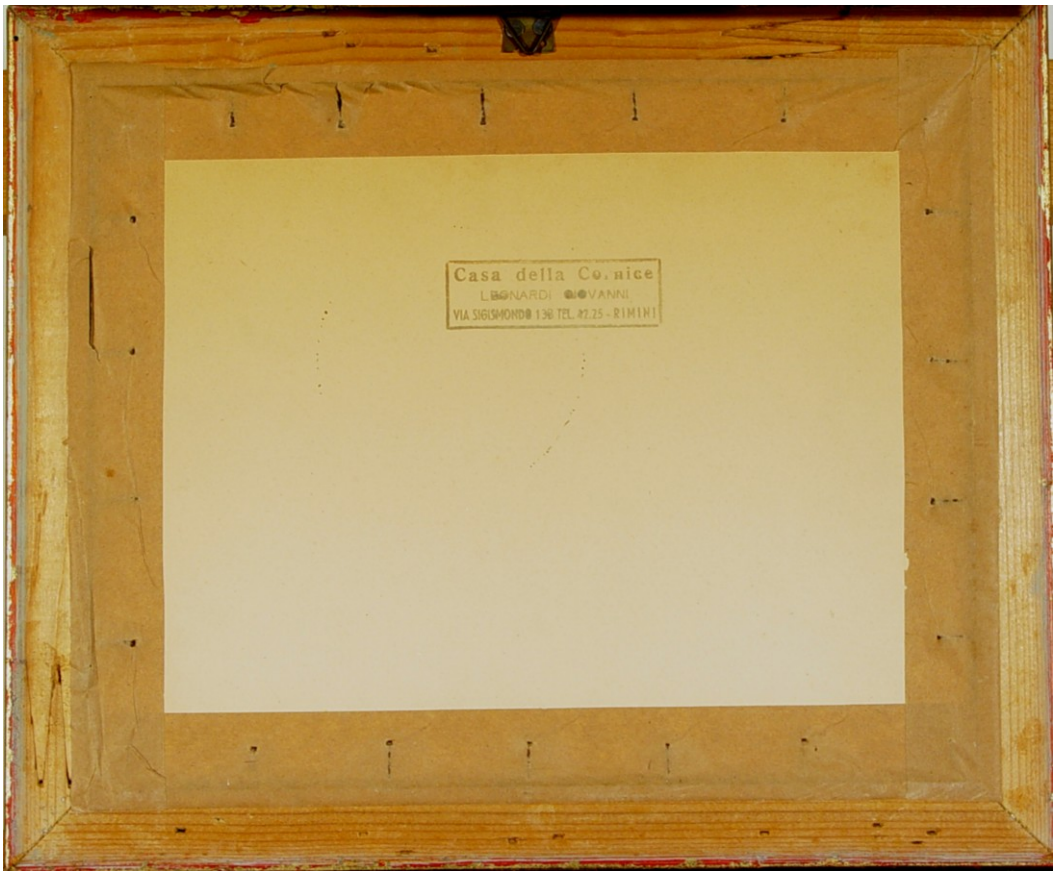

Fig 83 *Paesaggio di S. Marino*. Total in visible light, inside the frame (*verso*).

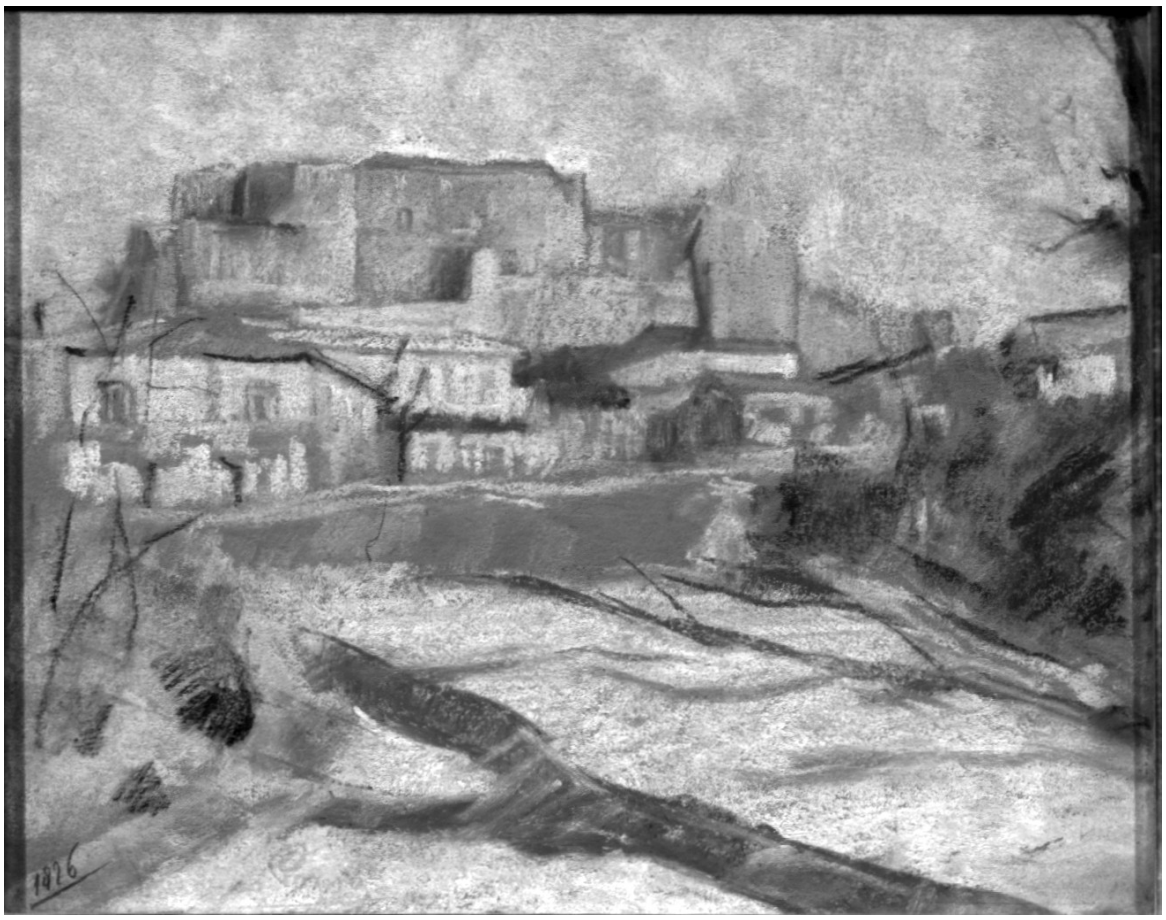

Fig 84 *Paesaggio di S. Marino* (*recto*).
Total in infrared reflectography (InGaAs scanner), showing decisive and dark lines of the drawing.

Fig 85 *S. Leo*, oil on cardboard, 1943. Total in diffuse light (*recto*).

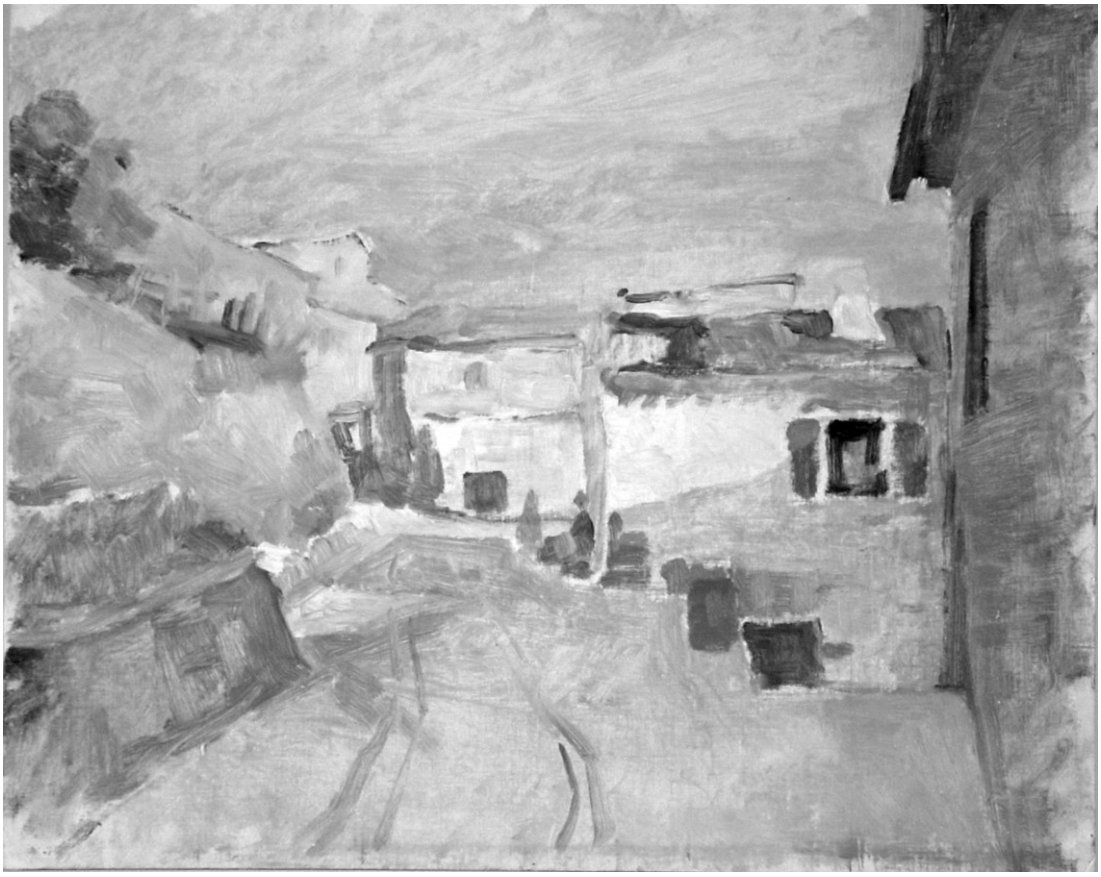

Fig 86 *S. Leo*. *Recto* in infrared reflectography, highlighting the features of materic brush strokes.

Fig 87 *Buoi*. Total in diffuse light (*recto*).

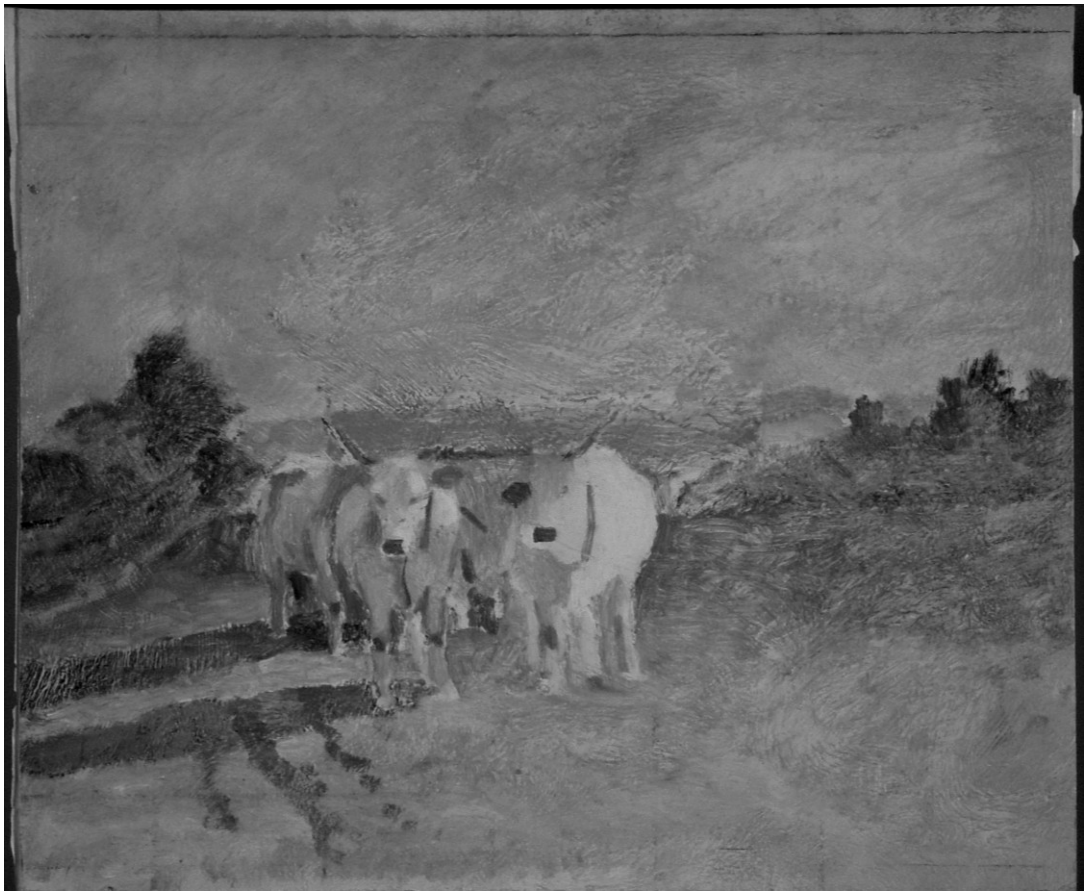

Fig 88 *Verso* in infrared reflectography, highlighting the squaring lines and the features of brush strokes.

Fig 89 *L'Azzurra vision di S. Marino*, oil on cardboard. Total in diffuse light in (*recto*).

Fig 90 *L'Azzurra vision di S. Marino*, oil on cardboard.
Recto in infrared reflectography (contrasted image) highlights traces of squaring lines, at the bottom.

Chapter 2

Applications of non invasive techniques to ancient artworks

During my PhD, some ancient and diversified works of art were investigated, too.
Indeed, also the numerous issues raised by non contemporary artworks, can be very different, as they are associated to the different nature of the objects examined.
Despite this, for ancient works of art, the use of materials and painting techniques is, at least, well established (Maltese, 2005). Unlike contemporary art, many texts and treatises about Italian and European painting are known and available. The most representative is *The Book of Art* by Cennino Cennini, containing information about pigments, brushes and painting techniques, and telling some tips and "tricks" of the trade (Frezzato, 2009).

The case studies presented below, concern exactly six artworks of different nature. Each of these was bringing questions, which often dictated the most appropriate investigations.

- The first one is a large altarpiece, whose great dimensions and weight were important issus to deal with, both while moving and investigating on it (Section 3.1).
- The second case study is represented by three samples taken from a fresco, and subjected to XRF analyses to formulate assumptions about the pigments used (Section 3.2).
- Then, a painting on canvas was investigated, soon revealing itself as an interesting case of reuse of a support (Section 3.3).
- Another peculiar artwork, a *desco da parto*, was studied, arising some doubts about the effective attribution to the Renaissance period (Section 3.4).
- Two artworks on paper, ascribed to the seventeenth century, were investigated by means of a microscope, allowing to appreciate the smallest details of the ink strokes (Section 3.5).
- Finally, some glazed ceramics of Iranian provenance were examined, to characterize their optical features (Section 3.6).

2.1 Giovanni Da Mel. *Madonna con il Bambino tra i santi Rocco e Sebastiano* (XVI century)

An artwork on wood panel, attributed to the second half of the sixteenth century, has been examined in the Larix laboratory in March 2011 (figs. 91, 92). With the priority of identifying the original paint layers, a radiographic image was required. As a matter of fact, the pictorial layer, raised in various points and then temporarily repaired with tissue paper, showed extensive repaintings.

The painting was digitally radiographed with the 2D scanner of the Department of Physics and Earth Sciences, University of Ferrara. Due to the size of the detector, which is 11 x 3.3 centimeters, 1500 images were totally acquired, and subsequently merged, in order to obtain the total image (fig. 93).

Fig. 91 The painting during the acquisition of radiographic images with the 2D radiographic scanner.

Some observations concern the support, starting with the three crosspieces, and three long reinforcements, which were intended to give greater strength to the structure during its movement. Some long nails are also evident, two different manufactures, on the top and on

the right edge. Six (butterfly shaped) joints, arranged on both ends, join the four axes which constitute the support.

The pictorial layer, corresponding to the portion of the sky (at the right of the Virgin), is non-uniform and fragmented, thus differentiating the original paint layer from subsequent repaintings.

Fig. 92 *Madonna con il Bambino tra i santi Rocco e Sebastiano*. Total in diffuse light (*recto*).

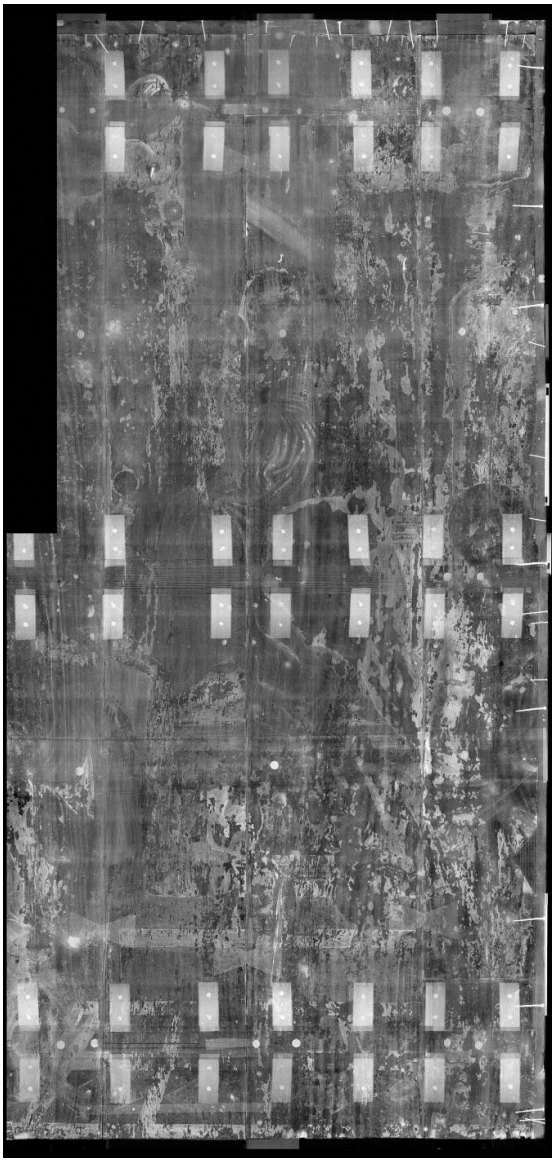

Fig. 93 Total digital radiography, showing the internal structure of the painting.

The cleaning test on the face of *St. Sebastiano* allowed a direct reference to the part of the original paint layer which is still present. At the same time, it enabled to observe the radiographic appearance, compared to that of the subsequent repaintings (fig. 94, 95). On the radiographic image, the appearance of original portions, rugged, minimal and irregular, is lighter than the background. These fragments are characterized by the presence of a

preparation, that X Ray fluorescence confirmed to be based on gypsum, probably with a superimposed *imprimitura* of *White Lead*. Where in the paint layers, additional amounts of lead or other radiopaque elements are present, the tone of the radiographic image appears clearer. The edge, thickened for the prominence of the colour applied by brush, is visible on the mantle of the Virgin (fig. 96, 97). On the musician angels, the radiographic image offers a further indication of the painting technique of Giovanni Da Mel. The strings of the instruments have been traced and retracted in some places, probably with the aid of a ruler (fig. 98).

Fig. 94 Cleaning test on the face of *St. Sebastian*.

Fig. 95 Radiography of the area around the cleaning test.

Fig. 96 Cleaning test on the mantle of the *Virgin*.

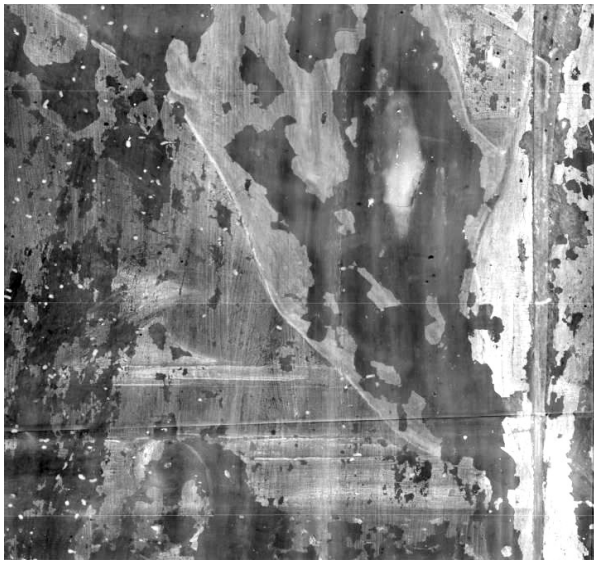

Fig. 97 Radiography of the area around the cleaning test.

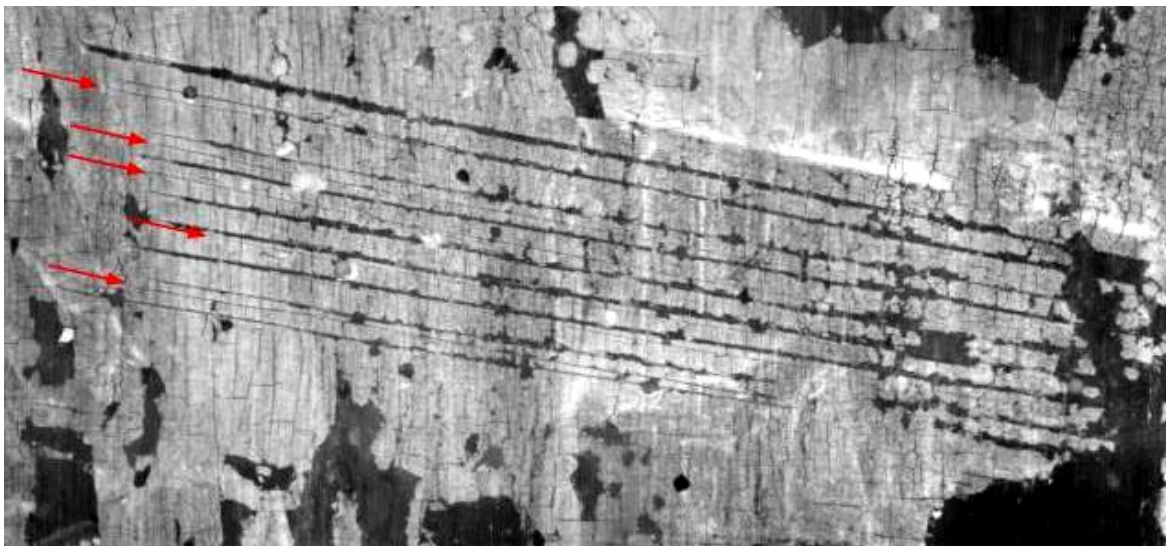

Fig. 98 Musician angel, on the left. Radiographic detail showing the arrows, that indicate some *pentimenti* on the strings of the instrument.

Additional information on the pictorial technique of the painting and its repaintings, come from the wide band infrared reflectography. This technique investigates a deeper level of the paint layer, with infrared radiation of longer wavelength (1.1 – 2.5 μm), compared with commercial applications (Section 4.1.1). The figure of the Child, the fragments of the original paint layer appear in dark tones in the reflectographic image. The same details that radiography reproposed, on the contrary, in light tones. In the repainted portions, instead, different gray tones correspond to the same number of levels of repaintings (fig. 99a-b-c). About the underlying drawing, traces of it can be seen along some figures, in the less compromised and repainted portions, as in the flesh tones. It is a rather thin contour, conducted in part by brush, in part, perhaps, with a black chalk. Since drawn on non-original parts, it was probably executed during repainting interventions, as demonstrated by the comparison with the radiography. Two details show the design on the eyes of St. Rocco (fig. 100, 101), and on the shoulder of St. Sebastiano (Albertin, 2013).

Fig. 99a Detail of the *Virgin* and *Child*. Photograph in visible light.

Fig. 99b Detail of the body of the *Child*. Radiography.

Fig. 99c Detail of the body of the *Child*. Image processing of IR and RX acquisitions: original parts in black, repainting in gray tones.

Fig. 100 Detail of the face of *St. Rocco*. IR reflectography.

Fig. 101 Detail of the face of *St. Sebastiano*. IR reflectography.

Finally, by X Ray fluorescence and the visible (VIS) reflectance spectrophotometry (G. Poldi, University of Bergamo), it was possible to speculate about the pictorial *palette* used in the painting. The XRF analysis identified, on the investigated points, some of the elements inside pigments (fig. 102).

Spectrophotometric measures and the subsequent comparison between measured reflectance spectra and reference spectra (available online), identified some pigments: calcium and lead, detected in conspicuous amounts on points in correspondence with the preparation, suggested *White lead* and *gypsum* as the pigments used on this layer.

On blue points, the significant presence of copper found in the XRF spectra (fig. 103), let assume the existence of a *Smalt blue*, which, however, must be found in the underlying layer (fig. 104). In fact, it wasn't identified by means of reflectance spectroscopy, which only operates at the surface. This technique, in fact, indicates only the presence of *Azurite* (fig. 105).

In correspondence of a repainting on the sky, iron was found by means of XRF. The reflectance spectrum has added an additional information, referring to the *Prussian blue*.

The green pigments investigated, appear to be all copper-based, due to the overwhelming presence of this element in the XRF spectra (fig. 106). The trend of the reflectance spectra is also compatible with the hypothesis of a *Copper green* (fig. 107), possibly mixed, in some points, with *lead-tin yellow*, or with small amounts of chromium and manganese.

The presence of iron on the red tiles on the floor, showed that they are made with *red ocher*. On the mantle of the Virgin (cleaning test), however, the outcome of investigations XRF revealed the presence of arsenic, which traced back to the use of *Realgar* (fig. 108). The reflectance spectrum for this point, excluding the presence of *Cinnabar* on the surface, left open the possibility of a glaze, based on red lake. This thin layer may be applied on underlying layers of *Realgar* and – maybe – *Cinnabar* (fig. 109) (Poldi, 2006).

Measure points	K	Ca	Ti	Cr	Mn	Fe	Co	Ni	Cu	Zn	As	Sr	Sn	Sb	Ba	Hg	Pb
White, preparation, cleaning test	0	161	0	2	0	55	13	5	1535	0	0	119	8	0	5	12	589
Dark blue, *Virgin*'s mantle, cleaning test	4	36	6	0	2	167	130	49	9038	0	113	50	0	0	0	0	1810
Blue, sky, cleaning test	2	14	2	0	4	35	20	9	2421	0	0	41	0	0	0	0	8451
Blue, sky, re-painting	0	81	0	23	1	202	3	0	8	5	0	124	0	29	22	21	1833
Green, throne basis	0	25	3	2	6	100	10	4	1138	0	0	56	13	0	0	299	7061
Light green, floor	0	57	3	3	2	124	0	0	1335	0	0	235	0	0	0	38	4485
Green, *St. Rocco*'s mantle	0	25	4	13	11	137	0	0	3152	0	0	112	0	0	0	36	3793
Red, *Virgin*'s mantle	0	55	0	1	36	612	0	0	66	3	3170	66	0	0	7	66	4895
Dark red, floor	0	35	0	4	7	1284	0	0	184	16	0	121	0	0	4	65	5223
Flash tone, *Angel*'s arm	0	30	0	0	6	115	0	0	9	0	0	87	0	12	0	240	6456

Fig. 102 Results of the XRF measurements. Counts per second, detected on the main peaks of each element, are reported. Data elaboration with software Bruker Spectra 7.2.5.0 .

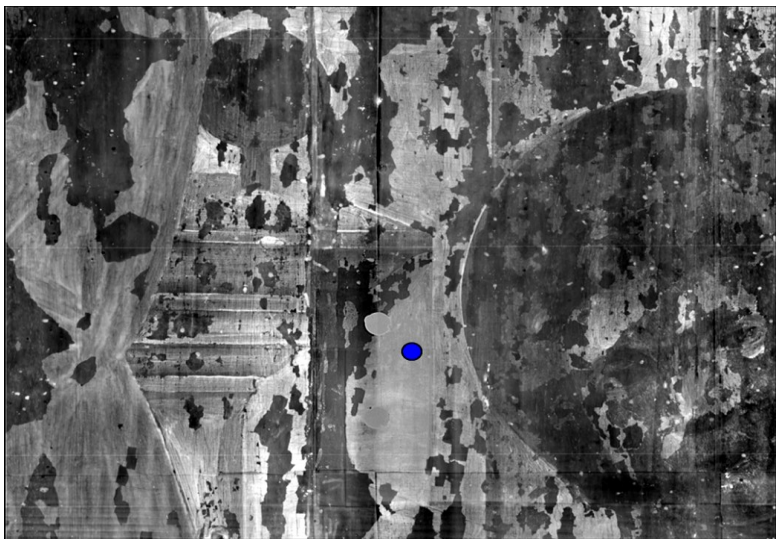

Fig. 103 Identification of the blue point on the sky, on digital radiography.

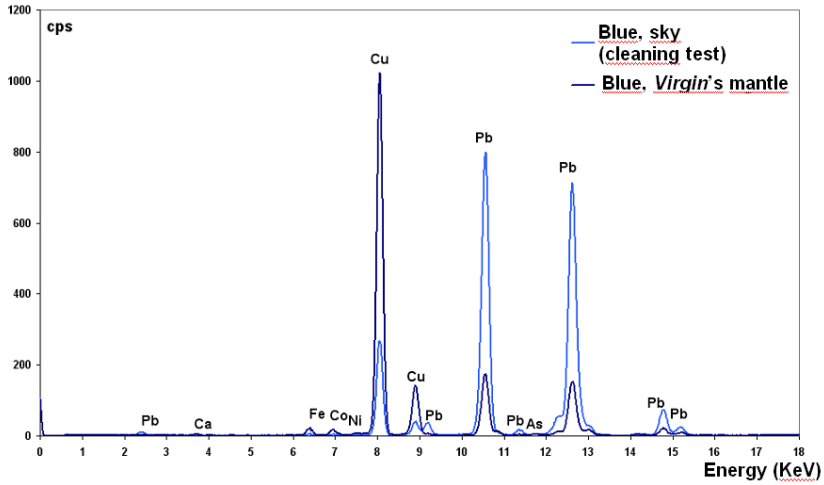

Fig. 104 X Ray fluorescence spectrum of two blue points (on the sky and the *Virgin*'s mantle), containing abundant *Azurite* (Cu) and *White lead* (Pb).

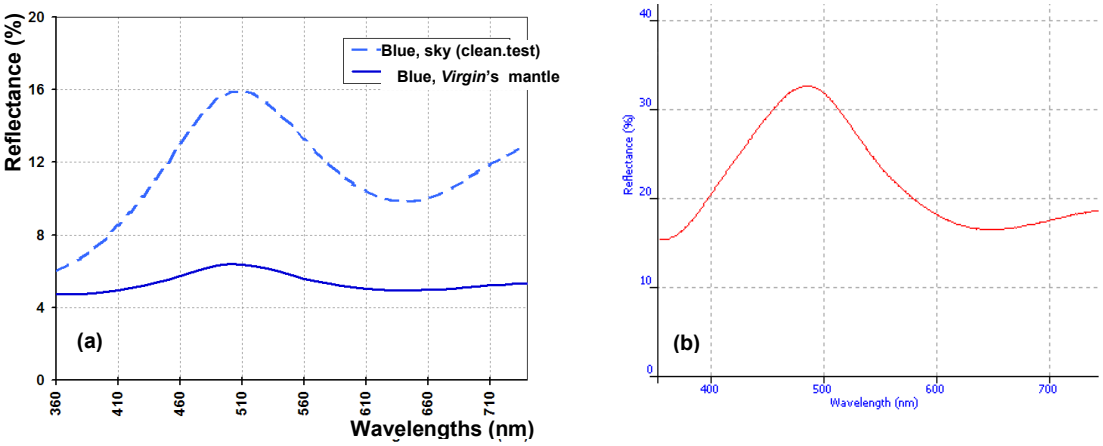

Fig. 105 Reflectance spectroscopy: a) spectra collected on the blue points of the previous figure, b) spectrum of *Azurite*. From http://fors.ifac.cnr.it/index.php

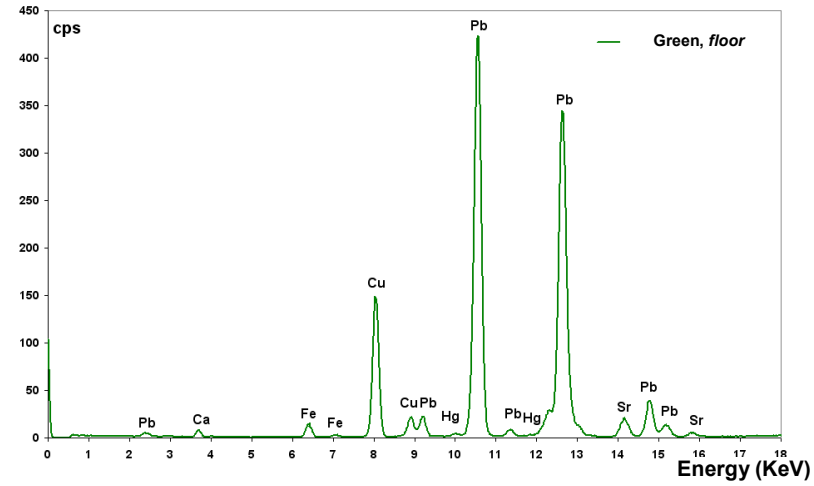

Fig. 106 X Ray fluorescence spectrum of a green point on a tile on the floor.

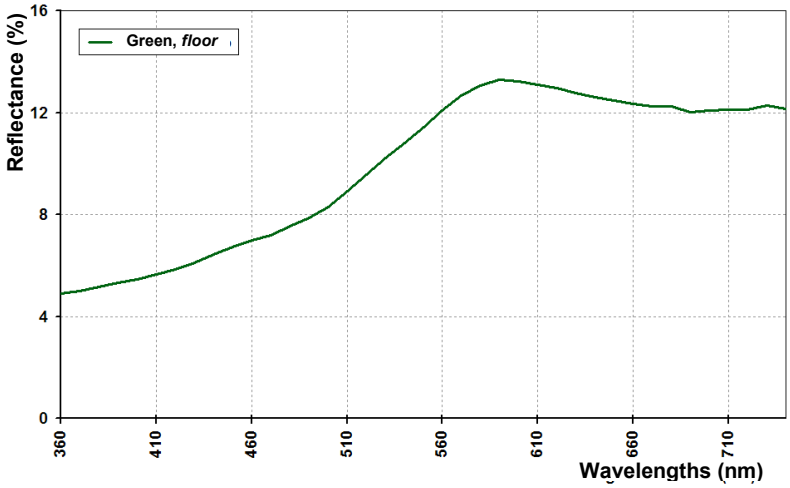

Fig. 107 Reflectance spectroscopy: spectrum detected on the green point from the previous figure.

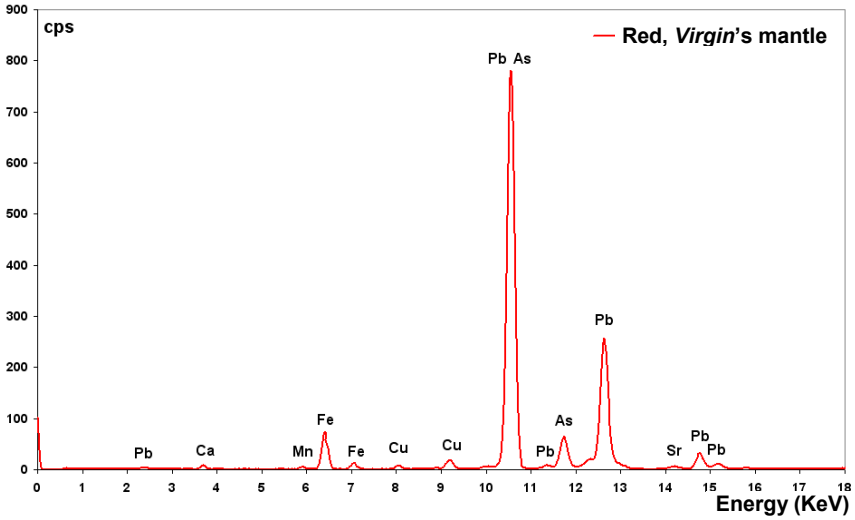

Fig. 108 X Ray fluorescence spectrum for a red point on the *Virgin*'s mantle.

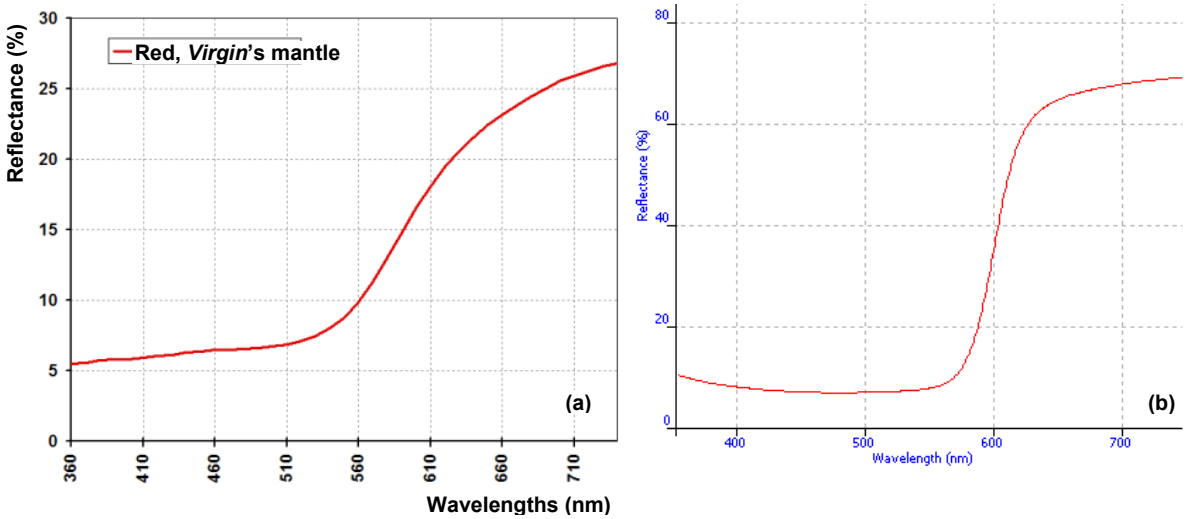

Fig. 109 Reflectance spectroscopy: a) spectrum detected on the red point in the figure above, b) spectrum of *Cinnabar*. From http://fors.ifac.cnr.it/index.php.

Conclusions

To sum up, radiographic and reflectographic images performed on the altarpiece provided an important cognitive basis to identificate the stratification of previous interventions. Integrated with spectrophotometric investigations in the visible range, and with X Ray fluorescence, image diagnostics gave information on execution technique and materials used.

The high definition of the radiographic image of the entire altarpiece, in particular, provided an indispensable tool for the general interpretation of the layer, on which the conservative intervention was later performed. Operational decisions were thus guided by the synergistic interpretation of results obtained from previous investigations.

The contribution of various skills, allowed to guide the restoration in a focused way, identifying areas where the original material was still present, and those where, instead, multiple layers of repainting were present. In addition, the results of the diagnostics also driven the cleaning operation, gradually conducted in a selective way, aimed to bringing back to light repainting portions of the sixteenth century, without demolishing the subsequent phases.

2.2 Marco Da Mel. Samples from a *fresco* in *Saint Bartolomeus Church*, Villapiana di Lentiai, Belluno (XVI century)

Measures on a wall painting concerned some samples taken from a *fresco*, realizaed by Giovanni Da Mel's brother, Marco, who was also working within the territory of Feltre.
The church of Saint Bartolomeus in Villapiana presents its actual form from the XV century. The church's interior frescos tell the story of Saint Bartolomeo, and show many signs of different over paintings, performed over time. As an example, precautionary measures were taken by the Venetian Republic in times of plague, by adding a layer of calcium plasters to avoid contaminations in church (Del Farra, 2013).
Anyway, in the currently visible frescos, Marco da Mel presents the scene of the *Leggenda Aurea* (*Golden Tale*), and the *Polimnio's Christening*.

X Ray fluorescence on fresco's samples

On the two pieces of fresco, three samples were taken, and submitted to X Ray fluorescence in order to better understand their composition. Both N1 and N2 samples presented a green colour, while the third one was collected from a dark red area (fig. 110a,b).

Fig. 110a *Male figure*. Total piece of the smaller *fresco* and sampling spot for sample N1 (green).

Fig. 110b *Polimnio's Baptize*. Total of the larger *fresco* and sampling spots for samples N2 (green) and N3 (red).

N1 sample, taken from a pale green area, showed a slightly painted surface. XRF measurements, carried out by placing the sample on a sponge, obtained as a result

spectrum and the elemental composition that do not allow a detailed characterization of the pigment. Nevertheless, it should be mainly composed by iron (fig. 111).

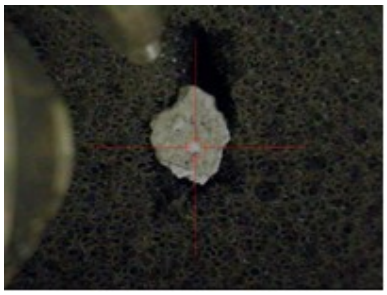

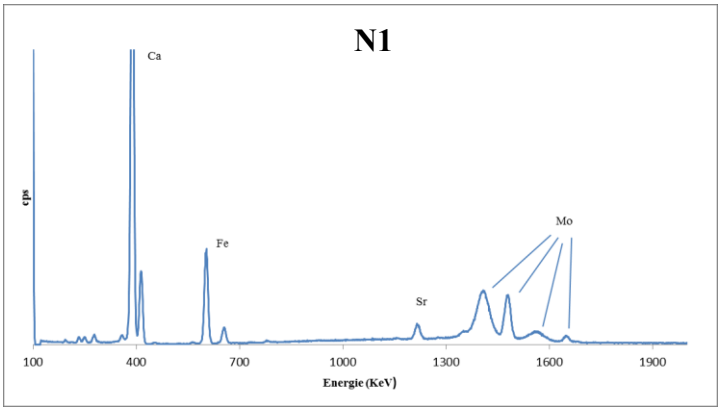

Line	Energy/keV	cps	Net	Backgr.
Ca $_{K\alpha}$	3.692	2136.2	256342	2795
Fe $_{K\alpha}$	6.405	267.7	32118	2662
Sr $_{K\alpha}$	14.165	29.9	3586	30440
Sr $_{L\alpha}$	1.806	1.2	148	2321

Fig. 111 XRF spectrum and relative counts per second (cps) detected for sample N1 (in the picture).

XRF measurement on N2 sample, taken from a bright green area, were carried out by placing the sample on a Mylar plastic wrapping on top of a sponge (fig. 112). The spectrum and the elemental composition identified the pigment as copper based green, differentiating it from the green one characterized for sample N1.

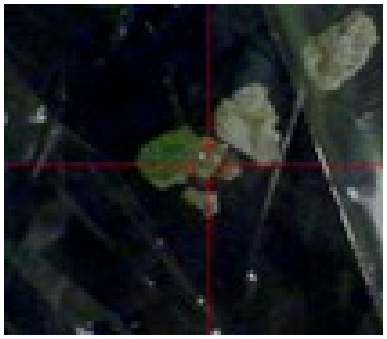

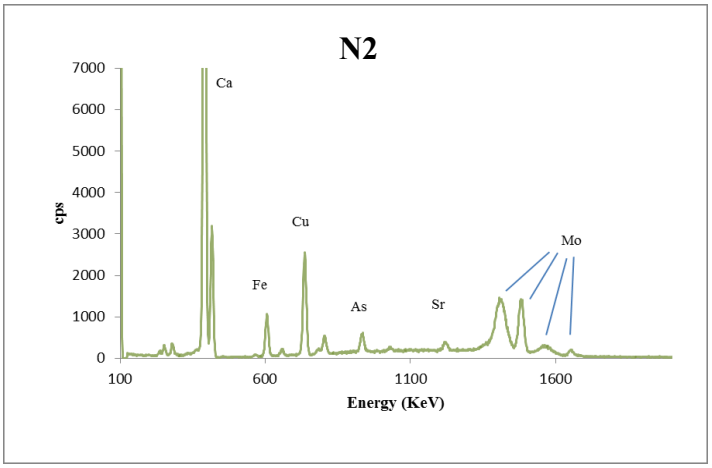

Line	Energy (keV)	cps	Net area	Backgr.
Ca $_{K\alpha}$	3.692	1942.4	233085	2770
Fe $_{K\alpha}$	6.405	255.6	30677	3435
Cu $_{K\alpha}$	8.046	6104.8	7325785247	0
As $_{K\alpha}$	10.543	354.9	42587	4339
As $_{L\alpha}$	1.282	0.5	62	2073
Sr $_{K\alpha}$	14.165	72.4	8689	6780
Sr $_{L\alpha}$	1.806	0.4	50	2043

Fig. 112 XRF spectrum and relative counts per second (cps) detected for sample N2 (in the picture).

N3 sample, collected form a dark red area, was placed on a Plexiglas support to carry out XRF measurements. The spectrum and the elemental composition indicated an iron based pigment (fig. 113).

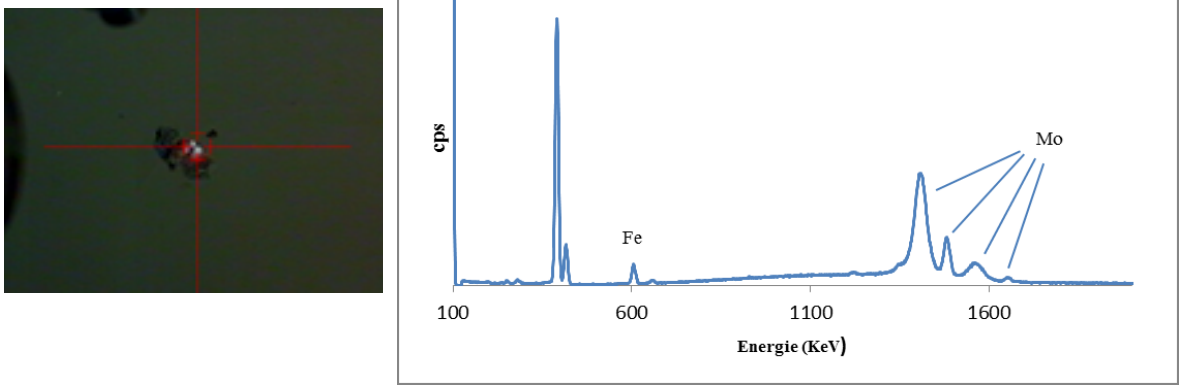

Line	Energy/keV	cps	Net	Backgr.
Ca $_{K\alpha}$	3.692	1628.1	195371	2476
Fe $_{K\alpha}$	6.405	135.2	16225	3069
Sr $_{K\alpha}$	14.165	24.3	2910	29794

Fig. 113 XRF spectrum and relative counts per second (cps) detected for sample N3 (in the picture).

Further XRF measurements, carried out *in situ* by means of a portable instrument, allowed to confirm, for N1 sample, the presence of a green earth, mainly composed by iron, as well as by K, Si, and Mg elements at lower concentrations (all consistent with the composition of the green earth).

Overall investigations performed on sample N2, included Raman analysis (Del Farra, 2013), confirmed *Malachite* as its main pigment, being copper the principal component and minor amounts of arsenic, generally found in copper minerals as an impurity (figs. 114, 115).

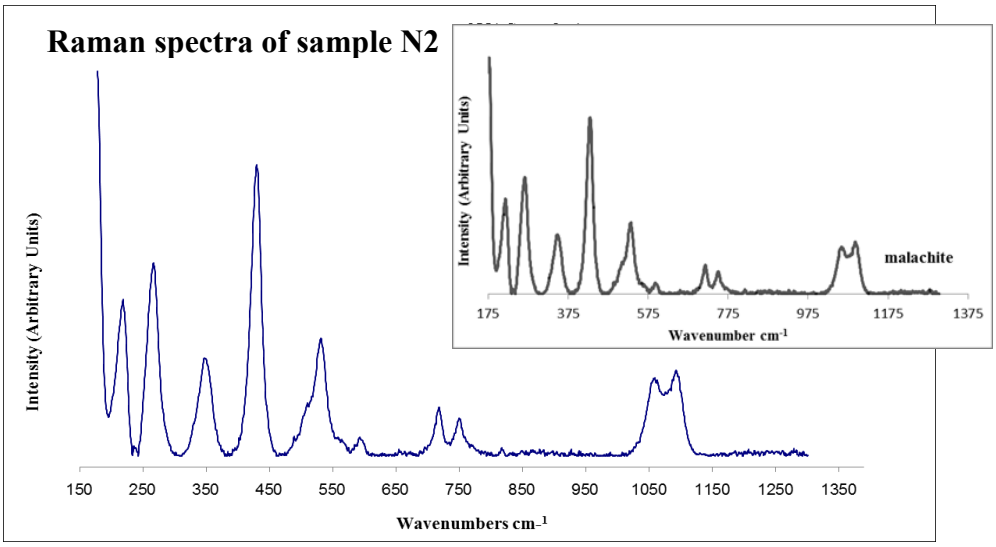

Fig. 114 Raman spectrum of the green crystal in N2 sample and a *Malachite* reference (Del Farra, 2013).

N3 sample was determined to be *Hematite*, as iron is the main element detected.

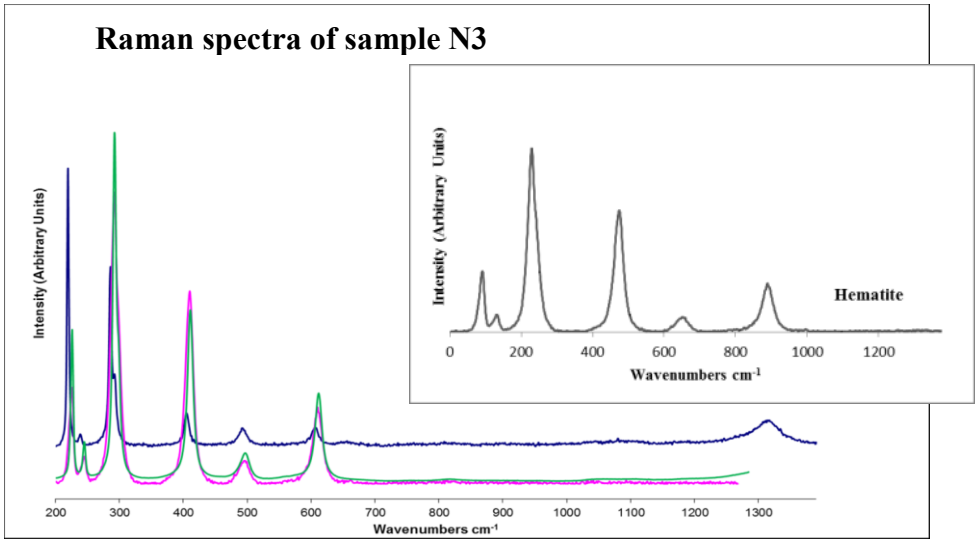

Fig. 115 Spectra of the three red crystal of sample N3 and reference compound (*Hematite*) (Del Farra, 2013).

Conclusions

Despite the small size of the samples and the consequent difficulty in carrying out the investigation, XRF analysis allowed to identify the pigments.

For all samples, the presence of calcium and strontium is due to the plaster, that is, the support of the painting.

For green parts, both *green earth* and *Malachite* were used, while on the red area *Hematite* was detected.

Further Raman analysis confirmed such findings, which were subsequently supported by further investigations XRF carried out *in situ*.

2.3 Anonymous, Portrait of *Giacomo Masino*

The reuse of paintings for new artistic productions became a common practice since the sixteenth century, together with the habit of resizing the support to meet new aesthetic or functional demands. Therefore, rearranged works of art can be found, when investigating inside the paint layers by diagnostic techniques.
This is the case of a canvas of the sixteenth century, depicting a mercenary called Giacomo Masino, a half-length portrait (fig. 116).

Fig. 116 *Portrait of Giacomo Masino*. Total in diffuse light (*recto*).

From a direct observation of the painting, some details immediately appear inconsistent with the visible portrait. In correspondence of the armature, in fact, a decoration not relevant to the subject, emerges (fig. 117). In raking light it appears in relief with respect to

the paint surface (fig. 118), and through some abrasions (fig. 119), a paint layer is visible below.

Furthermore, looking at the left edge of the canvas, there is a uniform pattern of red colour, even this not attributable to the details of the present painting, but due to an underlying layer (fig. 120). The same type of pigmentation emerges in different areas of the painting, on the uniform upper background, and is visible in some lacks of the paint layer surface (fig. 121).

Fig. 117 Detail, diffuse light.

Fig. 118 Detail, raking light.

Fig. 120 Detail of the edge, diffuse light.

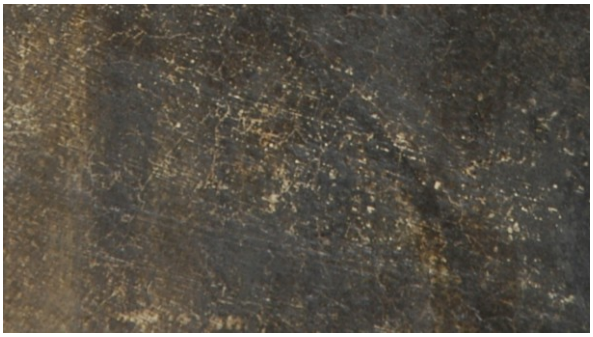

Fig. 119 Detail, diffuse light.

Fig. 121 Detail of a lacuna, raking light.

Wide band infrared reflectography

Infrared reflectography with a CCD silicon, in the spectral range 800-1100 nm (Section 4.2.4), did not disclose other details than those observed in visible light.

Instead, using the InGaAs detector (Section 4.1.1), with sensitivity in the range 1000-2500 nm, inserted into a scanner, some details were observed, not visible to the naked eye.

In fig. 122, results obtained on three different areas with the wide band scan, are shown.

The scanning revealed, below the corresponding part of the bust (fig. 122b) and of the inscription (fig. 122c), some lines, diagonally positioned with respect to the lines of the visible painting.

Analyzing the entire left side of the work of art, light backgrounds, not corresponding to the uniformity of the upper background, were highlighted. These findings insist on the red area already highlighted in the previous investigations.

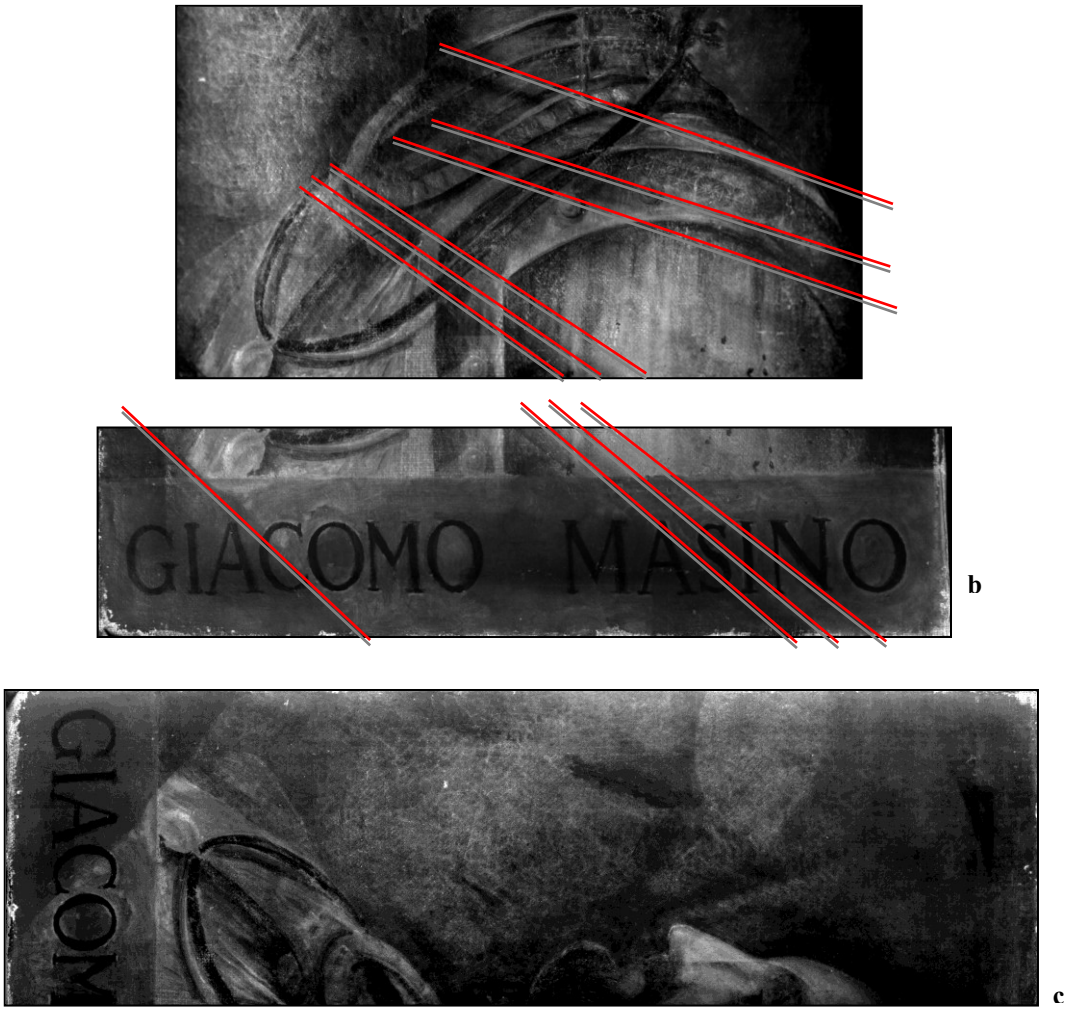

Fig. 122 A wide band IR Reflectography. The **c** detail has been rotated 90 ° to allow a better comparison with the radiography.

Radiography

Digital radiography clearly showed the presence of an underlying painting, representing a figure in a sitting position (fig. 123), and missing the face and part of the bust, for the resizing of the canvas. The investigation was carried out with a digital scanning radiographic system, described in chapter 4 (Section 4.1.2) (irradiation parameters: anode voltage of 24 kV, 2 sec exposure time).

The reduced thickness of the paint layer and the good visibility of the underlying painting in radiography, suggest the use of pigments containing elements of high atomic number, such as lead and mercury. The hypothesis of the latter element is supported by the observation of the red colour, later attributed to cinnabar.

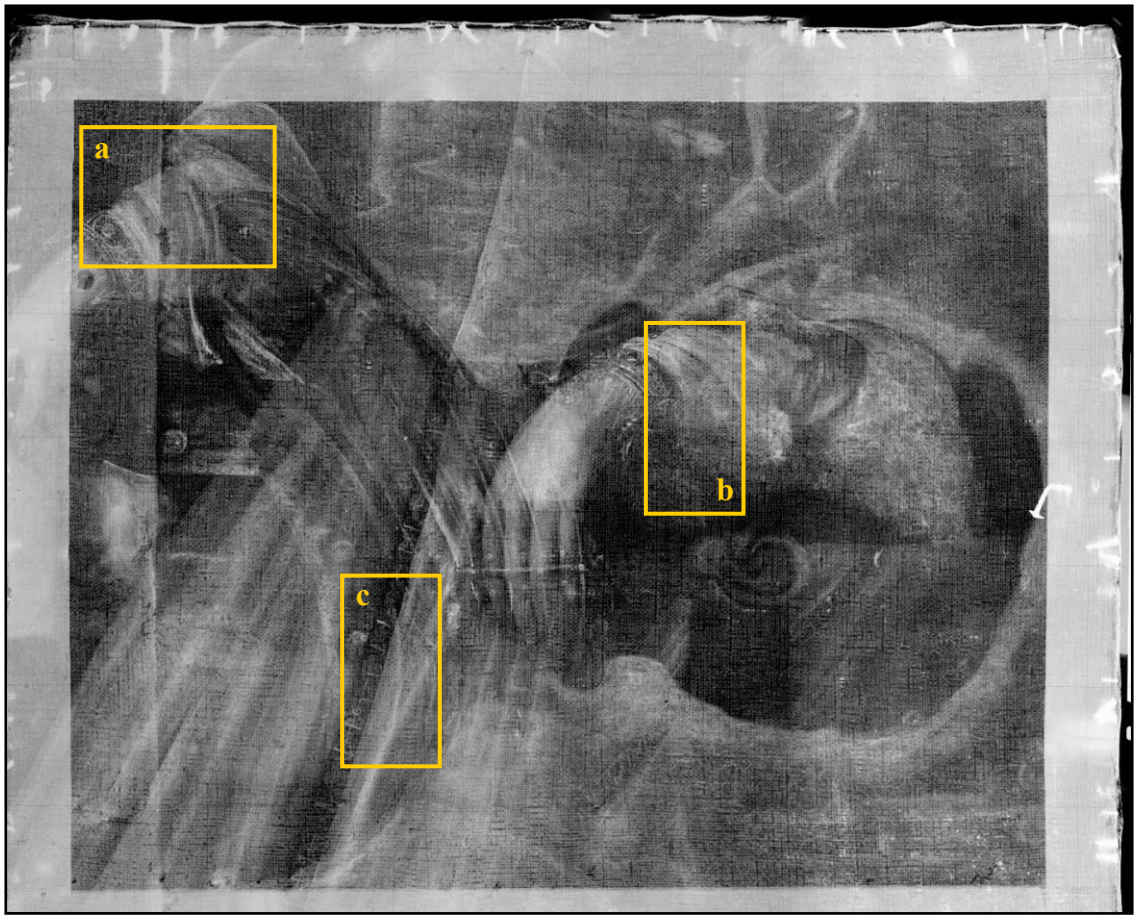

Fig. 123 Complete digital radiography of the work of art. The frames a, b and c indicate the details shown in following figures.

K-edge differential radiography

Further investigations were aimed at non invasively characterize the pigments, to obtain a clearer understanding of details, and thus to speculate about the materials used by the artist. This was possible by mapping out the elements by means of K-edge differential radiography.

Differential K-edge radiography allows, exploiting the monochromatic X-rays, to map the distribution of an element, on a painted surface. In fact, two radiographies with energies of X-rays very close, one just below and one a little above the K-edge of the element to identify, are performed. Using, then, a mathematical method to logarithmically subtract the two images, the distribution of the surface density of the element under investigation, is obtained. A brief description of the K-edge instrumentation is provided in Chapter 4 (Section 4.1.3).

In the case of the painting concerned, the mapping of lead was carried out by exploiting the L-edge at 13 keV, in three different areas of the painting surface, in correspondence with the decorations of his robe. For the irradiation, an anode voltage of 25 kV, with a current of 100 mA, and exposure of 5 sec, was used. Images obtained are shown in fig. 124.

In conventional radiographies the lead, likely associated to *White lead* ($2PbCO_3 \cdot Pb(OH)_2$), is primarily highlighted because of its high atomic number. Other effects, such as the variable density of the canvas and the different thickness of the preparation, reduce the contrast of details.

In differential images, on the contrary, radiographic contrast is only due to the presence of lead, and thus the lighter parts of the image represent larger amounts of that element. As a consequence, the best definition emerged on the embroidery, while a complete absence of details emerged on the visible painting, evidently treated with different materials.

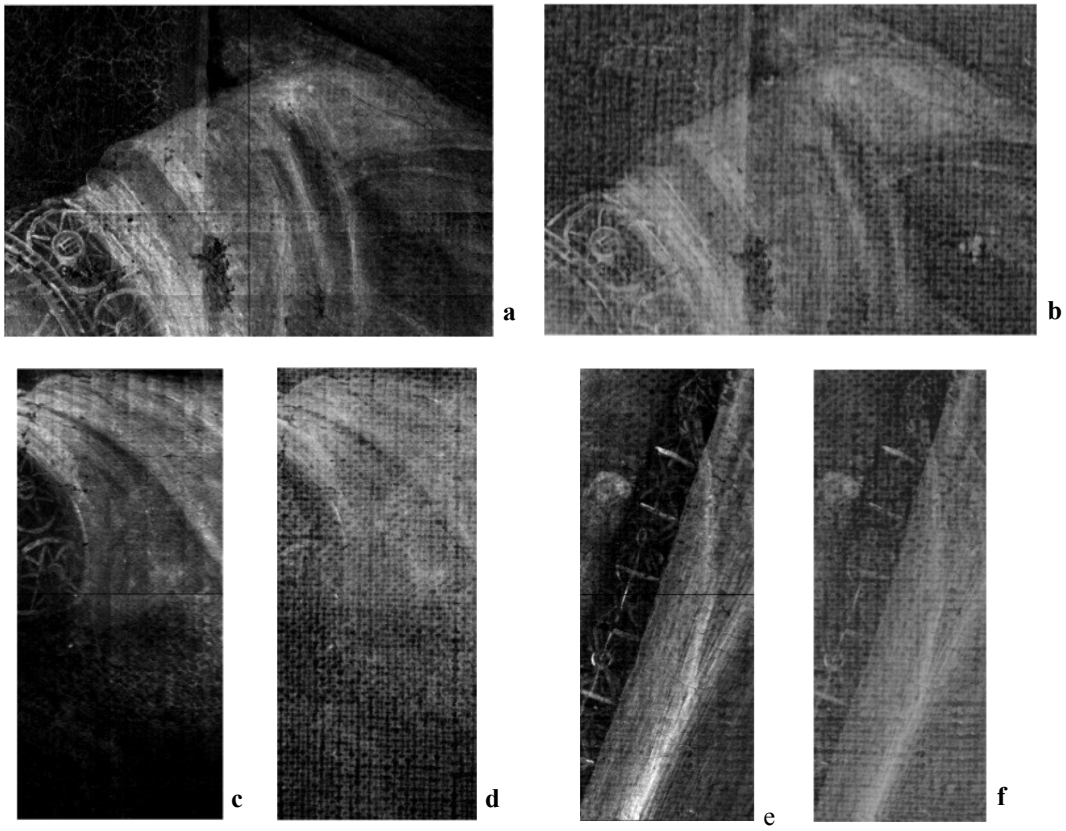

Fig. 124 Comparison between K-edge analysis (a-c-e) and digital radiography (b-d-f) of some details.

X Ray fluorescence analysis

Punctual X Ray fluorescence technique later confirmed and deepened the hypotheses about the constituent materials of the pictorial film.

White Lead was mapped in various details of the original painting, as well as mercury, due to the *Cinnabar* used for the dress. The integration of image diagnostics with the XRF analysis provided an overall knowledge, which is compatible with the first art-historical evaluation of the original painting.

X Ray fluorescence analysis, performed on 24 points (fig. 125), revealed elements with Z> 19, which compose the paint layers. This allowed to advance some hypotheses about the pigments used, both for the portrait of the commander, and for the painting below. In addition, three points on the back of the canvas: points 25 and 26 in correspondence of points the 8 and 11 points, and point 27, were analyzed.

The analysis was carried out using a Bruker Artax instrument 200, with molybdenum anode, and exposure parameters 30 kV, 1.3 mA and 120 sec.

On all points investigated, with the exception of points 17 and 19, traces of zinc were found, and the most intense signals of that element were revealed at the dedicatory zone,

on the bottom of the painting (points 1, 3-13). The analysis of the corresponding points to this area and, simultaneously, to part of the robe of the figure below, revealed a large amount of zinc and lead (point 8), this latter already mapped with K-edge differential radiography (fig. 126). The analysis of the spectra acquired at the back, on points 25 and 26 (in correspondence of points the points 8 and 11 on the front), revealed zinc and lead. Here, the lower counts are caused by the absorption of X-rays from preparatory layers (points 8 and 25) (fig. 127). Also, on the back, the ratio of counts Zn/Pb is inverted with respect to the front. For these observations, the presence of zinc in the paint layer surface was hypothesized.

On red areas of the superficial paint layer (points 18 and 19), the elements associable to red pigments are iron and mercury. On these points, the signal of the mercury is, however, much lower than that detected in the *lacuna*, in correspondence with the mantle of the figure below. The combination of these considerations would lead, on the one hand to identify the cinnabar as a pigment characterizing the mantle, on the other hand to doubt the presence of this material in the red backgrounds of the surface layer. Consequently, the red parts of the second portrait, could have been obtained with a red ocher (Fe_2O_3).

Points 21 and 22 are acquired on white brush strokes, but correspond to different parts of the figure below. Both are characterized by a strong presence of lead, attributable to lead white, while zinc is present only in low amounts. The absence of mercury on point 21 allows to assume that this part of the dress was not realized with cinnabar.

On all investigated points, the presence of calcium, probably related to a preparation or *imprimitura* based on gypsum or calcite, was found. Weak fluorescence lines of strontium, found on many of the acquired spectra, could be considered associated to calcium, as an impurity (Albertin, 2012 (c)).

Fig. 125 Measuring points analyzed by XRF.

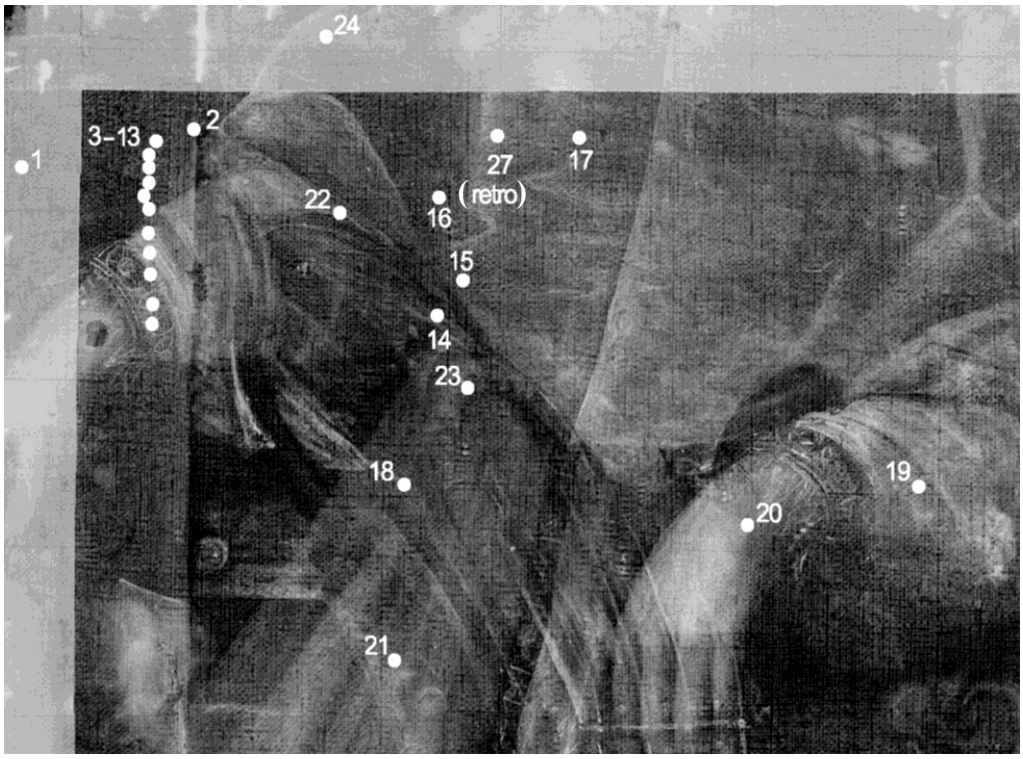

Fig. 126 Measuring points analyzed by XRF, indicated on the radiography.

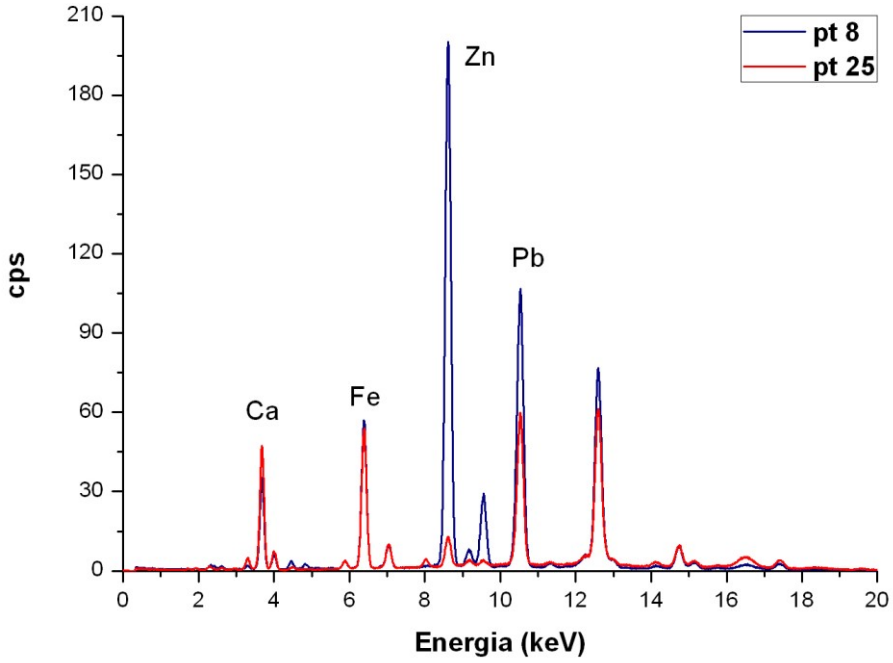

Fig. 127 XRF spectra of the measure points 8 and 25, corresponding on the *recto* and on the *verso*.

Conclusions

The case just presented, is a very interesting example of re-use of a support. Radiography played here a crucial role in the recognition of another character below the visible pictorial film. Whose identity remains, however, unknown, due to the lack of the upper portion of the (original) painting. Punctual XRF investigations carried out on the painting, subsequently allowed to try to locate the hypothesized pigments.

2.4 Desco da parto

Image and punctual investigations also involved a *desco da parto* (figs. 128, 129). This peculiar object was mainly used in the fifteenth century, acting as a tray to bring food and drink on to new mothers.

Fig. 128 *Desco da parto*. Total in diffuse light (*recto*).

Fig. 129 *Desco da parto*. Total in diffuse light (*verso*).

The iconography depicted, *Vulcano* forging the wings of *Cupido* and a dressed *Venere* with a lance in her hand, is compatible with the late fifteenth century.
On this object, integrated physical and chemical investigations allowed to further deepen the artistic and historical knowledge, arising some doubts about the dating of the art.
Image diagnostics mainly added information about materials and conservative state of the work of art. X-ray radiography, for example, provided data on the wooden support, important to protect and preserve the artwork.
SEM analysis, carried out in an external restoration laboratory, was supportive and helpful in suggesting areas to be investigated with X Ray fluorescence, that subsequently allowed to characterize the constituent materials of the pictorial layer, particularly on areas not affected by the sampling (Farioli, 2012).

A first UV fluorescence inspection, showed a substantial homogeneity of the table, indicative of the presence of a superficial varnish film. In addition, the pictorial layer appeared to be quite homogeneous (fig. 130).

Infrared investigation (fig. 131) showed, underneath, an indecision regarding the foot of the female figure (fig. 132), that presented uncertain lines, probably due to the study of its position. In correspondence with the hunting scene, no preparatory drawing underlying was detected, thus suggesting a direct application of colours. Instead, in correspondence with the city and the walls, well defined in their geometry, the preparatory drawing showed changes in the height of the central towers, which was originally greater and with a different shape, than in the final version (fig. 133, 134). On the back of the *desco*, a decoration was also well highlighted by means of infrared investigation, that is, a circular pattern repeating four inscribed circles, with a stylized floral design (fig. 135).
Nonetheless, the best delineated area on the entire painting, appeared to be in correspondence with the figure of *Vulcano*, where the design of the head and clothes was evident (fig. 136).

The painting was thus radiographed, in order to better investigate its internal structure. In the radiographic image, light areas indicated a higher absorption of the radiation from the material. White areas along the edge of the frame precisely localized the position of original nails, while a vertical fracture through the entire painting revealed, on some parts, the texture of an interposed canvas (*incamottatura*). On all the support, numerous tunnels and holes, filled, or not, produced by xylophages insects, were clearly evident.

Furthermore, in the radiographic image, colour falls appeared as dark areas, well defined in outlines (fig. 137). Nonetheless, the missing feedback of such evidences in the visible image, suggested that they were retouched with lower atomic number materials, which differently respond to radiographic examination.

Fig. 130 Ultraviolet fluorescence of the materials on the surface of the *desco*.
A homogeneous situation can be noticed.

Fig. 131 Total in infrared reflectograhy, *recto*.

Fig. 132 Detail of the *pentimento* on the *Venus*' foot.

Fig. 133 Detail of the towers, on the background, in diffuse light.

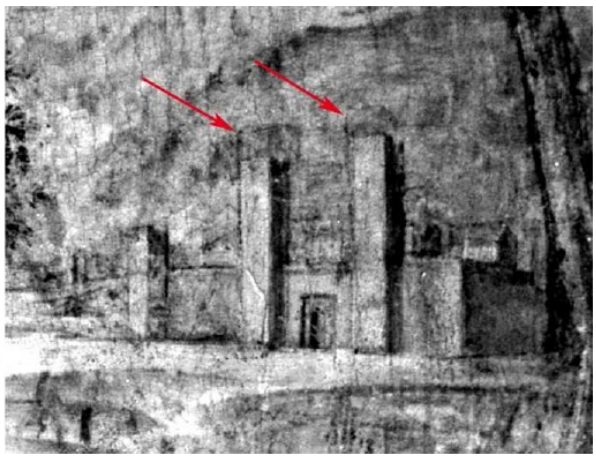

Fig. 134 The same detail of the towers, in infrared reflectography.

Fig. 135 Scaled image of the total, in infrared reflectography, and enlarged detail, emphasizing a stylized floral design.

Fig. 136 *Vucano* forging the wings of *Cupid*o, detail in infrared reflectography.
The lines defining the character are already well delneated in the preparatory drawing.

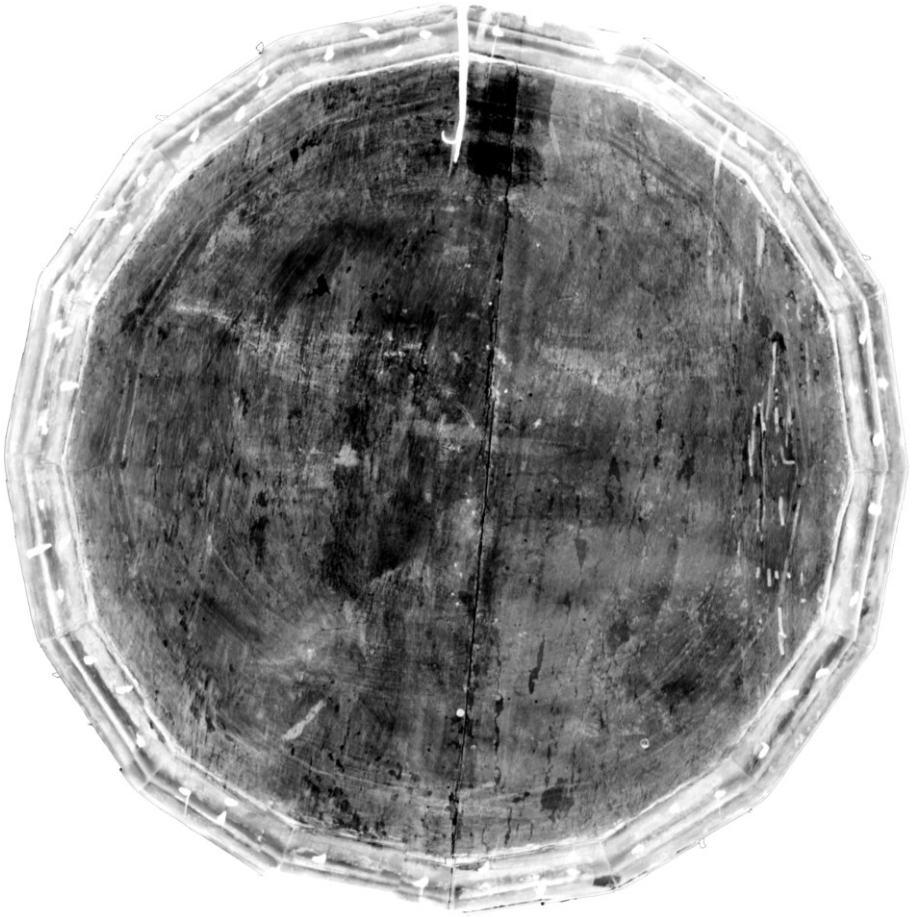

Fig. 137 Digital radiography of the entire painting.
Nails along the frame and holes produced by xylophages insects are shown.
Colour falls appear as dark areas, well defined in outlines.

From XRF analysis performed on the painting, high quantities of lead were found in each investigated area, as well as on the back of the painting. Counts were also pretty high for strontium, which could result from a preparation based on gypsum.

The presence of iron was almost constant in all the investigated points and, on the external golden frame, is due to the *bolo* preparation for gilding. In correspondence with the polygonal frame, a certain presence of gold was detected, together with copper and zinc, and probably caused by the layer of brass leaf, as an imitation of gold.

It is also interesting to focus on some areas on the sky. On point 4, as an example, copper was detected, suggesting the presence of azurite. Point 5 instead, characterized by a different blue, appeared likely attributable to be a retouch, because of the large amount of zinc and cobalt attributable to a blue cobalt-based, mixed with a zinc white. Both of them are modern pigments, as well as those found on other zones. As a matter of fact, while on the yellow point 2, corresponding to the painted frame, a large amount of arsenic was detected (compatible with ancient pigment such as *Realgar*), significant quantities of zinc characterized, instead, a point located on the hair of the female figure. Similarly, on point 3, a dark red, the presence of mercury was detected. This is attributable to *Cinnabar* (natural), or *Vermilion* (artificial), possibly mixed with *ocher* or *earth* (for the strong presence of iron). On other red points (18 and 19) a suspicious, additional presence of zinc, together with iron and mercury, was found. On brown point 9, localized on a rock, the iron responsible for the brown colour is accompanied by a substantial amount of copper, zinc, and chromium. The last two elements, in particular, must probably be related to modern pigments.

Overall, such findings confirmed the hypothesis of the coexistence of old, well established in use, and recent pigments (figs. 138-140).

Fig. 138 The *desco*, while performing XRF analysis.

Fig. 139 Measuring points analyzed by XRF (I recognition).

Fig. 140a Map of the modern pigments found on the surface by means of XRF analysis (I recognition).

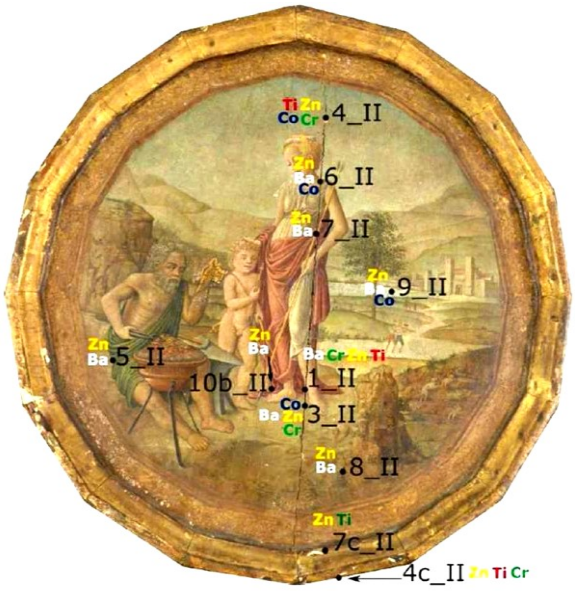

Fig. 140b Map of the modern pigments found on the surface by means of XRF analysis (II recognition).

Conclusions

Just comparing the different data obtained, an anachronism in the pigments on the *desco* was highlighted. Particularly, by integrating observations arising from both the iconographic and the scientific approach (characterization of materials), some conclusions were reached: the preparation was made of *gypsum* and glue, which is compatible with an old preparation. On the contrary, the paint film is not always consistent with a fifteenth century's palette, suggesting a remake or, at least, a rearrangement of an ancient work on an ancient preparation.

2.5 Artworks on paper (XVII century)

Further investigations also involved works on a different kind of support: is this the case of two artworks on paper.
Both of them, coming from a private collection, were attributed to Adrien Van Ostade, a Dutch painter who lived between 1610 and 1685.

The first item, entitled *The country fair*, is a laid paper glued on cardboard (fig. 141).

Fig. 141 *The country fair*, size 227 x 178 mm.

The work of art appears squared in red, perhaps with a colored pencil. It seems to be inspired by a print reproducing the painting *The country fair*, by the same A. Van Ostade (fig. 142). As of this print, the work examined reproduces a part, the question was whether this could be a pen drawing, or if it could be another print, used for the realization of the model.

Fig. 142 *The country fair*, Reproduction of the painting "The country fair" by A.Van Ostade. Etching, second half of the seventeenth century. Size: 347x 243 mm. Location: Pinacoteca Repossi, Chiari (Brescia).

According to the perfect, specular superimposition of the artwork to part of the print image from Brescia, it is possible to infer that the author owned the original, or a copy.

The microphotography in raking light, highlights the thickness of the ink stroke, which appears uniform, even at intersections. The red color of the squaring is superimposed to the fibers of the paper and to the ink (figs. 143, 144).

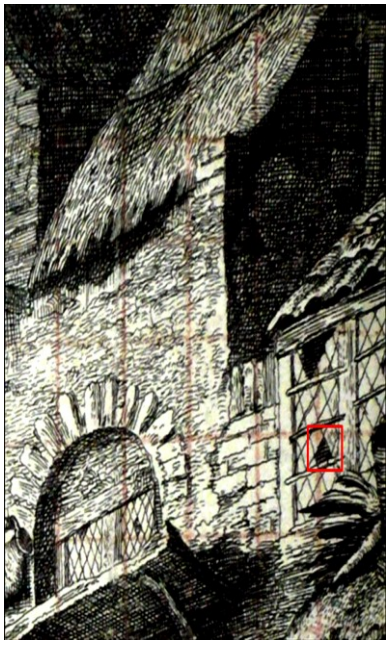

Fig. 143 Part of the print, with detail of window in the frame.

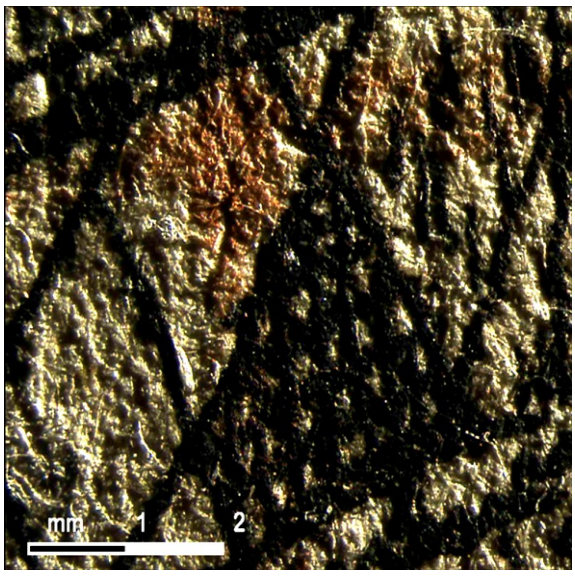

Fig 144 Detail of figure 143, enlarged under the microscope.

The second artwork, signed at the bottom, left: "*Van Ostade inc et pinxit*", represents an indoor environment (fig. 145). The subject is taken from a model by A. Van Ostade, and the support is a thin laid paper.

In this case, the question was whether it was a pen drawing or an engraving.

Fig. 145 *Indoor environment*, size 207 x 160 mm.

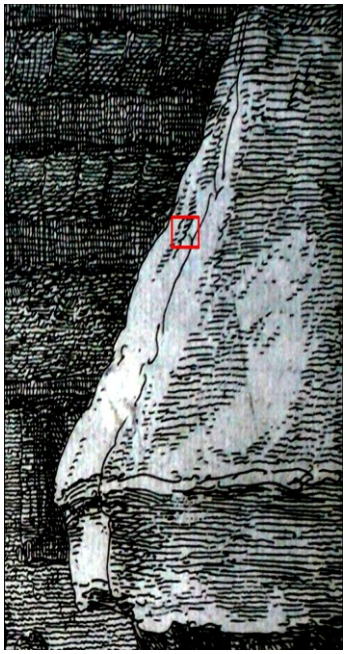

Fig. 146 Part of the print, with detail of window in the frame.

Fig 147 Detail of figure 146, enlarged under the microscope.

Macrophotographs at the microscope (figs. 146, 147), were taken by illuminating the surface in raking light. The thickness of the ink stroke, conducted with great fluidity, was this way highlighted.
Furthermore, the doubling of the thickness, where strokes overlap, can be noticed while, in the straight sections, the fibers appear covered by ink.

For a better understanding of both nature and executive technique of both works, the observations made at the microscope were further supplemented with appropriate considerations of a specialist.
Tests carried out by the restorer F. Antolini on the edges of both artworks, on different points, showed the presence of oil-based ink.
Such a finding makes it difficult to think about a pen drawing, also for the thinness of the lines. In all likelihood, the two objects are prints, also due to the agility of the strokes.
Moreover, the presence of squaring lines in the first case, with an oily and no removable pigment, suggests a model, while, in the second case, the good paper quality leads back to a precious copy.

2.6 Characterization of polychrome ceramics from Iranian artworks (XVII century)

In the framework of a PhD thesis (Holakooei, 2013), spectroscopic approaches were adopted to investigate on seventeenth century polychrome overglaze *half rang* tiles, originating from Iran (fig. 148). The combination of techniques used, made it possible to identify some technical and compositional features of the *half rang* technique.

The objects of spectroscopic investigations were *haft rang* tiles, comprising of different parts, from the bottom to the top of the tile: a body, a white substrate glaze, and the upper layer with the coloured glazes. Black line, finally, acts by separating the different coloured glazes.

Different techniques were used to their characterization: besides ultraviolet-visible (UV-VIS) spectroscopy, performed at Archaeometry laboratory, also X Ray fluorescence, energy dispersive X-Ray spectroscopy and micro-Raman spectroscopy were exploited.

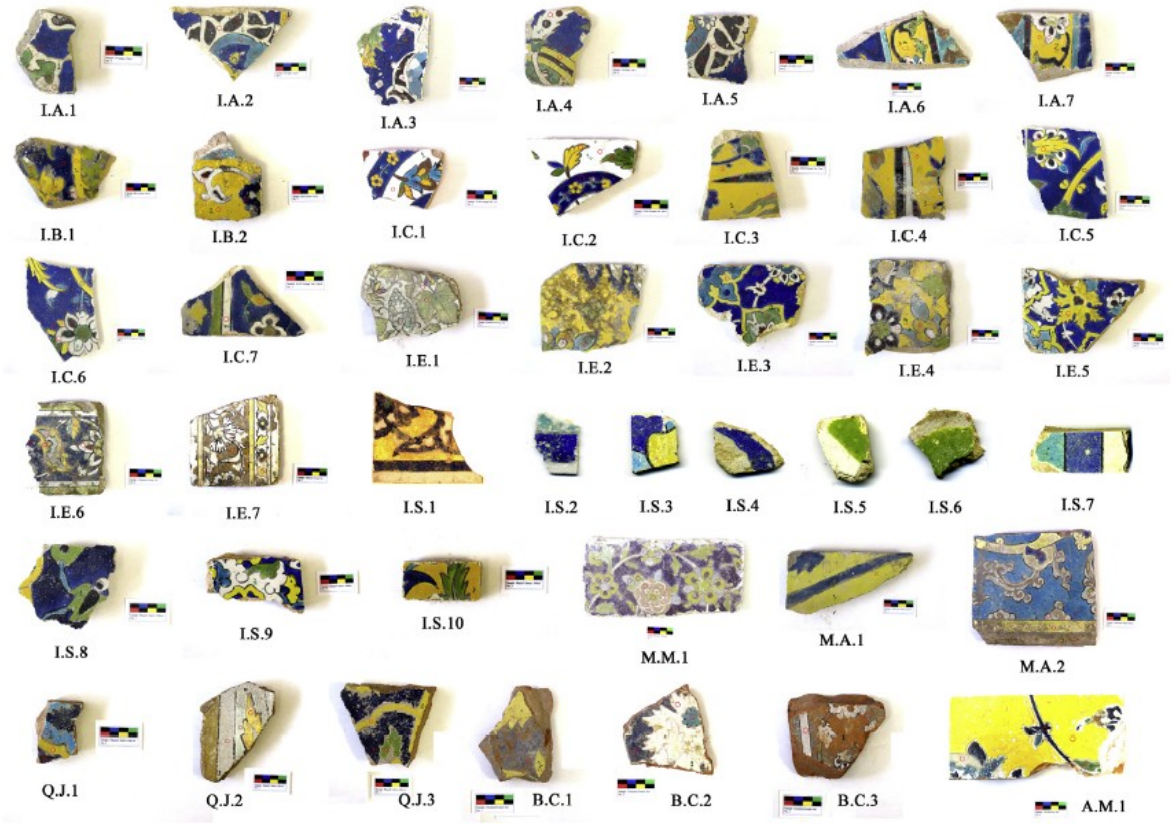

Fig. 148 Pictures showing the forty three investigated *haft rang* samples (with labels) (Holakooei, 2014).

In this context, spectrophotometric and colorimetric measurements were performed with the only aim of characterizing the investigated samples.

The forty three fragments, investigated by means of UV-VIS spectroscopy, were collected from nine different Iranian sites. Coloured glazes applied on the tiles consist of white, yellow, brown, black, green, blue, turquoise and violet hues.

More than 460 *diffuse* and *total* reflectance measurements on surfaces of the coloured glazes were acquired in the range 360–740 nm, using a Konica Minolta spectrophotometer CM-2600-d equipped with a *barium sulphate* integrating sphere with a d/8° configuration (Chapter 4).

Colour coordinates, univocally describing a color according to its attributes of *hue*, *lightness* and *saturation*, in a numerical form, were plotted in the CIE*L*a*b** colour system, with reference to the illuminant D65, while spectroscopic data were processed with the SpectraMagicNX software.

To have an overall idea about the chemical composition of the glazes, a principal component analysis (PCA) biplot of the samples for Na_2O, MgO, Al_2O_3, SiO_2, K_2O, CaO, and PbO variables was plotted, based on the EDS results (fig. 150).

PCA revealed itself as a suitable statistical approach to interpret the dataset (Armanino, 2011). As shown in fig. 149, blue, turquoise, violet, and white glazes were found to be alkali glazes, due to the relatively high alkali content (K_2O and Na_2O). On the contrary, brown, yellow, and green glazes are high-lead glazes, due to the high lead content in their glassy matrix.

A glassy matrix cannot be deduced, instead, for black lines, due to their behaviour. (Holakooei, 2014).

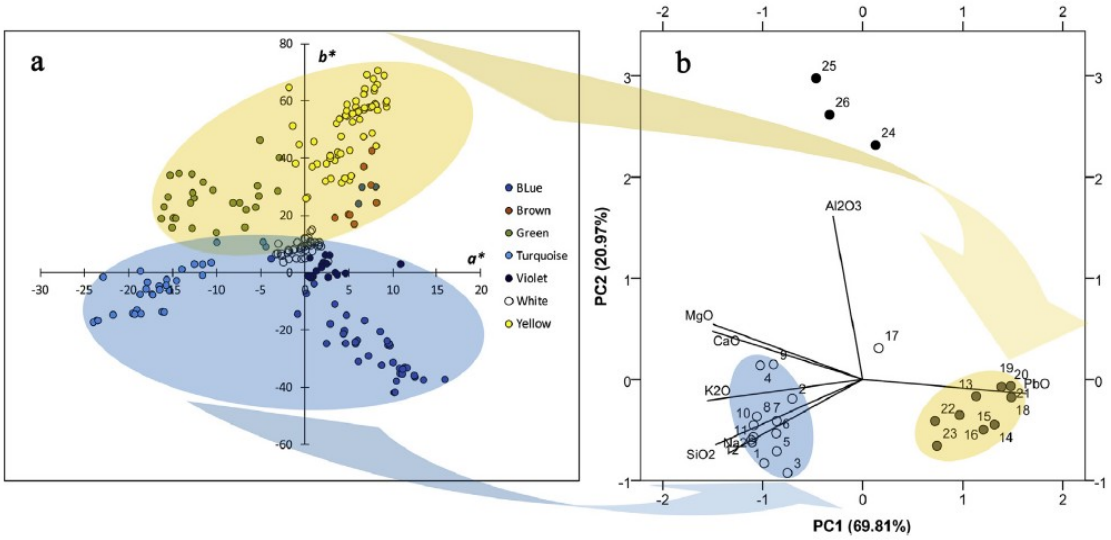

Fig. 149 (a) Projection of a* and b* values of the coloured glazes (Specular Component Excluded), on CIEL*a*b colour plane; **(b)** PCA biplot of the first two Principal Components resulted from EDS data (Holakooei, 2014).

n.	Glaze	Label	Na_2O	MgO	Al_2O_3	SiO_2	K_2O	CaO	Fe_2O_3	MnO	CoO	PbO	CuO	SnO_2	ZnO	PbO/SnO_2	Na_2O/K_2O	Maturing T (°C)[a]
1	Blue	I.C.5	18.6	1.9	1.7	65.9	4.7	4.2	2.1	n.d.[b]	0.2	0.7	n.d.	n.d.	n.d.	n.c.[c]	4.0	770
2	Blue	I.E.5	6.1	1.4	3.6	66.6	4.7	5.0	4.2	n.d.	0.8	6.3	1.4	n.d.	n.d.	n.c.	1.3	942
3	Blue	I.S.8	12.6	1.2	4.2	58.8	12.0	3.6	3.9	n.d.	0.4	3.4	n.d.	n.d.	n.d.	n.c.	1.0	787
4	Turquoise	I.A.2	15.0	2.1	7.2	54.4	4.1	6.5	2.4	n.d.	n.d.	5.4	3.0	n.d.	n.d.	n.c.	3.7	819
5	Turquoise	I.A.3	17.7	1.5	4.8	47.3	5.1	4.5	2.3	n.d.	n.d.	8.6	2.7	5.6	n.d.	1.5	3.4	708
6	Turquoise	I.A.7	20.9	3.5	4.2	52.3	3.2	3.5	n.d.	n.d.	n.d.	11.5	0.8	n.d.	n.d.	n.c.	6.5	637
7	Violet	I.A.3	15.1	1.4	3.9	46.1	5.4	4.9	1.6	2.2	n.d.	19.2	n.d.	n.d.	n.d.	n.c.	2.8	613
8	Violet	I.C.3	8.5	2.3	2.8	63.1	6.6	6.4	1.7	3.9	n.d.	4.6	n.d.	n.d.	n.d.	n.c.	1.3	888
9	Violet	I.E.5	15.4	1.6	5.9	44.0	4.9	5.2	1.3	2.2	n.d.	19.4	n.d.	n.d.	n.d.	n.c.	3.2	615
10	White	A.M.1	16.8	2.3	4.9	53.6	4.6	5.3	n.d.	n.d.	n.d.	9.7	n.d.	2.8	n.d.	3.5	3.6	843
11	White	I.C.2	11.7	2.1	2.8	57.4	6.1	6.0	2.1	n.d.	n.d.	7.9	n.d.	3.9	n.d.	2.0	1.9	902
12	White	I.C.7	11.9	1.9	3.6	51.4	8.2	4.9	0.8	n.d.	n.d.	9.3	n.d.	7.9	n.d.	1.2	1.5	844
13	Brown	I.A.7	4.8	1.0	3.0	28.6	2.1	1.9	1.2	0.4	n.d.	46.5	n.d.	10.4	n.d.	4.4	2.3	616
14	Brown	I.C.1	5.3	0.7	2.2	34.4	1.1	0.9	1.2	0.7	n.d.	44.4	n.d.	9.1	n.d.	4.9	4.9	627
15	Brown	I.E.2	6.2	0.4	2.1	33.4	2.0	1.8	1.0	n.d.	n.d.	46.3	n.d.	6.9	n.d.	6.7	3.0	545
16	Brown	I.E.4	2.9	0.7	3.6	35.2	3.5	2.0	1.5	0.2	n.d.	41.4	n.d.	7.3	1.7	5.7	0.8	664
17	Brown	M.A.2	7.8	1.6	6.7	34.3	3.4	2.5	5.3	n.d.	n.d.	38.5	n.d.	n.d.	n.d.	n.c.	2.3	547
18	Green	I.A.4	2.4	0.5	2.0	30.4	0.3	1.4	1.6	n.d.	n.d.	44.6	1.0	15.0	0.7	3.0	7.2	755
19	Green	I.A.7	3.8	0.4	2.4	29.0	1.5	2.2	2.7	n.d.	n.d.	49.5	0.5	7.4	0.6	6.7	2.5	551
20	Green	I.C.2	3.7	0.5	2.2	25.8	0.3	2.5	1.4	n.d.	n.d.	54.2	1.5	6.8	1.2	7.9	12.0	497
21	Yellow	I.C.6	3.8	0.5	3.8	29.8	1.3	1.1	n.d.	n.d.	n.d.	50.8	n.d.	9.0	n.d.	5.6	3.1	585
22	Yellow	I.C.7	2.2	0.8	3.1	40.9	2.1	1.9	1.8	n.d.	n.d.	37.0	n.d.	10.1	n.d.	3.7	1.1	783
23	Yellow	I.S.9	8.4	0.6	2.8	35.4	1.9	3.0	n.d.	n.d.	n.d.	40.1	n.d.	7.7	n.d.	5.2	4.5	596
24	Black line	I.A.4	1.4	1.8	7.7	33.3	2.5	7.4	9.9	1.8	n.d.	33.2	1.0	n.d.	n.d.	n.c.	0.6	1168
25	Black line	I.C.4	3.6	3.1	16.8	35.6	4.0	11.7	6.8	11.5	n.d.	7.1	n.d.	n.d.	n.d.	n.c.	0.9	1176
26	Black line	I.E.7	4.5	2.3	12.7	38.9	4.1	4.3	8.8	19.7	n.d.	4.7	n.d.	n.d.	n.d.	n.c.	1.1	1159

[a] Temperature at which 10^4 P of viscosity is achieved. Calculations based on Fluegel et al. (2006).
[b] Not detected.
[c] Not calculable.

Fig. 150 Table showing the results of EDS microanalysis on *haft rang* glazes (normalised to 100%) (Holakooei, 2014).

As a general result, that can be noticed on all glazes, the opaque appearance of fragments is confirmed by the lack of difference between total and diffuse reflectance curves, and the colorimetric parameters.

Furthermore, the presence of lead, suggested by the absorption band around 450 nm in the reflectance spectra, involved almost all the investigated samples.

Reflectance spectra will be presented below, separated according to the different hues and accompanied by some XRF spectra, to trace the elements responsible for the coloration of glazed ceramics.

White glazes

UV-Vis reflectance spectra of white glazes showed higher values in the red region, probably due to iron oxide content in the tiles bodies, while lead presence (later detected by means of XRF measurements) is also confirmed by the typical absorption in the near ultraviolet and blue region of the spectra (fig. 151a-b).

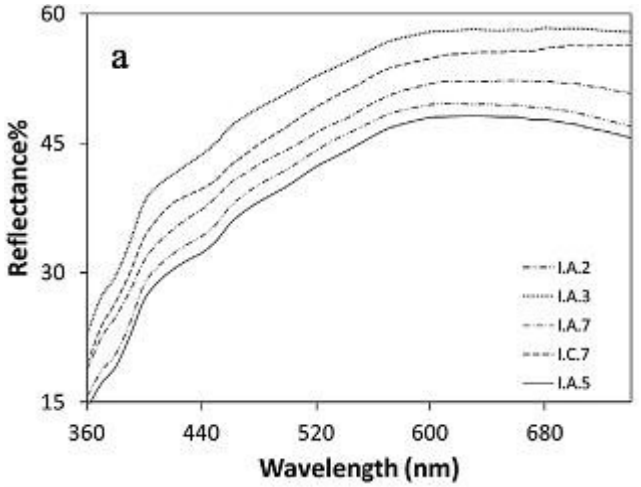

Fig. 151a UV-VIS spectra of total reflectance for five white glazes (Holakooei, 2014).

Such kind of absorption is responsible for the increasing scattering in that region of the spectra, which enhances the whiteness of the glaze.

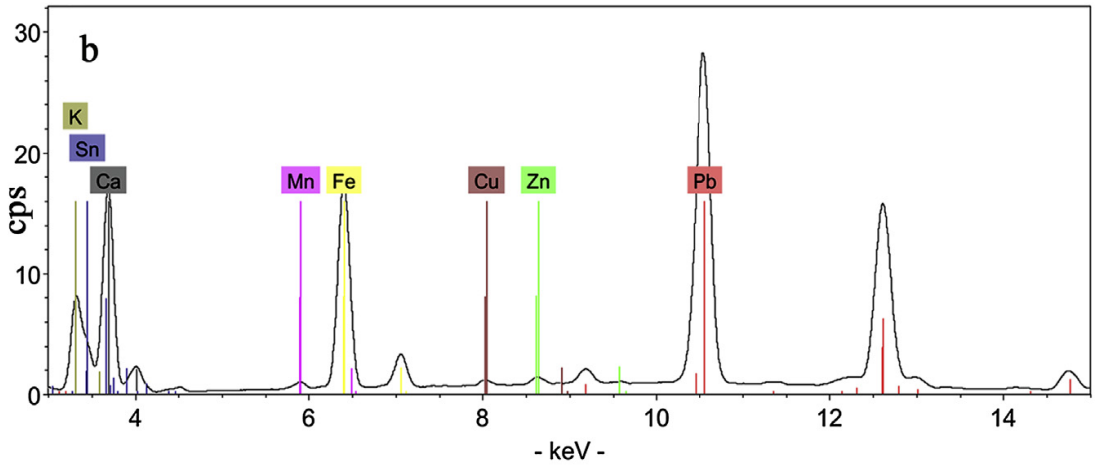

Fig. 151b XRF spectrum of the I.C.2 white substrate (Holakooei, 2014).

Yellow glazes

According to the XRF results, yellow glazes contained Pb, Ca, Sn, and traces of Fe (fig. 152a-b), whose quantity was measured with EDS. In the UV-Vis spectrum, an absorption at wavelength lower than 450 nm confirms the presence of lead, suggesting *Lead-tin yellow type II* as pigment used.

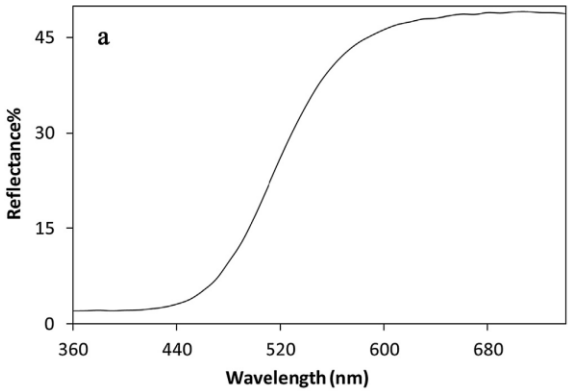

Fig. 152a UV-VIS spectra of total reflectance of the I.C.2 yellow glaze (Holakooei, 2014).

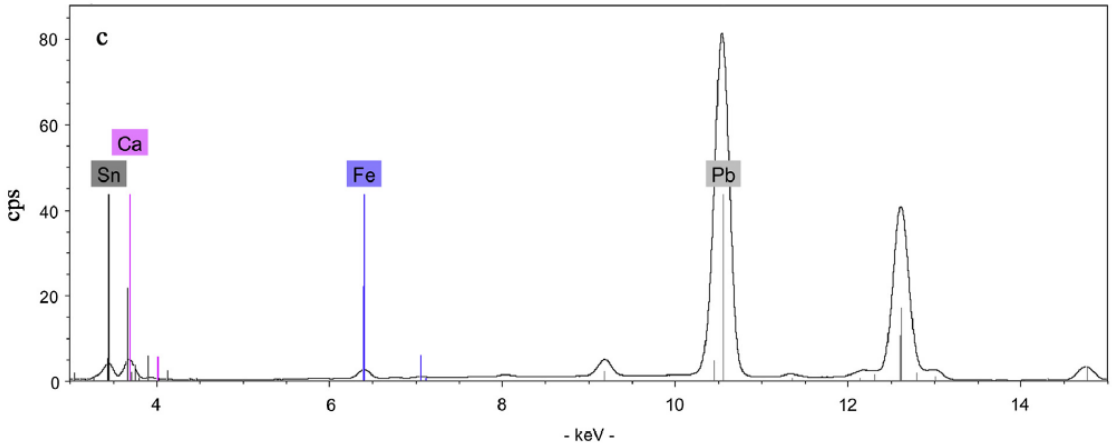

Fig. 152b XRF spectrum of the A.M.1 yellow glaze (Holakooei, 2014).

Turquoise glazes

UV-Vis spectra of turquoise glazes showed a typical trend of a copper(II) based pigment, in an octahedral symmetry (Holakooei, 2014), as indicated by the slight absorption bands at 450 and 720 nm (fig. 153a-b). Characteristic absorbance bands of a sodium silicate glass, at 450 nm (shoulder) and 720 nm, are also clearly observed. The minimum absorption for the turquoise glazes is shifted to 480 nm, probably due to the sodium content of the glazes, while a low content in lead is suggested by the absorbance in wavelengths lower than 400.

XRF spectrum shows a relative large amount of copper, followed by Pb, Ca, K, Sn, Cu, and traces of Fe in the composition of the turquoise glazes.

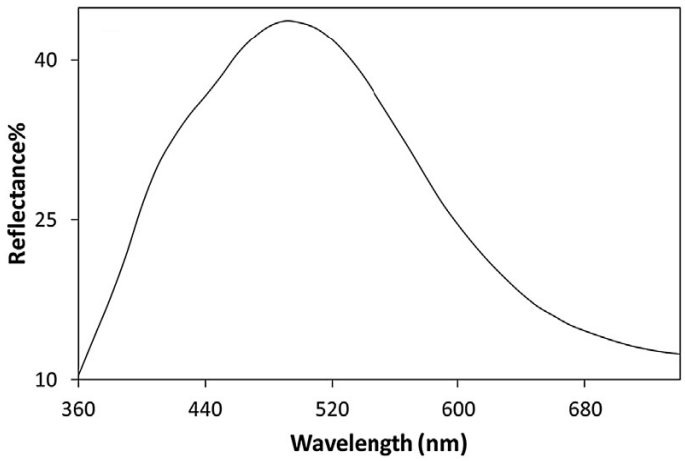

Fig. 153a UV-VIS spectra of total reflectance of the I.A.3 turquoise glaze (Holakooei, 2014).

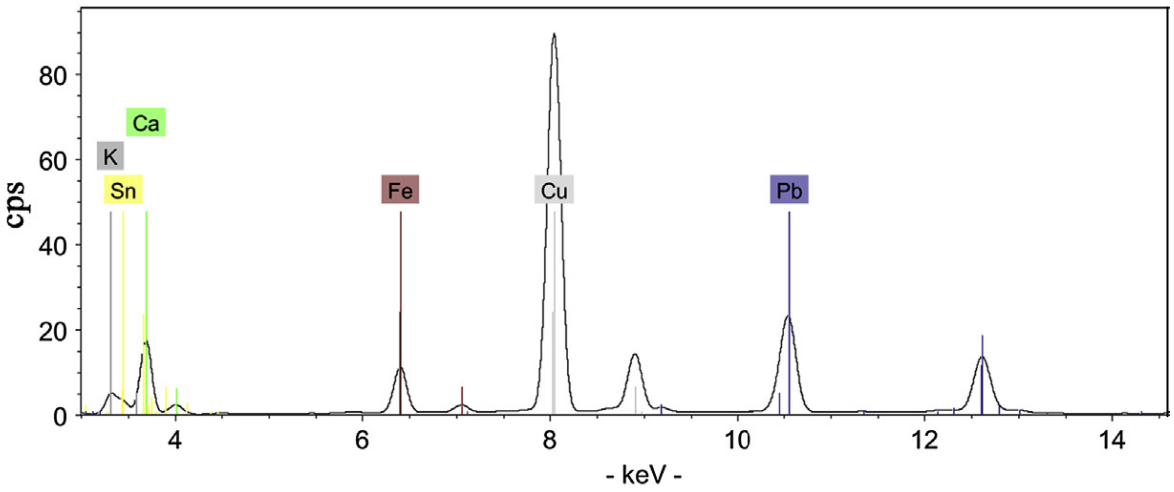

Fig. 153b XRF spectrum of the I.A.5 turquoise glaze (Holakooei, 2014).

Blue glazes

UV-Vis spectra of blue glazes show absorbance bands at 540, 590 and 650 nm, suggesting the presence of a glassy matrix in which cobalt(II), in a tetrahedral symmetry, has yielded a deep blue colour. The absorption band at 540 nm, and the weak shoulder at about 450 nm (fig. 154a-b), suggests the probable presence of a potash and soda glassy matrix. XRF spectrum of the sample also returns a certain amounts of copper, suggesting the co-presence of this element together with cobalt, possibly to confer a particular shade on the final hue.

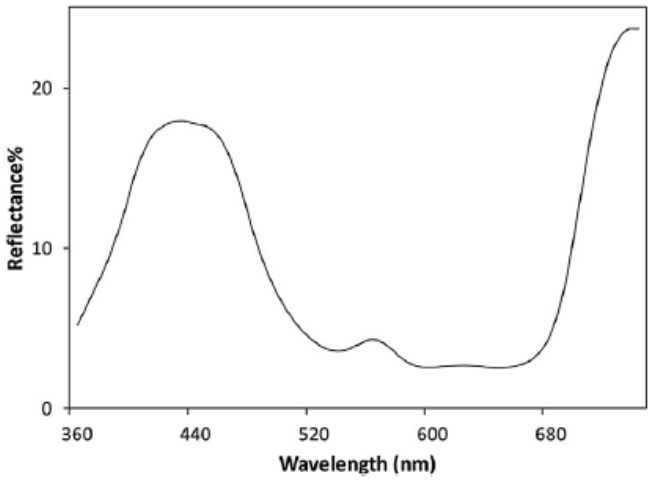

Fig. 154a UV-VIS spectra of total reflectance of the I.C.5 blue glaze (Holakooei, 2014).

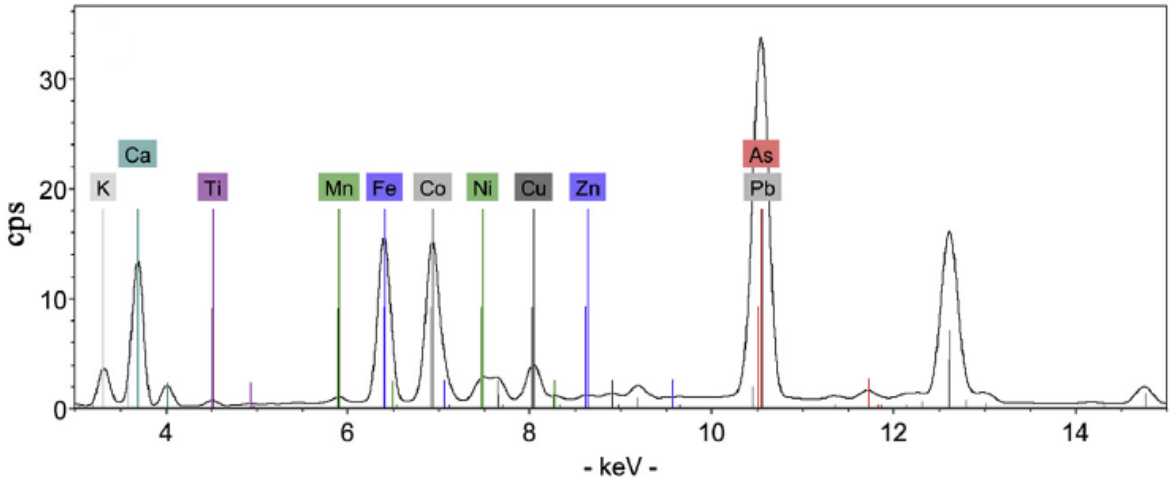

Fig. 154b XRF spectrum of the M.A.2 blue glaze (Holakooei, 2014).

Green glazes

High reflectance values characterized the spectra of green glazes at almost 550 nm while a broad absorption band is present after 720 nm. As on turquoise glazes, XRF analyses indicated the presence of copper, which could be considered as the responsible element for the green coloration of the pigment used (fig. 155a-b).

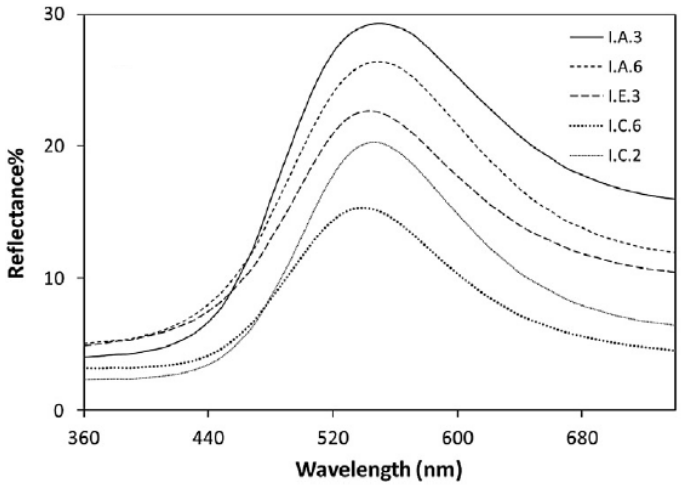

Fig. 155a UV-VIS spectra of total reflectance of five green glazes (Holakooei, 2014).

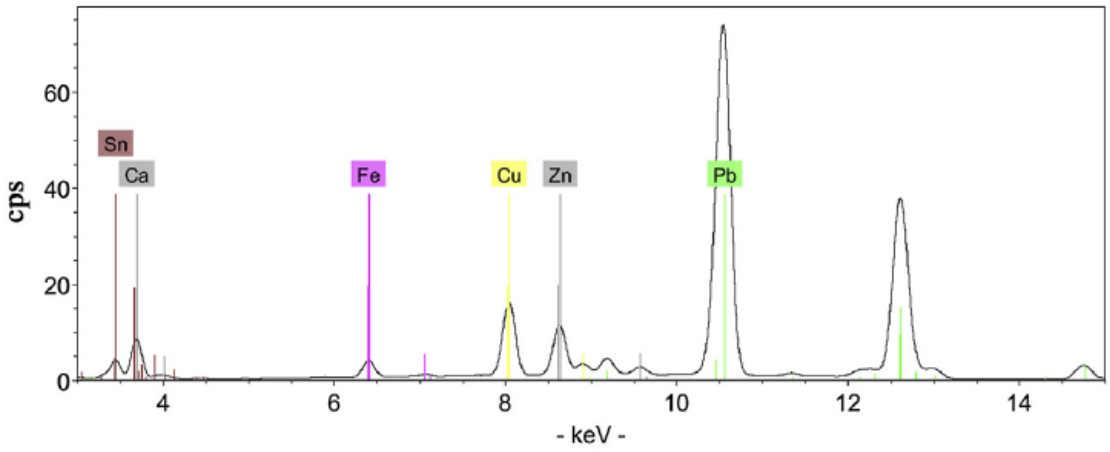

Fig. 155b XRF spectrum of the A.M.1 green glaze (Holakooei, 2014).

Violet glazes

Violets spectra present a wide band, centred at 490 nm, and a weak shoulder at about 680 nm, both of them to be related to manganese(III) ion in glaze, as a responsible for such a coloration (fig. 156a-b).

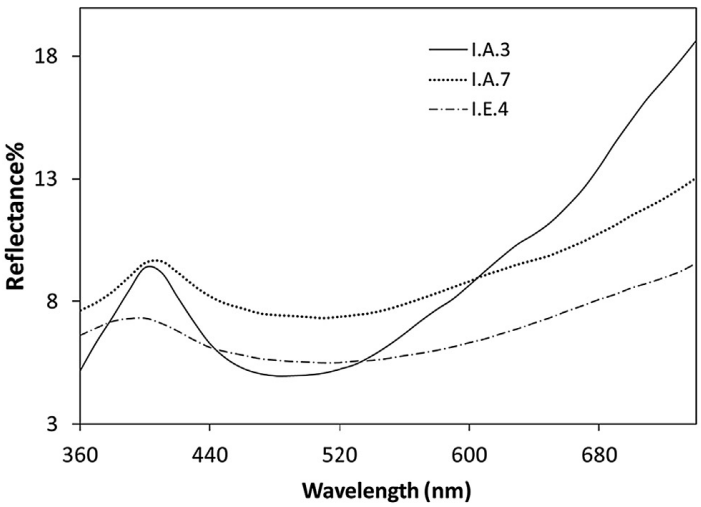

Fig. 156a UV-VIS spectra of total reflectance of three violet glazes (Holakooei, 2014).

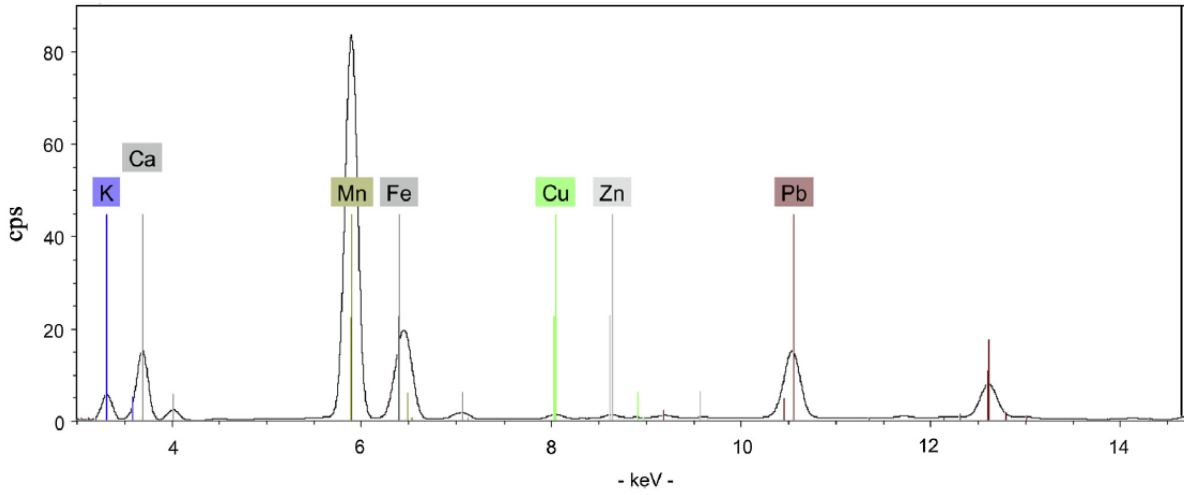

Fig. 156b XRF spectrum of the I.C.3 violet glaze (Holakooei, 2014).

Brown glazes

Brown glazes spectra resulted similar to the yellow ones, due to the absorption band at wavelengths lower than 480 nm, related to the presence of *lead*. Besides, other elements like *iron(III)* and *manganese(III)* should have yielded the brown hue. EDS results confirmed brown glazes as opacified by lead-tin yellow, where iron and manganese created a brown colour (Holakooei, 2014).

XRF spectra acquired on black lines of two samples (I.C.3 and I.E.5), finally, show the presence of iron and manganese and chromium as the responsible elements for the dark colouration (figs. 157, 158).

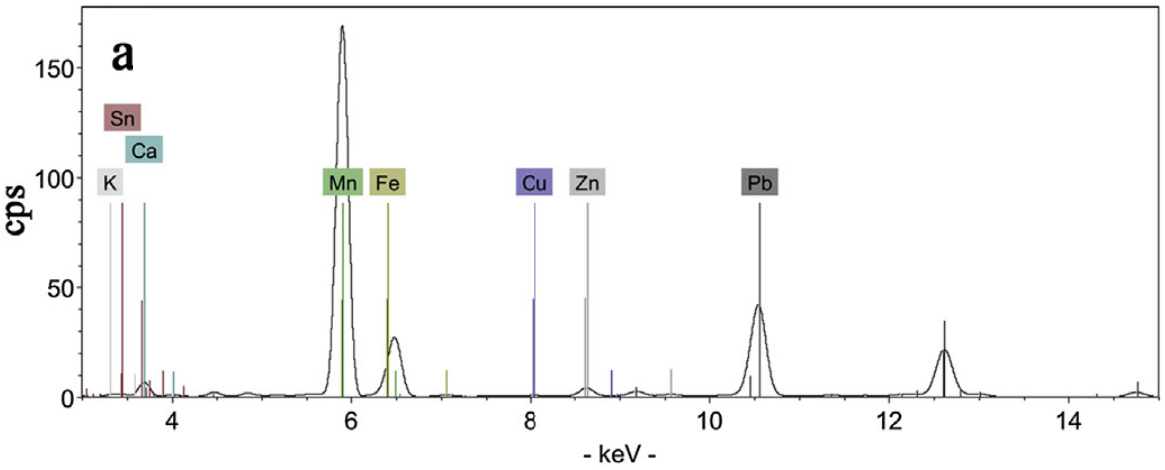

Fig. 157 XRF spectrum of the I.C.3 black line (Holakooei, 2014).

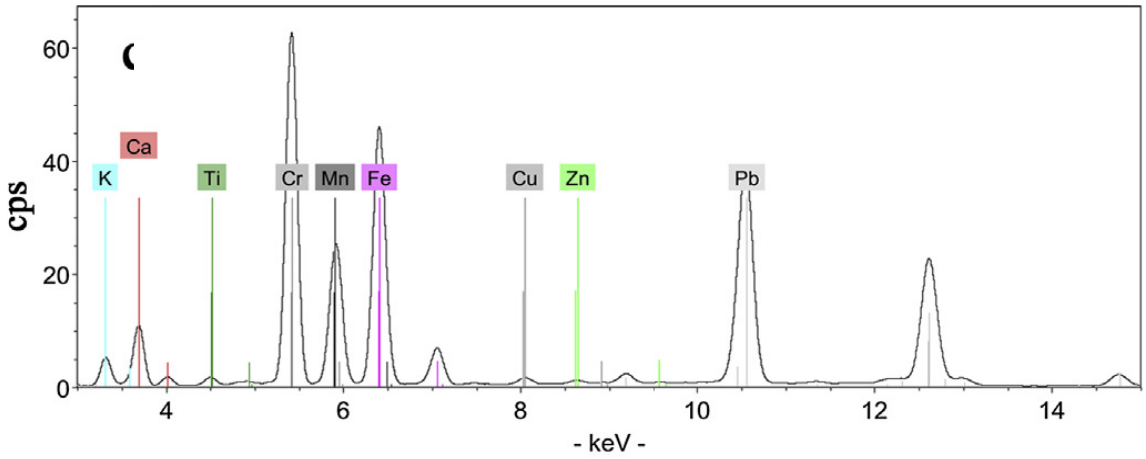

Fig. 158 I.E.5 black lines (Holakooei, 2014).

To conclude, table of fig. 159 presents a summary concerning the elements found in the coloured layers, and the estimated colouring agent for each hue.

Glaze	pXRF results	Colouring agent
White	Sn, Pb, Ca, K, (Zn, Fe, Cu, Mn)[a]	No
Yellow	Sn, Pb, Ca, (Fe)	No
Turquoise	K, Pb, Ca, Sn	Cu, (Fe)
Blue	K, As, Pb, (Ni, Zn, Ti)	Co, (Cu, Fe)
Violet	Pb, K, Ca, (Cu, Zn)	Mn, (Fe)
Brown	Sn, Pb, K, Zn, (Cr)	Fe, Mn
Green	Sn, Pb, K, Zn	Cu, (Fe)
Black lines	Ca, K, Zn, Sn, Pb, (Cr[b])	Mn, (Fe)[c]

Fig. 159 Summary of XRF analysis results, on the colouring agents of the glazes (Holakooei, 2014).

Conclusions

As a partial result of all the study on the Iranian ceramic artworks, spectrophotometric and colorimetric investigations allowed to characterize the tiles from an optical point of view. For each hue, characteristic trends in the reflectance graphs and colorimetric values were identified. XRF analysis later performed on the samples, their elemental composition was found out. The comparison with similar data, but obtained on specimens from elsewhere, was this way facilitated.

Chapter 3

Non invasive techniques for materials and artistic techniques

From the early avant-gardes, at the beginning of the XX century, artists' works have gradually released from mimetic and narrative needs, by adopting new compositional criteria and, most importantly, new techniques and materials, whose characteristics that determine their alteration are today often ignored.

Ways of expression and artistic techniques were influenced by discoveries and innovations, produced by industrial development. New materials were put into every day life and the contemporary world, with its enormous scientific, technological, industrial development, provided the artists with great possibilities to elaborate new techniques.

Among the most impacting materials, in the art world, there were the synthetic and semi-synthetic, polymeric materials, as pictorial binders. Alkyd and acrylic resins are the most diffused.

Since the 40s of the twentieth century, pictorial materials based on alkyd resins were introduced. Widely used in Europe ten years later, variations in their formulation could provide richer and opaque colours, and a film with the desired flexibility. Alkyd resins were soon preferred by artists to oil painting, because they were cheaper and easier to find, for their particular optical properties, for the possibility of getting thick layers of pigment, and for the variety of colours available. The interest raised in the artists for new materials encouraged producers of colours to develop specific products, based on the new synthetic polymers.

In the late '40s, the first acrylic paints in tubes were produced. Among their properties, fast drying, intensity and purity of the colours that could be obtained, immediately grabbed the artists. A close collaboration with the artists were thus established, improving the products by trying to meet the specific needs they asked (Chiantore, 2005; Siqueiros, 1976).

The degradation of materials in contemporary art

The assembly of different materials for expressive purposes, is one of the causes of the complexity in the approach to the conservation of contemporary art. Besides the heterogeneity of materials, in fact, there is the diversity of processes of aging and degradation, that these may experience. The materials of contemporary art are mainly synthetic compounds, based on complex formulations. However, they are rarely designed for artistic purposes, and frequently used as they appear in the industrial market. In

addition, little is known about their durability. These are compounds whose expected survival goes from some years to a few decades, and their proper management for reasons of stability and maintenance, which requires the constitution and potential degradation processes are known. The identification of synthetic materials requires sophisticated investigative techniques, mostly of chemical nature and often of a destructive nature, aimed at recognizing the constituent parts (molecules, macromolecules). In rubbery materials, where flexible macromolecules predominate, for example, the speed of the degradation processes is higher. The effect of the presence of additives on aging and loss of physical properties of the material, such as mechanical and optical properties, are also to be considered. Among the effects of degradation, in fact, there may be the appearance of coloration and the loss of gloss, in addition to weakening and crumbling. The physical aging, in particular, is a phenomenon that only involves the organization of molecules, creating problems of deformation, fracture, rigidity and fragility, summarized in changes in appearance of the material.

Regarding the conservation aspects of polymer materials, the degradation induced by the combined action of light and atmospheric oxygen is the most important. The energy needed for the breaking of chemical bonds comes from a small fraction of the solar light (solar ultraviolet), whose wavelengths lie between 300 and 400 nm. Environmental contaminants can also accelerate the degradation processes, as well as temperature and relative humidity contribute to the loss of physical characteristics of the materials (Chiantore, 2005).

In the following paragraphs, the results of some tests on restoration materials *as they are*, are presented.

In the first case, frequently used consolidants, applied to monochrome layers to better focus on the materials, are considered.

In the second case, the behavior of different *associations* of materials: pigment, binder and eventual varnish, subjected to natural or induced aging, is evaluated and compared over time.

3.1 Study on materials: *Evaluation of the optical properties of consolidants for restoration*

The behaviour of a product used in restoration always requires a preliminary evaluation of its features. Among conservative interventions involving Cultural Heritage, the consolidation is a structural and comprehensive treatment, as it deeply acts by affecting all layers of a painting. It is therefore a risky procedure, as it could compromise both the structure and the aesthetic appearance of work of art, modifying its message. As the readability of an artwork is of fundamental importance, the application of a consolidant requests a specific attention to its optical characteristics such as transparency, the absence of coloration and of glossiness. Such an issue was investigated in a bachelor thesis (Labate, 2011).

Just with this aim, a test experiment was set up, having available specific materials for the purpose.[1] The optical behaviour of few synthetic consolidants such as Plexisol P550, BEVA 371, a polyurethane resin, Gelvatol and Aquazol 200 (all frequently used in the restoration of paintings), was thus investigated with image diagnostics and punctual techniques, with the main purpose to monitor their features over time (fig. 160). An innovative polyurethane resin was added to the test, for a comparison.

Fig 160 Total of the sample, in diffuse light.

[1] Such materials were kindly provided by Dr. Giovanna Scicolone, art restorer.

To address this need, the products were applied on white and black paint layers of matt acrylic tempera, on three equal test cardboards.
One of these **(C1)** will be submitted to artificial aging in a climatic chamber, with circadian cycles of temperature and relative humidity.
The second sample **(C2)** has been used as a control sample, being subjected to natural aging (normal condition of temperature, lighting and relative humidity).
As first step, just on these two samples, the main goal of measures presented in here was to verity the comparability of data, ahead of the future comparison after different agings.
The third sample **(C3)**, on which most of the observations were carried out, was subjected to UV-VIS-IR irradiation for 300 hours with a solar lamp (PHILIPS TL 29D model), forcing a possible early alteration. In this case, the radiation selectively involved the sample: its central part, being covered with a black cardboard, represented the non-irradiated part. Data presented in here about the third sample were thus aimed to find out eventual changes occurred after the irradiation.

In a first inspection, features not appreciable by naked eye have been visualized by image diagnostics.
Photographs in specular reflected light enabled the visualization of the distribution of consolidants on the surface (figs. 161-163), while ultraviolet fluorescence and visible pictures reached the lower layers.
Pictures taken of ultraviolet fluorescence showed a non homogeneity on layers of fluorescent consolidants (figs. 164-166).

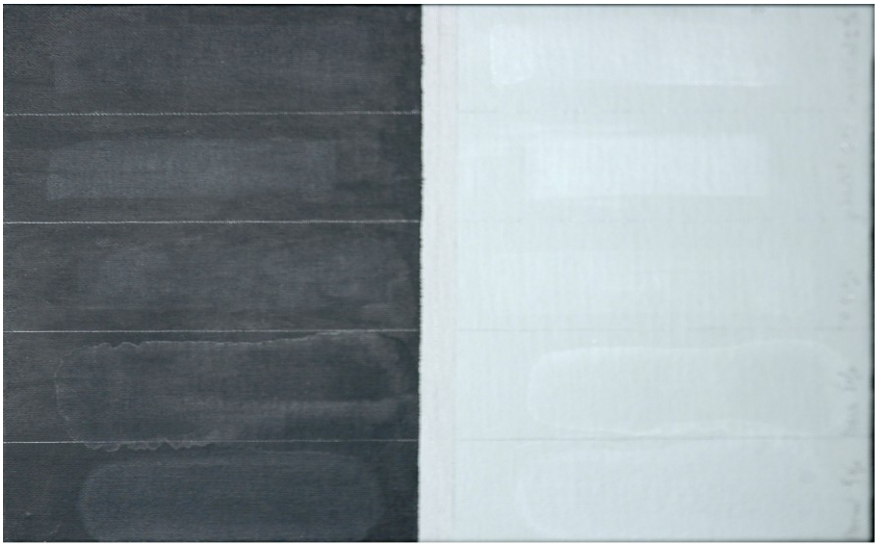

Fig 161 Photograph of the sample in specular reflected light.

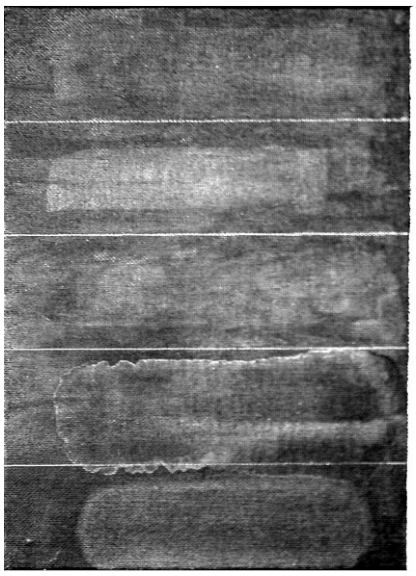

Fig 162 Elaboration of the previous picture, on black portion. Areas where consolidants were applied are well evident.

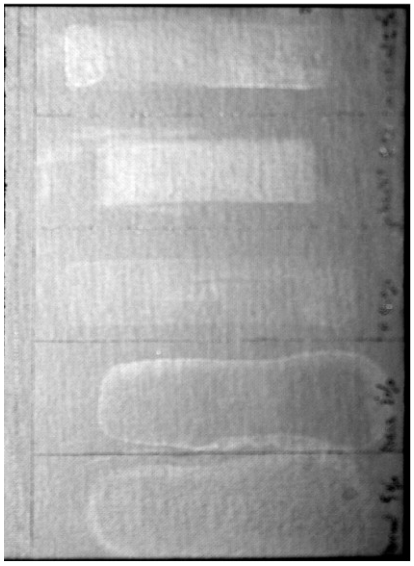

Fig 163 Elaboration of the previous picture, on white portion. Areas where consolidants were applied are emphasized.

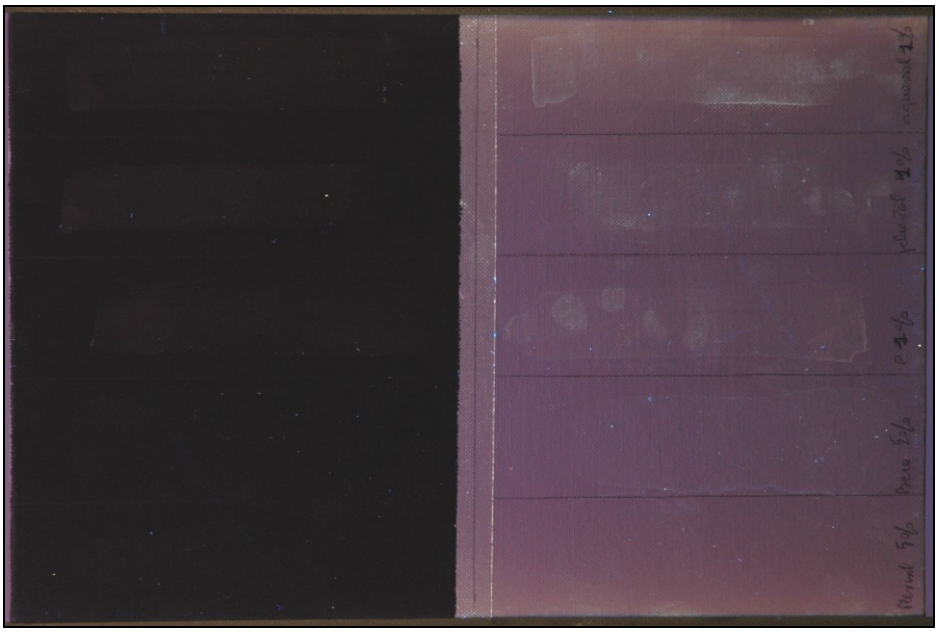

Fig 164 Photograph of the sample in ultraviolet fluorescence.

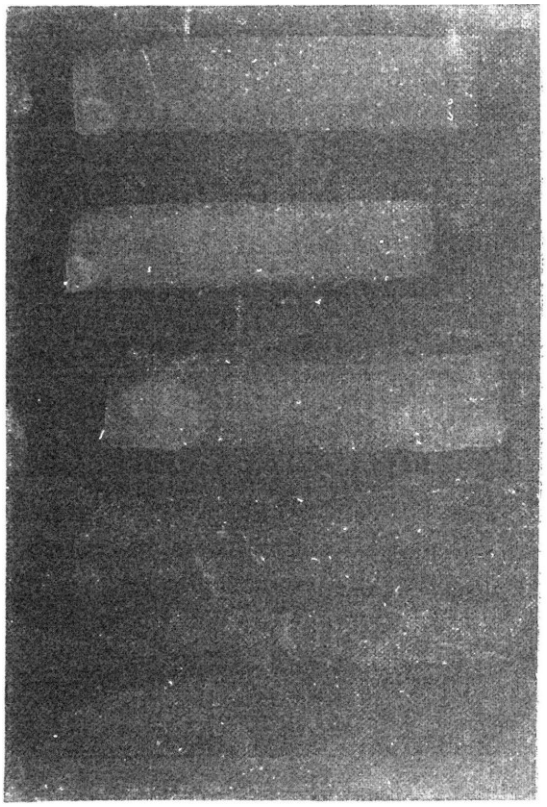

Fig 165 Elaboration of ultraviolet fluorescence photography, on black part.

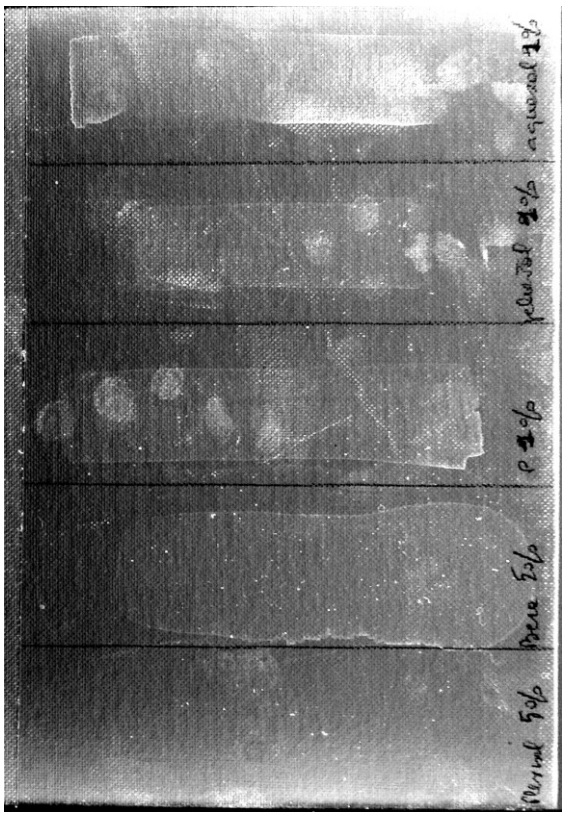

Fig 166 Elaboration of ultraviolet fluorescence photography, on white part. The strong contrast highlights some traces of fingerprints.

Further punctual spectrophotometric and colorimetric analysis, performed on samples according to the diagram shown in fig. 167, and combined with the principal component analysis (PCA), was employed in order to better understand the spectral behaviour of layers (Heck,1987).

Acquired spectrophotometric data, showing a certain uniformity in the behaviour of consolidated areas, revealed negligible differences between consolidated and non-consolidated areas (figs. 168, 169).

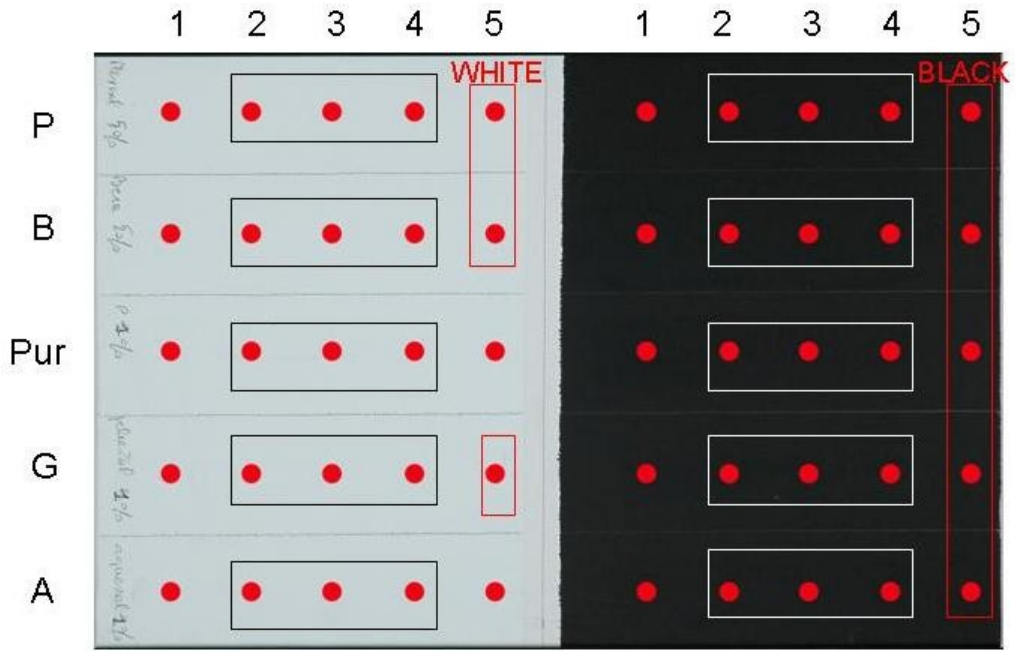

Fig 167 Diagram showing the position of spectrophotometric punctual measurements (Labate, 2011). Black and white frames, on the central portions of the two halves, individuate the three points on which measures were averaged. Red frames on black and white halves identifies the averaged measurements taken as a reference for the non consolidated areas.

In general, colorimetric data collected on samples C1 and C2, showed a uniformity in the response of consolidants.

As a matter of fact, all data collected are distributed within $\Delta E < 1$ (fig. 168). For each pictorial area in both tables, detected values for the different products, as well as being similar to each other, did not differ from those related to areas without consolidant (white and black).

It is therefore not possible to make considerations about differences between the values of each consolidant. In fact, as part of the systematic error of the instrument, it can be considered negligible.

Also the principal component analysis (PCA), confirmed the substantial comparability between spectrophotometric and colorimetric data of the samples. This similarity in the application of products on both the samples, represents a fundamental starting point for the aging test in which, as already said, one of the sample will act as a reference for the other one (figs. 170, 171).

PCA analysis also allowed to identify the most significant colorimetric coordinates for the examination of these measures. By applying it to colorimetric data L*, a* and b*, the major contributions to the first and second principal components respectively, resulted from the L* and a* variables. These results allowed thus to identify the changes as “more/less bright” and “more/less greenish”.

Colorimetric coordinates, defined as measurable by the International Commission for Lighting (CIE), take into account the lightness and the hue of a colour, specifying it in three numbers:

- the overall amount of light reflected in the whole visible spectrum (Lightness, L*);
- the red/green aspect (coordinate a*);
- the yellow/blue aspect (coordinate b*).

The difference between two colours is measured by a quadratic difference (ΔE) of the three coordinates.

Consolidants	L*(D65)	σ L*	a*(D65)	σ a*	b*(D65)	σ b*
Plexisol	95.27	0.04	-2.47	0.04	2.05	0.04
BEVA	95.37	0.03	-2.52	0.04	2.12	0.04
PUR	95.00	0.20	-2.54	0.03	2.28	0.09
Gelvatol	95.28	0.02	-2.53	0.01	2.24	0.02
Aquazol	95.2	0.20	-2.48	0.06	2.20	0.10
WHITE	95.26	0.06	-2.36	0.06	2.07	0.06

Fig 168a Sample1. Colorimetric data L* a* b* on white layers.

Consolidants	L*(D65)	σ L*	a*(D65)	σ a*	b*(D65)	σ b*
Plexisol	95.06	0.04	-2.35	0.03	1.98	0.07
BEVA	95.27	0.02	-2.43	0.03	2.05	0.04
PUR	95.00	0.20	-2.40	0.02	2.41	0.23
Gelvatol	94.90	0.10	-2.41	0.06	2.35	0.07
Aquazol	94.70	0.10	-2.39	0.03	2.50	0.2
WHITE	95.10	0.10	-2.29	0.13	-2.29	0.05

Fig 168b Sample2. Colorimetric data L* a* b* on white layers.

Consolidants	L*(D65)	σ L*	a*(D65)	σ a*	b*(D65)	σ b*
Plexisol	24.70	0.10	0.05	0.01	-0.48	0.06
BEVA	24.52	0.07	0.03	0.01	-0.58	0.01
PUR	24.88	0.09	0.06	0.02	-0.49	0.04
Gelvatol	25.52	0.24	0.08	0.02	-0.48	0.09
Aquazol	25.23	0.20	0.10	0.01	-0.34	0.03
BLACK	25.38	0.33	0.18	0.02	0.13	0.04

Fig 168c Sample1. Colorimetric data L* a* b* on black layers.

Consolidants	L*(D65)	σ L*	a*(D65)	σ a*	b*(D65)	σ b*
Plexisol	24.69	0.14	0.02	0.01	-0.47	0.01
BEVA	24.38	0.22	0.00	0.01	-0.55	0.05
PUR	24.51	0.08	0.08	0.01	-0.42	0.05
Gelvatol	25.36	0.09	0.03	0.02	-0.51	0.02
Aquazol	25.20	0.10	0.08	0.02	-0.45	0.03
BLACK	24.80	0.30	0.15	0.01	0.09	0.01

Fig 168d Sample2. Colorimetric data L* a* b* on black layers.

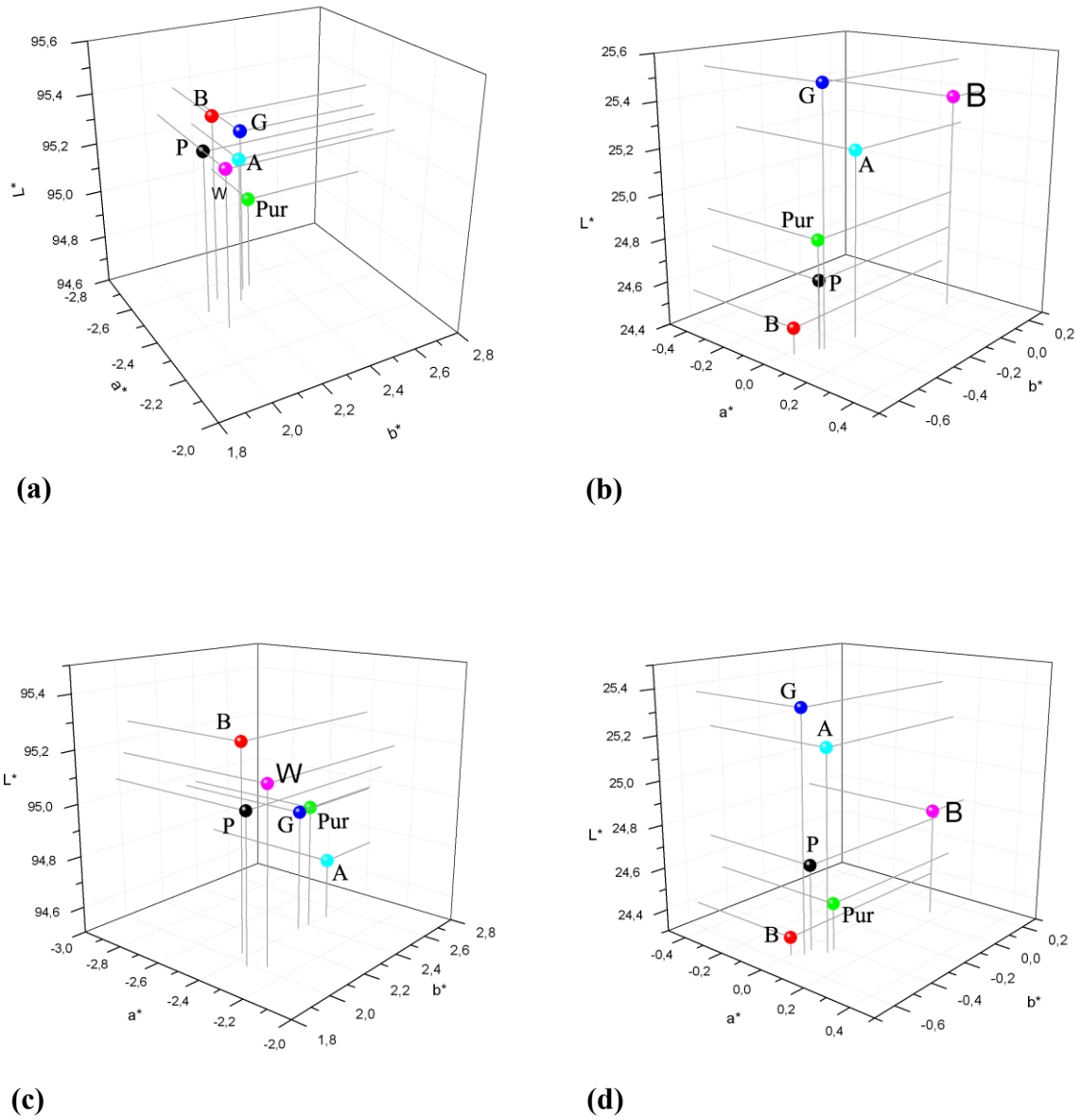

Fig 169 3D diagrams, showing detected values for the different products (Labate, 2011).
(a) L*a*b* initial values detected on the white half (Sample1).
(b) L*a*b* initial values detected on the black half (Sample1).
(c) L*a*b* initial values detected on the white half (Sample2).
(d) L*a*b* initial values detected on the black half (Sample2).
On both the halves, L*a*b* values detected are similar to each other.

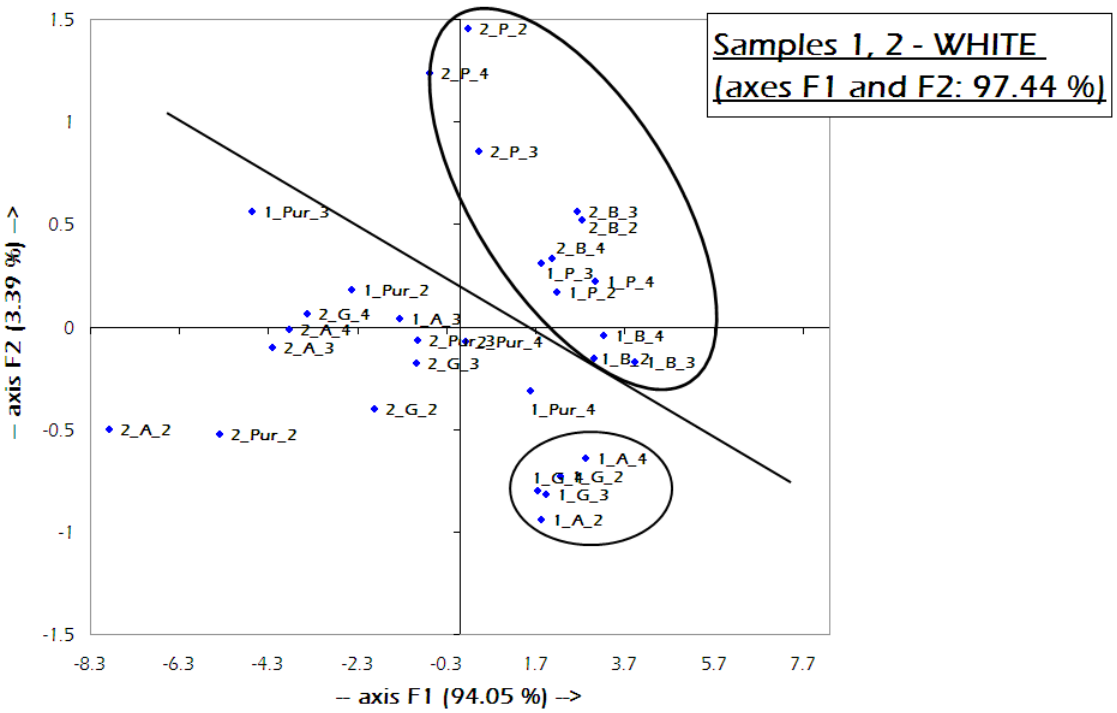

Fig 170 1-2 Samples. PCA on the reflectance values of the white halves.

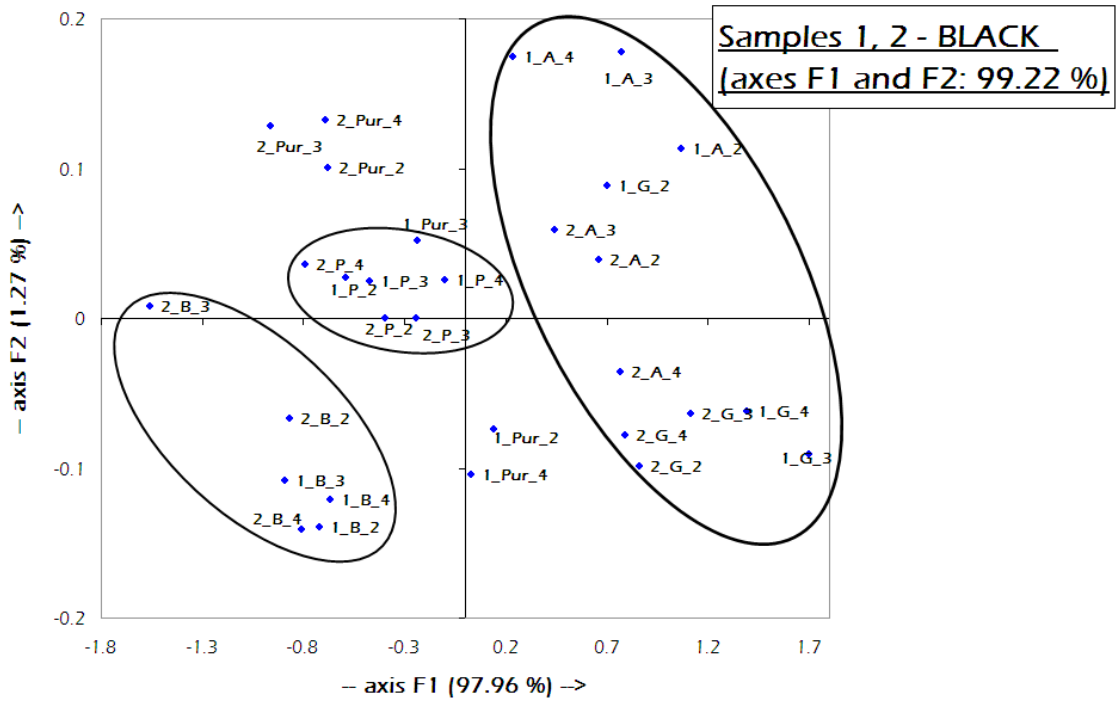

Fig 171 1-2 Samples. PCA on the reflectance values of the black halves.

Even on sample C3, colorimetric measurements were carried out, to detect any possible difference - in the visible - range after irradiation. As the variations observed both for spectral data and colorimetric data were under the threshold of visibility, it can be

concluded that no differences induced by irradiation with solar lamp could be appreciated in the visible range.

On the contrary, photographs of the ultraviolet fluorescence (figs. 172-174), taken after irradiation, showed a slight difference between the area subject to irradiation and the central one, protected by the black cardboard. This evidence was better appreciated on the white part, where the irradiated portion is less fluorescent, as shown in fig. 174c-d (Labate, 2011).

Fig 172 Photography of the total fluorescence in the ultraviolet, before irradiation.

Fig 173 Photography of the total fluorescence in the ultraviolet, after irradiation.

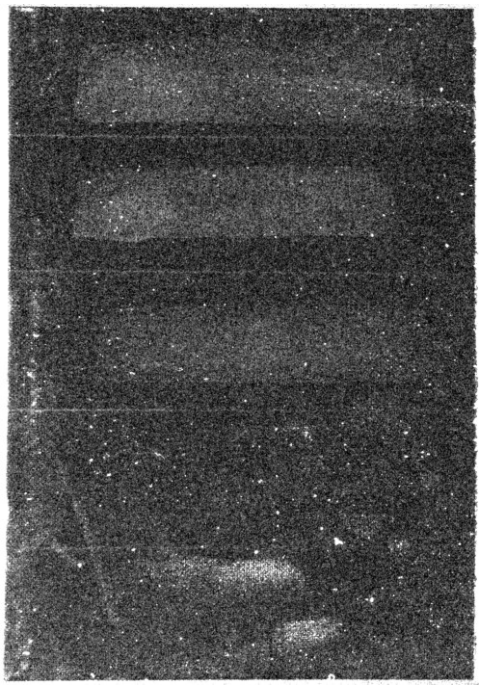

Fig 174a Elaboration (by contrast) of picture in ultraviolet fluorescence of the black half, before irradiation.

Fig 174b Elaboration (by contrast) of picture in ultraviolet fluorescence of the black half, after irradiation.

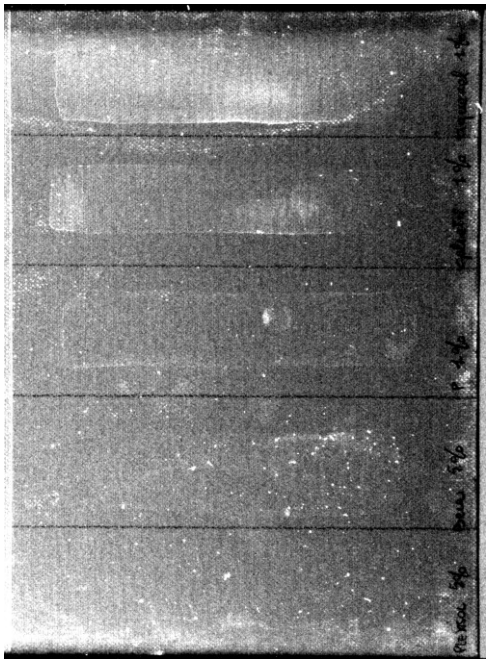

Fig 174c Elaboration (by contrast) of picture in ultraviolet fluorescence of the white half, before irradiation.

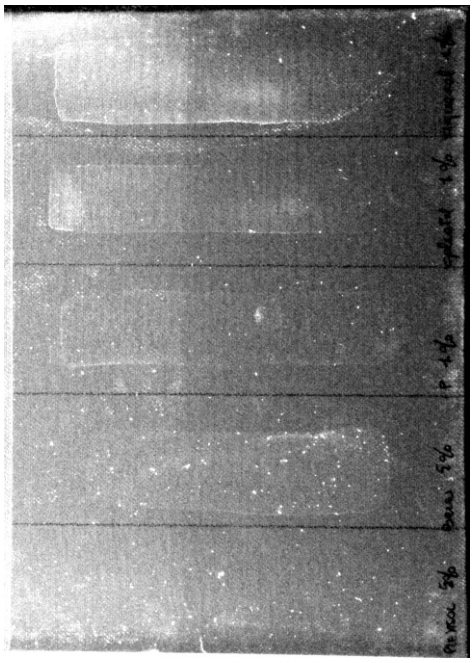

Fig 174d Elaboration (by contrast) of picture in ultraviolet fluorescence of the white half, after irradiation. A greater difference between irradiated and non irradiated parts, can be noticed on this half.

Conclusions

In conclusion, photographies in specular reflected light, allowed to visualize the distribution of consolidants on the surface layers of the test paintings.

Images of the ultraviolet fluorescence highlighted, instead, the lack of homogeneity on the layers of consolidants, particularly on the sample subjected to artificial aging. However, on consolidated areas, punctual analyzes by means of a spectrophotometer, showed a certain uniformity of behaviour. Acquired data presented, in fact, negligible differences between consolidated and unconsolidated areas.

Colorimetric measurements demonstrated a good uniformity in the preparation of the samples, which is confirmed by the principal component analysis (PCA). This is a useful requirement for the subsequent testing phases. As samples distribution is within $\Delta E < 1$, they can therefore be considered indistinguishable. Future phases of the project will provide additional measures for monitoring purposes.

3.2 Monitoring of contemporary painting layers. Test painting: Image spectroscopy and PCA to monitor modern materials

The aim of this study was to validate a method of measurement and analysis, in order to early detect phenomena of chromatic alteration. To this end, punctual non invasive spectrophotometric measurements were made by contact.

The monitoring over time of reflectance spectra and colorimetric parameters (CIELab 1976) of some chromatic layers, realized with *Titanium white*, was carried out.

On reflectance data, Principal Component Analysis (PCA) was also used, to identify and discriminate the variations observed on these samples.

Reflectance spectra and, thus, colorimetric data, were acquired by means of the spectrophotometer CM2600-d Konica Minolta (Chapter 4), operating in the 360-740 nm wavelength range, with a sampling pitch of 10 nm and a d/8° measurement geometry. Standard illuminant chosen was the D65 (CIE, 1964), while the Standard Observer was the 10° (CIE, 1964). The diameter of measurement area was set on 3 mm. Measurements were performed on a test painting, consisting of layers of *Titanium white*, *Ultramarine Blue* and *Siena Earth* (fig. 175). Nonetheless, in this work, observations relate on some of white layers, whose lower section of each frame (as in all the other coloured layers), was subject to artificial aging by irradiation with ultraviolet and infrared radiations.

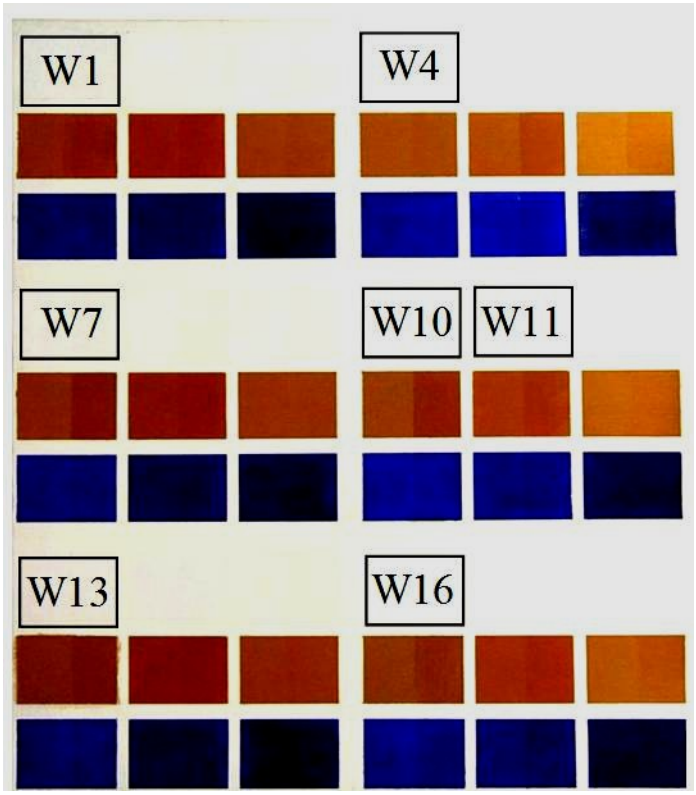

Fig. 175 Image, in visible light, of the test painting.
The codes of the investigated frames are reported.

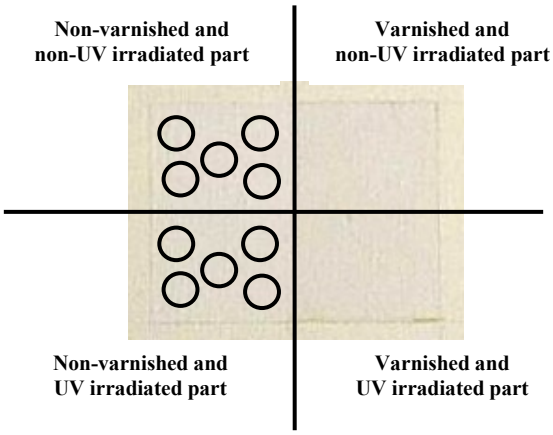

Fig. 176a Subdivision of each frame and the sampling points.

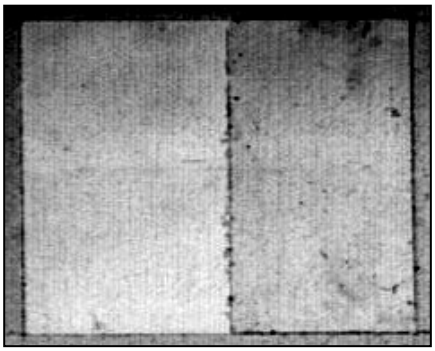

Fig. 176b Image (530 nm) of a frame where difference between varnished and not varnished part is visible.

Measurements were carried out on five different points on the unvarnished portions (fig. 176a).

Initially, the portions of the six layers in acrylic binder, not subjected to artificial radiation, were considered, with the aim to evaluate the inherent variability of layers. This variability was calculated taking into account the initial error, which proved to be of about 0.25.

Secondly, for the same binder, the effects of artificial and natural irradiations were investigated. A layer with alkyd binder was also taken into account to evaluate the contribution of different binders to the changes induced by artificial irradiation.

Layers in acrylic binder

The PCA distinguishes the layers in two well-separated clusters (fig. 177b), indicating that frames W1, W4, W7 and W13 have common characteristics, but different from those of the frames W10 and W16. It was also confirmed by the data of 2003 (fig. 177a), though there are only those related to the frames W10, W16 and W4. The latter, considering the results obtained in 2011, can be reasonably assumed to be representative of the frames belonging to cluster 1. In any case, the graphs showed the presence of a net, initial separation between the two groups. In addition, the intrinsic characteristics of the various frames remained almost unchanged. Such a distinction is also recognizable in the reflectance spectra for 2011 (fig. 178a), although with less evidence. The analysis of the colorimetric parameters put further emphasis on the greater contribution of the L* - Lightness) parameter, to negligible differences between the two groups. In the case of frames W10 and W16, that parameter is slightly higher - $\Delta L^* = 0.6 \pm 0.2$ with $\Delta E^*ab = 0.7$ (fig. 178b).

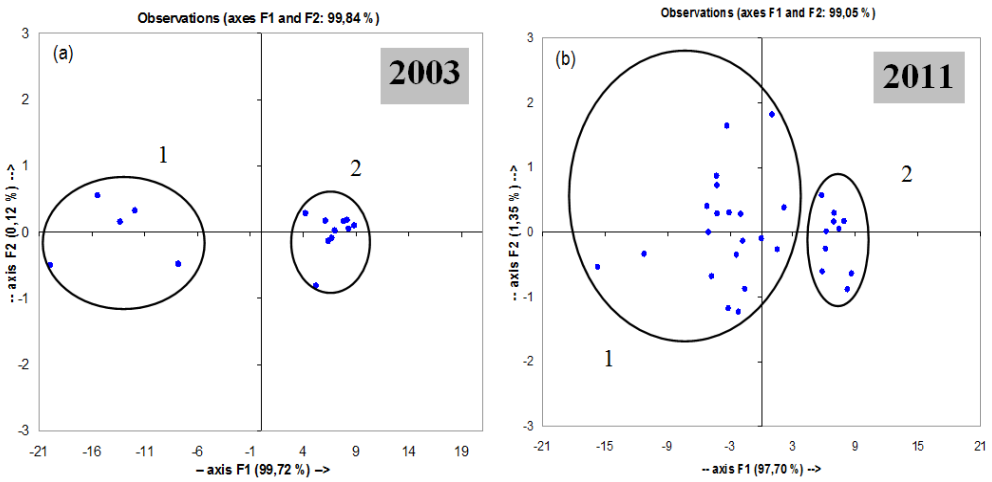

Fig. 177 Results of the PCA on the frames in acrylic binder, not subjected to UV irradiation. **(a)** Frames W4, W10 and W16 - measures 2003. **(b)** Frames W1, W4, W7, W10, W13, W16 - measures 2011.

Fig. 178 (a) Average relative reflectance spectra of frames analyzed in 2011. **(b)** L* (lightness) values of the same frames.

Irradiated layers in acrylic binder

The effects due to artificial aging, on portions irradiated with ultraviolet radiation, were investigated on the frames presented above. Data related to 2011 were analyzed.

Considering the results obtained on frames W10 and W16 through the use of PCA, an evident separation between irradiated and non-irradiated part (fig. 179) emerged. This distinction occurred according to the first principal component, indicating that the most significant differences were determined by direct artificial irradiation. Variability between the two frames was found, instead, on the second principal component, confirming their similarity. A similar situation, though less pronounced, was found on frames W1, W4, W7, W13. In fig. 180c, the frames W4 and W7 are presented, in which the separation occurred on the first principal component, while for the frames W1 and W13 (fig. 180a-d), the distinction took place on the second principal component.

Guided by the findings of PCA, analysis of colour parameters made it possible to assess the extent of their variations, as a result of the irradiation. Although differences found can be considered negligible (ΔE= 0.7), colorimetry allowed to highlight a contribution slightly greater of b*, in this variation. In fig. 181b, results for frames W10 and W16 were reported, on which this evidence was most clearly manifested.

Finally, reflectance spectra on the two frames confirmed what already found through colorimetry, also allowing to detect a decrease in reflectance values on frame W16, after irradiation, in the spectral range between 420 and 560 nm (fig. 181a) (Albertin, 2011 (a)).

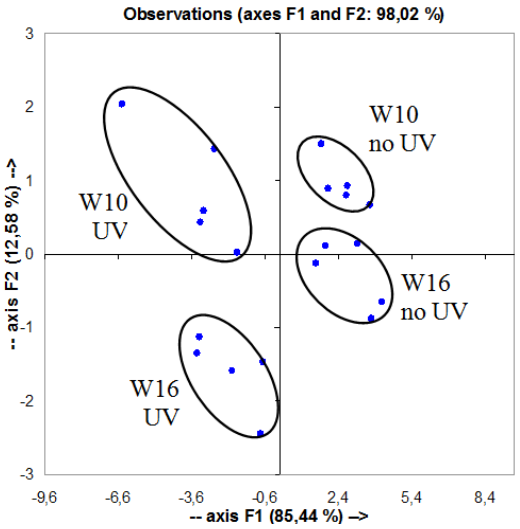

Fig. 179 Application of PCA on irradiated and non-irradiated portions of frames W10 and W16 in acrylic binder.

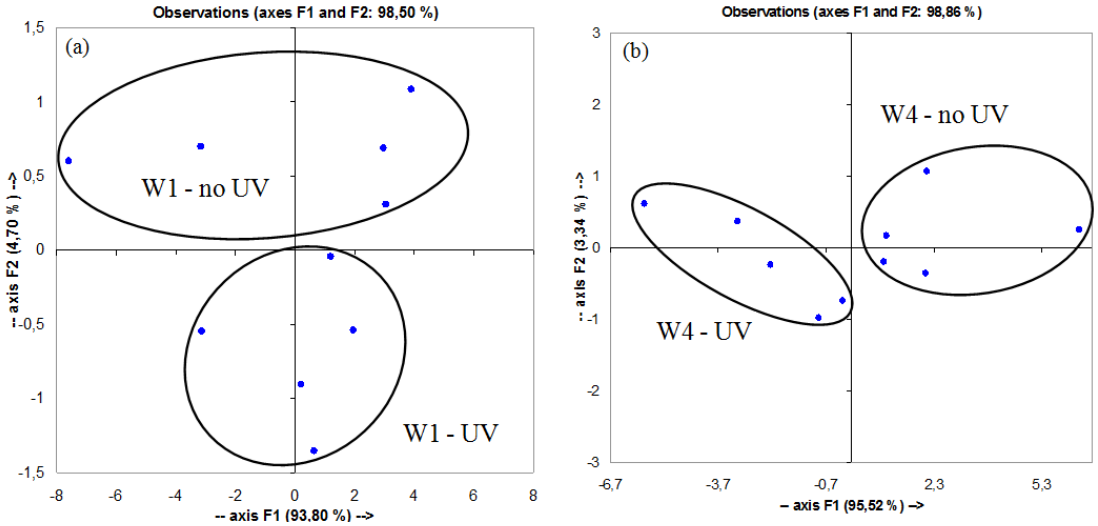

Fig. 180 Application of PCA on irradiated and non-irradiated portions of frames W1 **(a)** and W4 **(b)** in the acrylic binder.

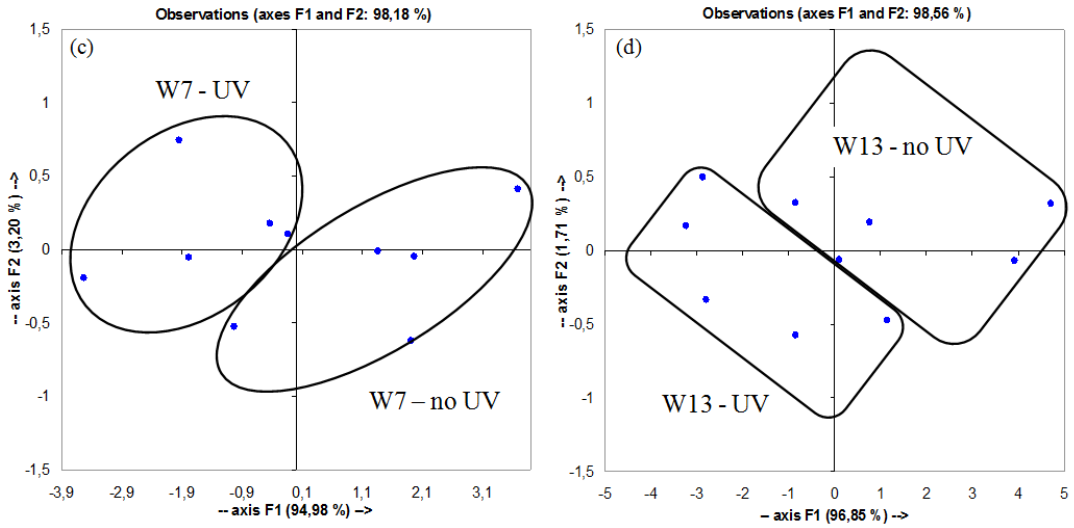

Fig. 180 Application of PCA on irradiated and non-irradiated portions of frames W7 **(c)** and W13 **(d)** in the acrylic binder.

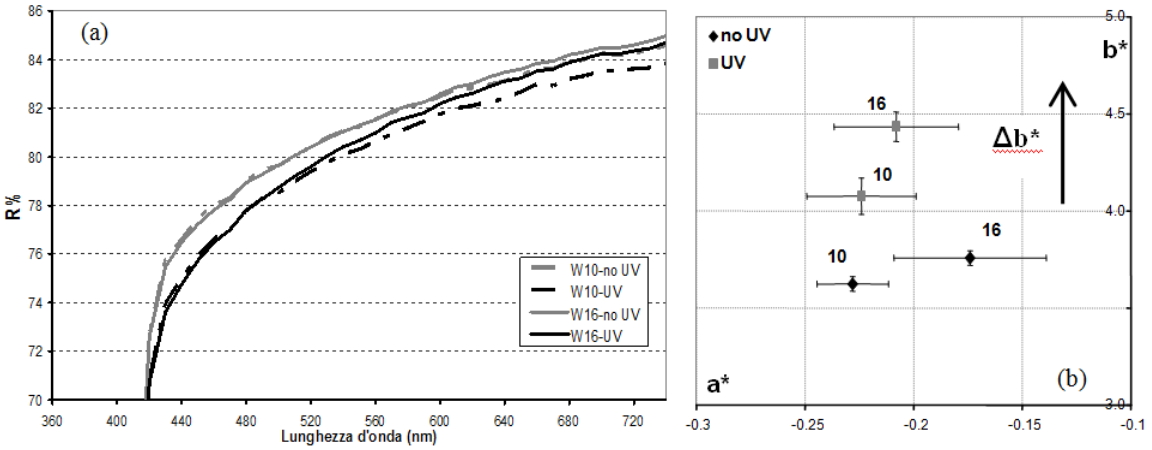

Fig. 181 (a) Average reflectance spectra of the measures carried out in 2011 on frames W10 and W16, with and without irradiation. **(b)** Colorimetric results, a* and b*, obtained on the same fields.

Irradiated layers in alkyd binder

Data obtained by PCA analysis showed a separation between irradiated and non-irradiated portion of frame W11, emerged on the second principal component (fig. 182a). These changes were not significant in colorimetric terms - $\Delta E = 0.2$ - (fig. 182b), while on individual wavelengths they amounted within the standard deviations. Anyway, alterations were evident only through multivariate analysis.

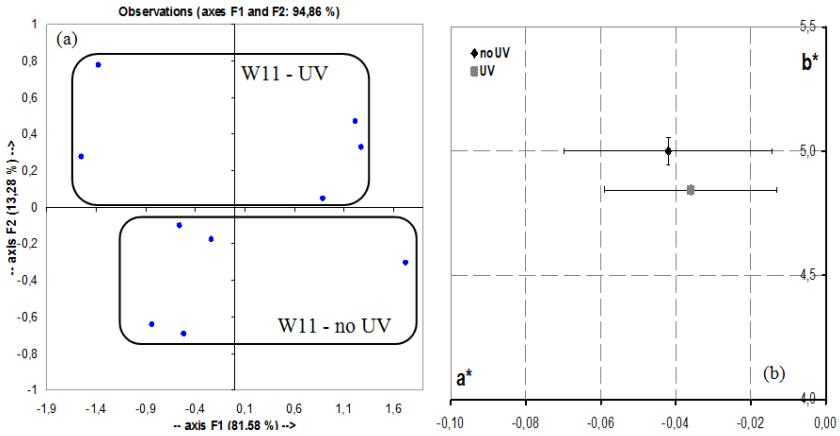

Fig. 182 (a) Application of PCA on irradiated and non-irradiated portion of frame W11 in alkyd binder. **(b)** colorimetric results, a* and b*, obtained on the same fields.

Natural aging of layers in acrylic binder

In order to evaluate the aging over time of the layers considered, data acquired with the same instrument in 2003 and 2011, relative to the frames W10 and W16, were compared. It was decided to focus on these layers, whose values obtained with the PCA were more clustered than those of the other cluster.

On portions not subjected to irradiation, PCA immediately highlighted a clear separation on the first principal component between data for the two years. In addition, measurements made in 2011 showed more pronounced separation between the two frames, which can be related to the effects of natural aging (fig. 183a).

Looking at the graph related to irradiated portions (fig. 183b), the UV irradiation caused a premature aging of layers. So much that measures of 2003 and 2011 on frame W10 are separated only on the second principal component.

Analysis of reflectance spectra showed that, as a result of natural aging (2011), irradiated and non-irradiated portions of the two frames presented comparable values, although starting from a different situation, reached after the first few years of aging (2003). In fig. 177a, as an example of this trend, the case of frame W16 is reported.

By a colorimetric point of view, the L* parameter (lightness) seemed to be the most sensitive indicator of changes observed over time. The common trend appears as a reduction in the values of L* (fig. 184b).

With regard to the two considered frames, after eight years of natural aging, values similar to those induced by the artificial irradiation in a short time, were achieved.

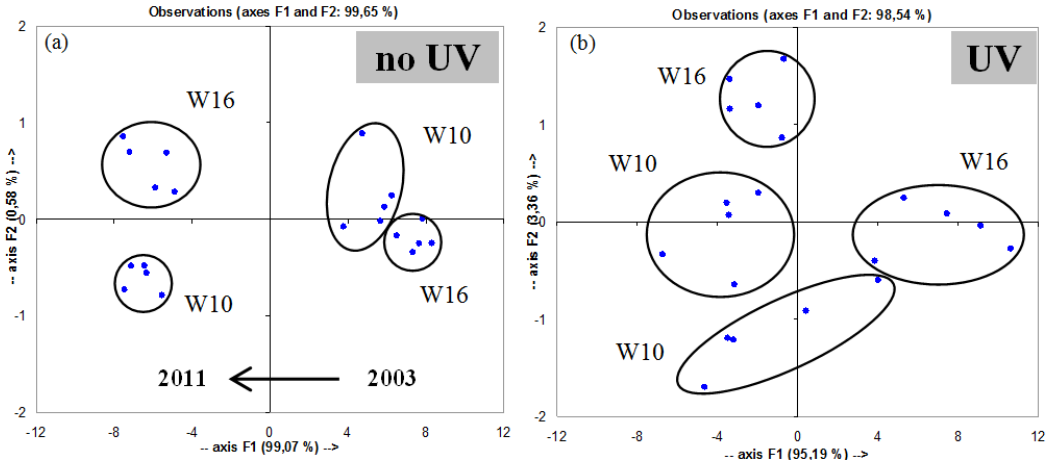

Fig. 183 PCA performed on spectral data collected in 2003 and 2011 on frames W10 and W16.
(a) Non-irradiated portions. **(b)** Irradiated portions.

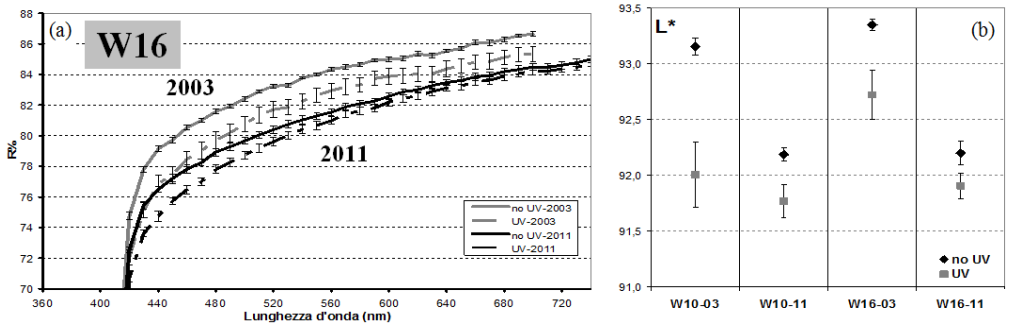

Fig. 184 (a) Comparison between the average reflectance spectra obtained from measurements made in 2003 and 2011, on frame W16, with and without UV irradiation.
(b) Colorimetric results related to L* parameter, obtained on frames W10 and W16.

Conclusions

This work confirmed the validity of the combination of spectrophotometry and multivariate analysis, for the early detection of alteration on painted surfaces.

Sensitivity to minor chromatic alterations was very good, thanks to the PCA analysis applied on wavelengths included in the visible spectral range (Petrucci, 2004; Pasetti, 2002). On the other hand, colorimetric coordinates firstly allowed to evaluate the low extent of the chromatic variations detected, quantifying them below the threshold of visibility ($\Delta E < 1$). Secondly, they were useful parameters to interpret colour changes over time. In this case, systematic non-uniformity in the layers of *Titanium White*, initially considered homogeneous (according to initial assumptions), were found. It has thus been demonstrated that this intrinsic variability (of hand-made painted layers), could overcome the effect of artificial aging induced by ultraviolet radiation. For conservation purposes, the need to measure, compare and to periodically monitor the reflectance features on the same points, emerged. Therefore, the availability of a diagnostic tool for remote sensing of reflectance spectra, is more reliable (Albertin, 2011 (a); Albertin, 2012 (b)).

3.3 Colour and texture characterization of a sample (Training at the *Centre for Fine Print Research*, Bristol)

3.3.1 The *BRDF* (*Bidirectional Reflection Functions*)

The bidirectional reflectance distribution function is a measure of the distribution of reflectance. It defines how much light is reflected on an opaque surface. The function considers the direction of the light that comes *in* and *from* the surface.
Specular reflection is the mirror-like reflection of light from a surface, in which light from a single incoming direction is reflected into a single outgoing direction.
So, bidirectional reflectance is given by contribute of both specular and diffuse reflection, where incoming light is reflected in a wide range of directions (fig. 185).

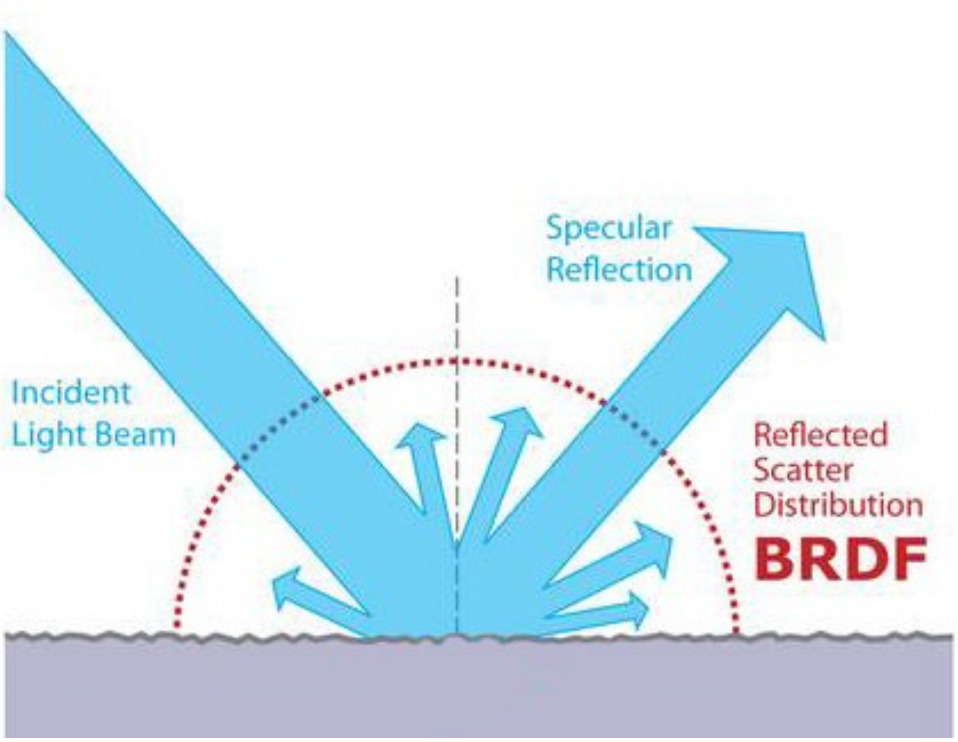

Fig. 185 BSDF (Bidirectional Scattering Distribution Function) describes the way in which the light is scattered by a surface. Such a phenomenon is usually split into the reflected and transmitted components, separately treated as BRDF (Bidirectional Reflectance Distribution Function) and BTDF (Bidirectional Transmittance Distribution Function). Picture taken and modified from: (http://en.wikipedia.org/wiki/Bidirectional_scattering_distribution_function).

As an example of the distinction between specular and diffuse reflection, would be glossy and matte painted surfaces. Matte paints have almost exclusively diffuse reflection. A glossy appearance characterizes, instead, surfaces that reflect the light in both ways (that is, also specularly).

3.3.2 The practical approach: construction of a system for the observation of prints, through a microscope

During the training at the *Centre for Fine Print Research*, Bristol, the work has been focused on a project related to the use of the raking light technique, in order to emphasize the effects of brushstrokes and the surface texture of prints.
An extra device was thus set up on a microscope, with the purpose of acquiring - at the same time - both colour and texture features of the sample. Just by means of a stereo microscope, a better and more detailed observation was possible, concerning these features, that can be summarized in the measure of *Bidirectional Texture Function*.
The result of such an investigation should consist in a better characterization of the sample (with its colorimetric and texture features), an easier digital reconstruction and, thus, a simpler reproducibility by printing.
In this first phase of the work, the apparatus was set up. It consists of an enclosed rotating dome under which a sample is placed, which must be of reduced size or, however, easy to handle (for example, a sheet of paper). A closed hemispherical covering, approximately 20 cm high, is placed above the sample, in order to guarantee a "micro-environment" with a constant geometry of illumination and observation of the sample (fig. 188).
On the external shell of the dome, two holes are present, through which two light sources were inserted, small lambertian bright 0.5W LED lamps (6000k) to illuminate the sample surface at different angles (fig. 187). To this aim, the dome can rotate around the fixed sample, to obtain both single pictures and a 360° rotating view.

Making the dome

The prototype of the dome was realized using newspaper and PVA glue (fig. 186). To ensure greater stability to the paper structure, a circular basis was created with plastic material, with an internal slit (sort of track), where to allocate the dome. This basis was realized with a 3D printer, at the *Centre for Fine Print Research*. The object was also realized in order to ensure a greater "smoothness", once inserted into the track on the wooden support, where to place the sample.
Some types of "brushstroke" were thus selected, in order to be reproduced with a "2.5 printer", with different types brushes. Several "styles" of painting could thus be selected, among those employed by some of modern and contemporary artists, for the most distinctive and recognizable style.

Prints produced, once dried, could be illuminated with raking light, again using the created device, and so be observed under the microscope at different angles (fig. 191-192).

Fig. 186 Phases of realization of the dome: gluing of sheets of newspaper with vinyl adhesive.

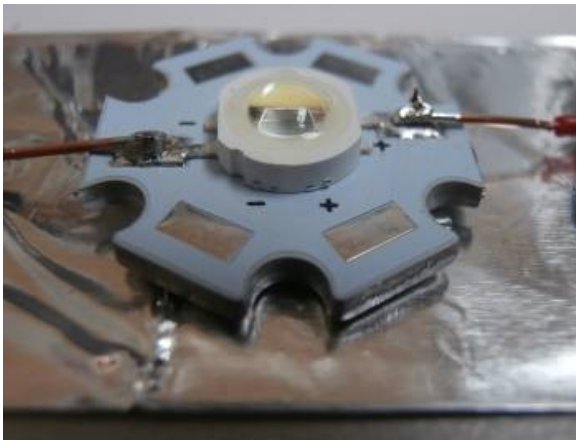

Fig. 187 Images showing wires soldering for the realization of the LED source.

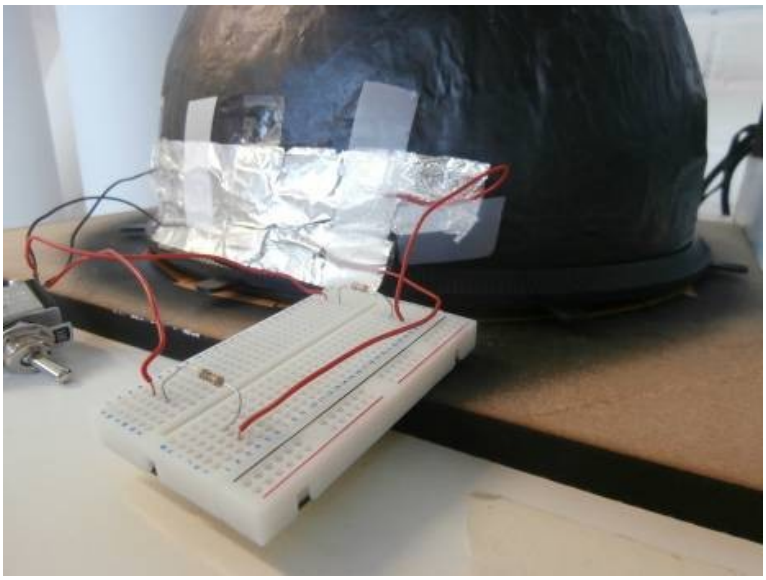

Fig. 189 Detail of the electrical circuit connected to the dome.

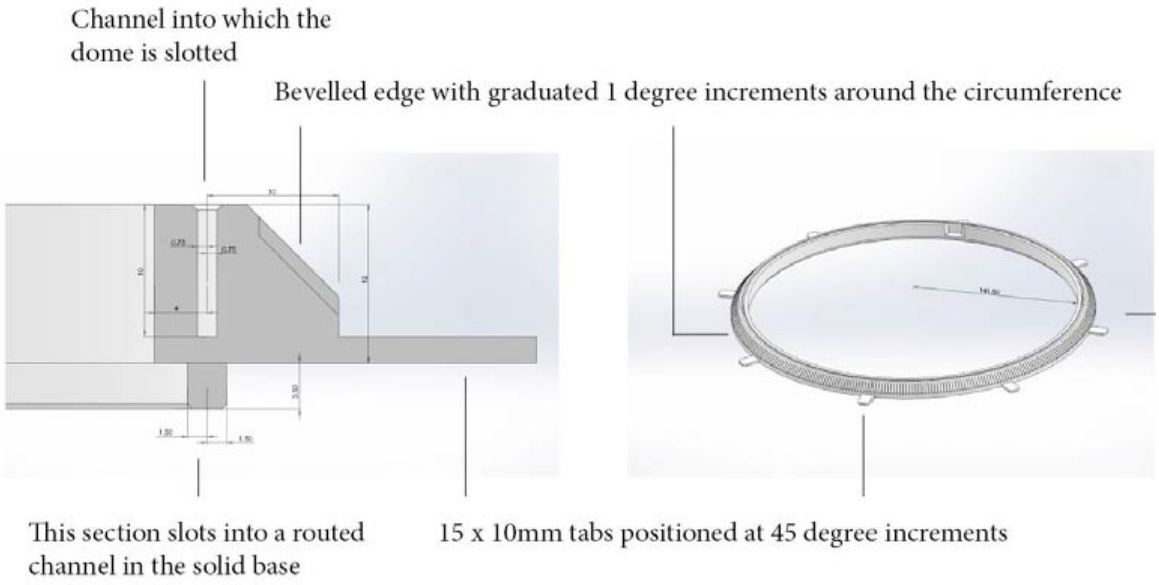

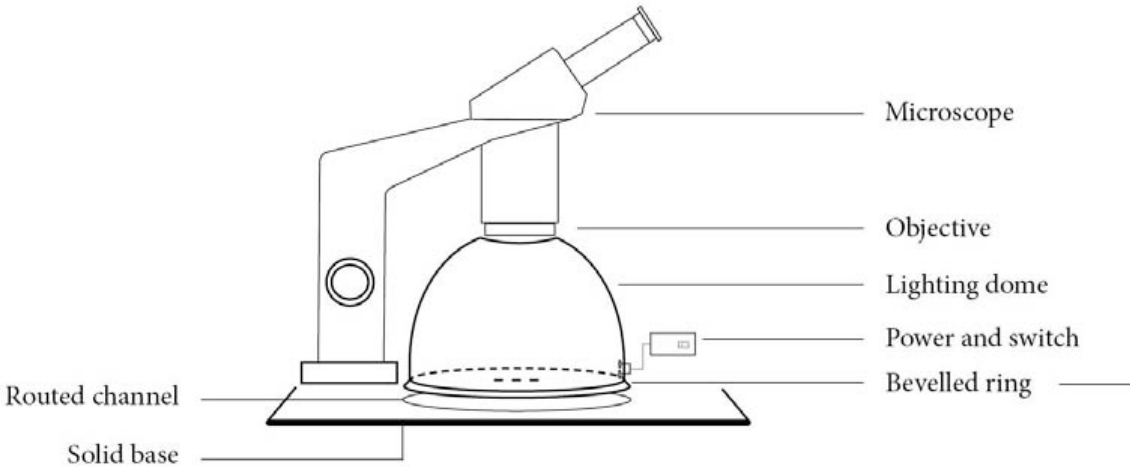

Fig. 188 Diagram showing side elevation (top left) and isometric view of the rigid bevelled ring (top right). The bottom figure shows the complete apparatus and the placement of the ring at the bottom of the dome (Parraman, 2014 (b)).

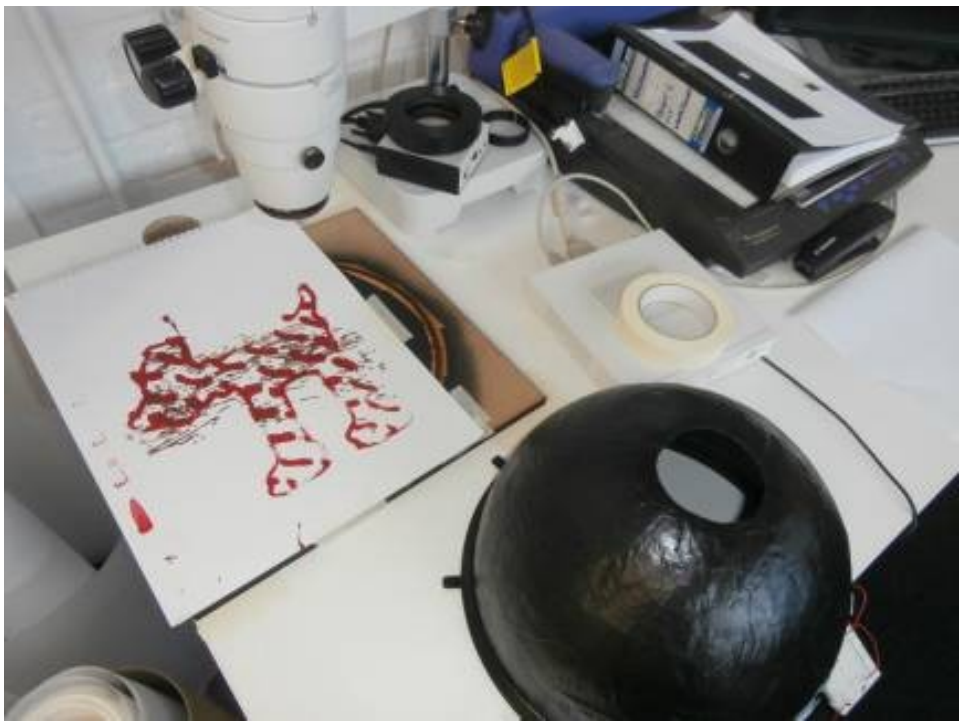

Fig. 190 Detail of the device, while acquiring pictures of a 2.5D printed sample.

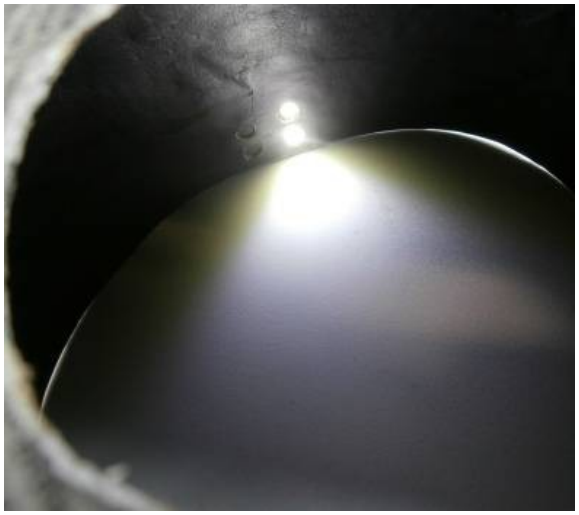

Fig. 191 Interior of the dome with both LEDs turned ON.

Fig. 192 Detail, in diffuse light, of a 2.5D print, emphasizing brush strokes and texture features.

Applications

The technique of raking light, when applied to prints and paper items, can reserve interesting and surprising details… perhaps even more if compared to what happens for paintings on canvas and wood. It has thus been searched among various methods and approaches, in order to deepen the knowledge about the artworks (http://www.whiteboardmag.com/3d-scan-van-gogh-perfect-replica-formart/).

Besides trying to obtain a very detailed observation of the sample from a qualitative point of view, future purpose would be a more precise and detailed characterization of the surface, both from the texture and the colorimetric point of view.

To this aim, experimental methods (approaches) have been sought.

As a first approach, special graphic processing, such as “bas relief” filter, available on Adobe Photoshop program, enabled to visualize images emphasizing their three-dimensionality. The further possibility of simulating the illumination angle, allowed to obtain a graphic rendering closer to the original visualization (fig. 193a,b).

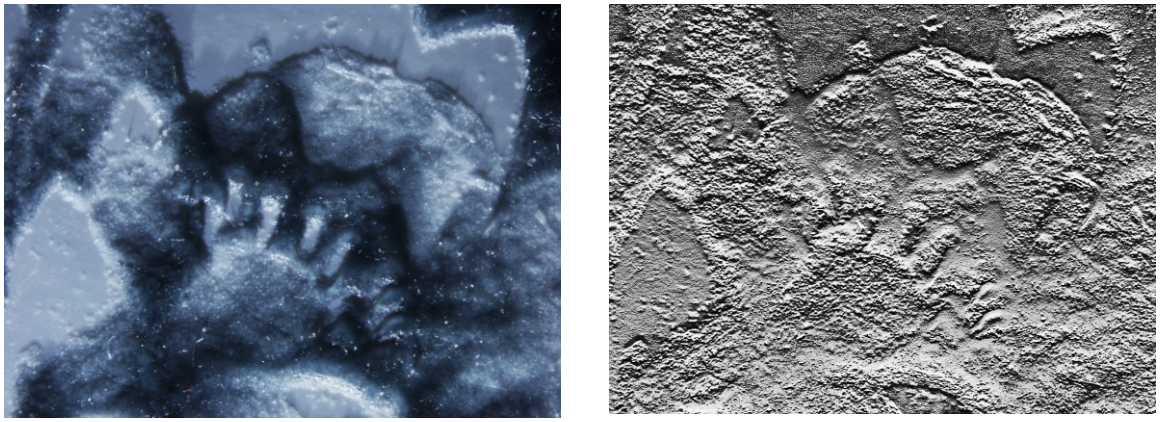

Fig. 193 (a) Detail of a silicon print under the microscope (1x magnification), elaborated **(b)** by means of “bas relief” filter, in Photoshop program.

A further attempt provided a more concrete approach.

As a matter of fact, by acquiring images of known thicknesses, at different magnifications, the intent would be to trace back to the different thicknesses that characterize the particular, investigated artifact, on its different superficial portions.

The expected final result is a grayscale image that could be "quoted", that is, where each gray level corresponds to a different thickness. Every thickness is constituted by both the paper and the overlying layer of paint or ink that, at least ideally, could be characterized and, therefore, accurately reproduced.

3.3.3 Photographs, at different magnifications, of samples illuminated with the dome stereomicroscope system

In figs. 194, 195 and 196, some examples are provided of the better understanding of the relationship between ink or paint on the different substrates, by examination of samples under a stereo-microscope.

Samples are captured using a Nikon SMZ800 stereo zoom microscope with a P-ED Plan 0.5x objective, attached to a G-US2 universal table stand so that a range of samples can be examined. Nikon Elements software was used as both a visualisation and measuring tool.

Images obtained emphasize the threedimensionality of every smallest detail, of a single brushstroke. In the following fig. 187, raking light is used at different angles, highlighting the shadows created by the reliefs of paint, the texture of the paint and paper.

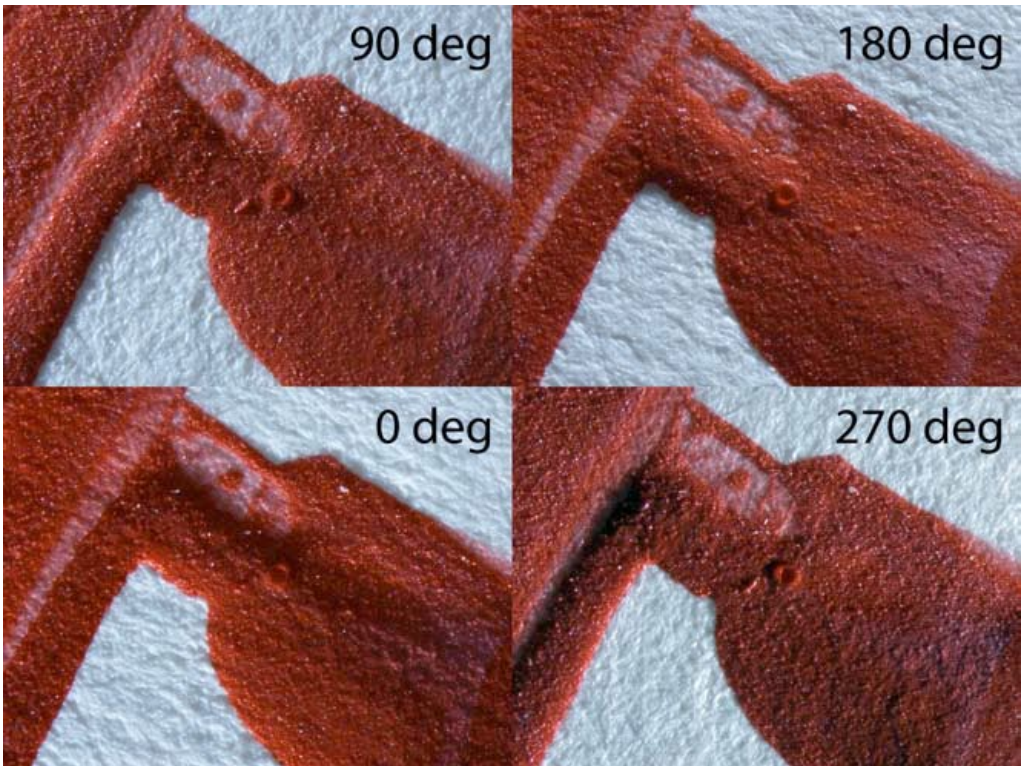

Fig. 194 Appearance of a painted sample acquired by using raking light at 0°, 90°, 180°, 270°.

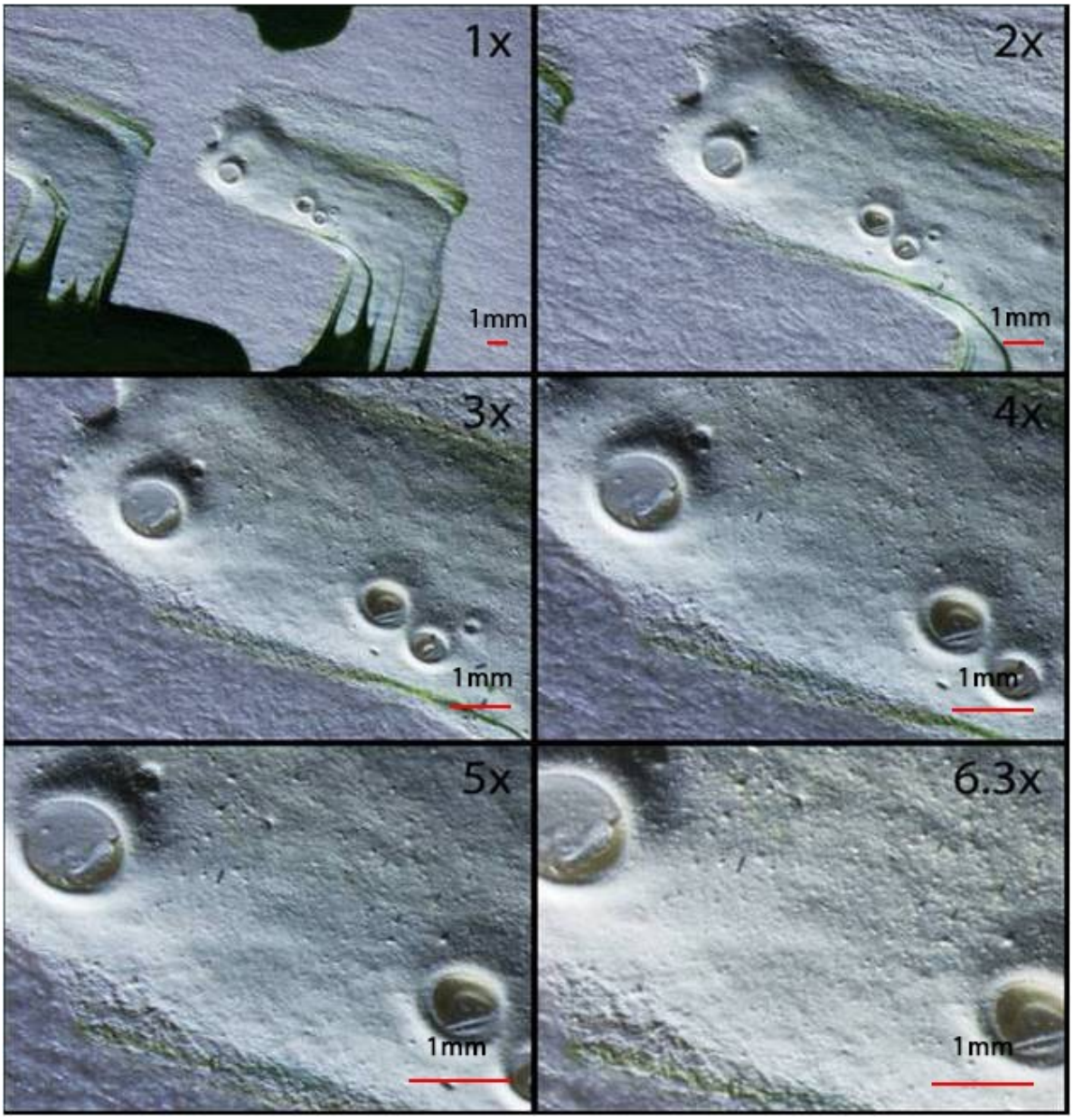

Fig. 195 Increasing magnifications of a detail from a 2.5D print.
The use of raking light emphasizes the three-dimensionality of the brush stroke.

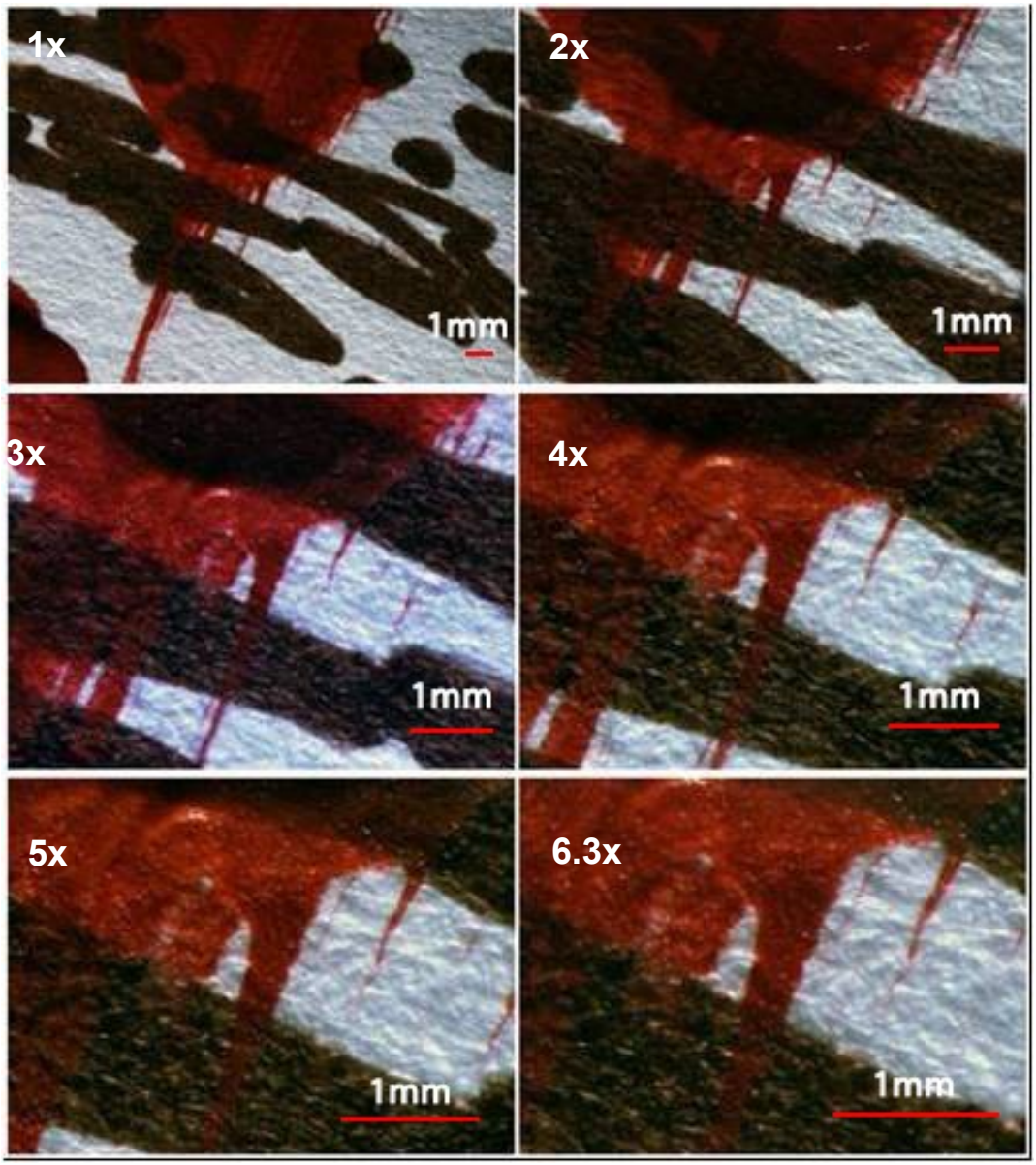

Fig. 196 Increasing magnifications of a detail from a 2.5D print (Parraman, 2014 (a),(b)) allow to better appreciate the succession of layers. Such a sequence initially occurred by 2.5D printing on paper a dense red color, followed by a brown marker.

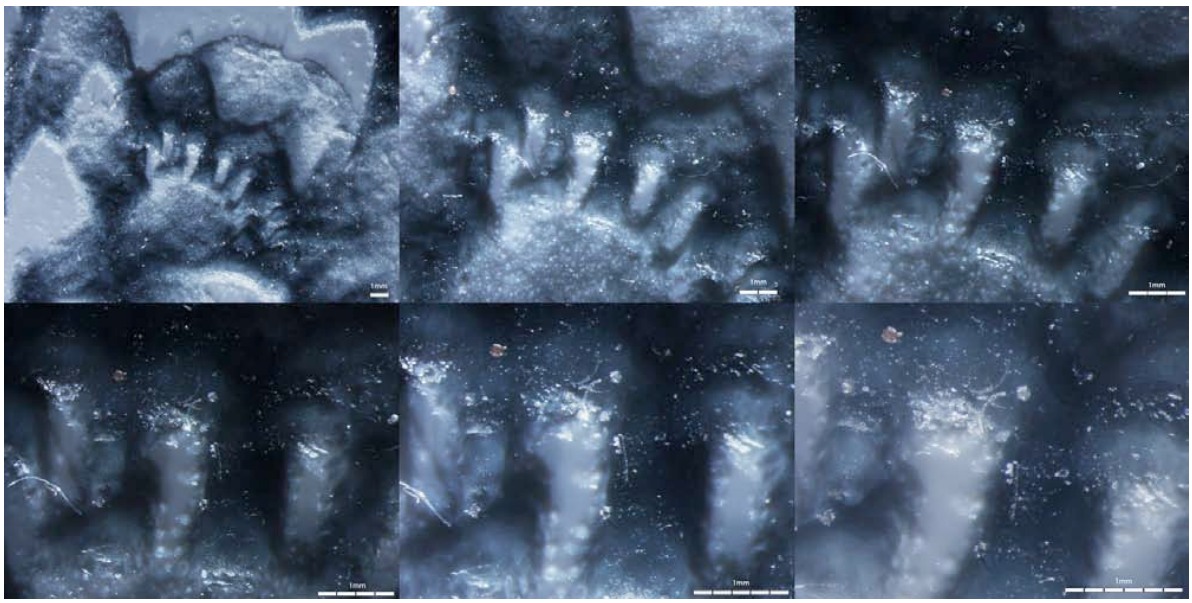

Fig. 197 Silicone melted print by P. McCallion (2013). Magnification increases from 1x up to 6.3x. Measurement bars (in white) = 1mm. Raking light source is positioned at 180°.

Finally, fig. 197 shows another example of the use of raking light in combination with magnification of the sample. P. McCallion (from the *Centre for Fine Print Research*, University of the West of England, Bristol) is investigating the use of CNC machining and casting using silicones to create texture in continuous tone digital images (McCallion, 2014). Such enlargements, using raking light (from the same position), highlights in this case the different depths of the silicone, the gloss and texture, dust and air bubbles.

Such an application suggests, on the whole, the validity of the combination microscope - raking light, in order to investigate in depth different types of material.

Conclusions

To sum up, a practical approach was adopted in the building of an illuminated dome, designed to be attached to a stereomicroscope.

The objective of such a work was to provide a useful tool to visualize, capture and compare fine surface textures and microscopic detail. A range of surfaces, including relief prints, were investigated by such a device.

As a fundamental application, raking light could enable better visualization of details, potentially contributing in methods of analysis for the field of conservation and Cultural Heritage.

As a potential, future purpose, such information could be used for further digital and texture applications.

Chapter 4

Equipment

In the field of Cultural Heritage, there is a great need for research techniques allowing to explore, in a non destructive way, the internal or hidden parts and, anyway, those invisible at a simple visual inspection and otherwise inaccessible.
Very often, physical-chemical characterization techniques are requested for a qualitative identification of materials, or for a precise quantitative analysis of its composition. Besides, for dating or authentication purposes, or to evaluate the degradation.
Different techniques have been used at the Archaeometry Laboratory. Among the instruments used for the investigations presented here, some are present on the market (section 4.2). These include a spectrometer for X Ray fluorescence, a spectrophotometer, a Wood lamp for ultraviolet fluorescence and a camera with a Silicon detector for infrared reflectography. On the other hand, non-standard instruments (section 4.1) like an apparatus for image spectroscopy, a scanner for wide band reflectography, a system for digital radiography and a device for K-edge radiographies, have been implemented with the valuable support of the Electronics and Mechanics workshops of Physics Department and INFN Unit in Ferrara.

4.1 Non standard instruments

4.1.1 Wide band infrared reflectography scanner

Infrared reflectography uses near infrared electromagnetic radiation (NIR) to investigate underdrawings on paintings. Nonetheless, the success of such a technique in accomplishing this task, significantly depends on the art technique of the painting. As an example, in paintings XIV up to XVI century, thin and uniform pictorial layers covering high contrast drawings on white priming, allows a good detection of underdrawing details. On the other hand, paintings from late sixteenth century often present dark preparations and thick paint layers, so that reflectography doesn't get the same good results. Extension of the spectral band to wavelengths longer than allowed by Silicon detectors, up to 2.5 μm, is a tool to improve reflectographic capability. The further introduction of scanner devices, together with the extension of the spectral sensitivity beyond the limit of Si detectors, resulted in a significant improvement in the definition of images obtained.

The new infrared scanning system adopted in here includes an InGaAs detector, with a spectral sensitivity extended up to 2.5 μm.
The scanning device (fig. 198) is constituted by four main parts, such as the mechanical structure, the optical and illumination system, the detector, and a PC with the acquisition software.

- The **mechanical asset** consists of two perpendicular motorized axes, allowing to scan an area of about $1m^2$.
- The **optical system** (fig. 199) consists of a binocular microscope head mounted on a Y-axis, provided by a revolver with selectable magnification steps. On an eyepiece tube, the detector is placed, while in the second one a camera is located, for positioning and focusing operations.

The use of the microscope offers some advantages, including:

- the enlargement of the area focused on the detector, to cover the active area of photodiode,
- the guarantee of a working distance of about 10 cm, to avoid damage to the painting,
- a depth of field of about 0.5 cm, which is compatible with the roughness of most pictorial surfaces.

- The **lighting** is provided by two halogen lamps (50W) placed at 45°, focused and filtered with silicon filters, to eliminate wavelengths shorter than 1100 nm. Thanks to the optical system, a spatial resolution of 4lp/mm with both detectors is obtained.
- The **detection system** is a Hamamatsu Two-colour K3413-08 detector, constituted by two single photodiodes Si and InGaAs, equipped with a thermoelectric cooling. The combination of the two semiconductors covers a wavelength range from 0.3 μm up to 2.5 μm.

  Due to the transparency of Silicon at wavelengths over 1100 nm, this detector delivers the possibility of simultaneously acquire two images in different spectral bands (fig. 200).
- The movement is handled by a **dedicated software**, while the **acquisition and digitization** of the images occurs via a National Instrument™ capture 6036E card, and a software developed on LabView™ platform (Peccenini, 2012).

Figures 217a-b present a comparison between results obtained by means of a Silicon detector (with a limited response in the visible spectral range), and those achieved by using the wide band infrared scanner, described in this section.

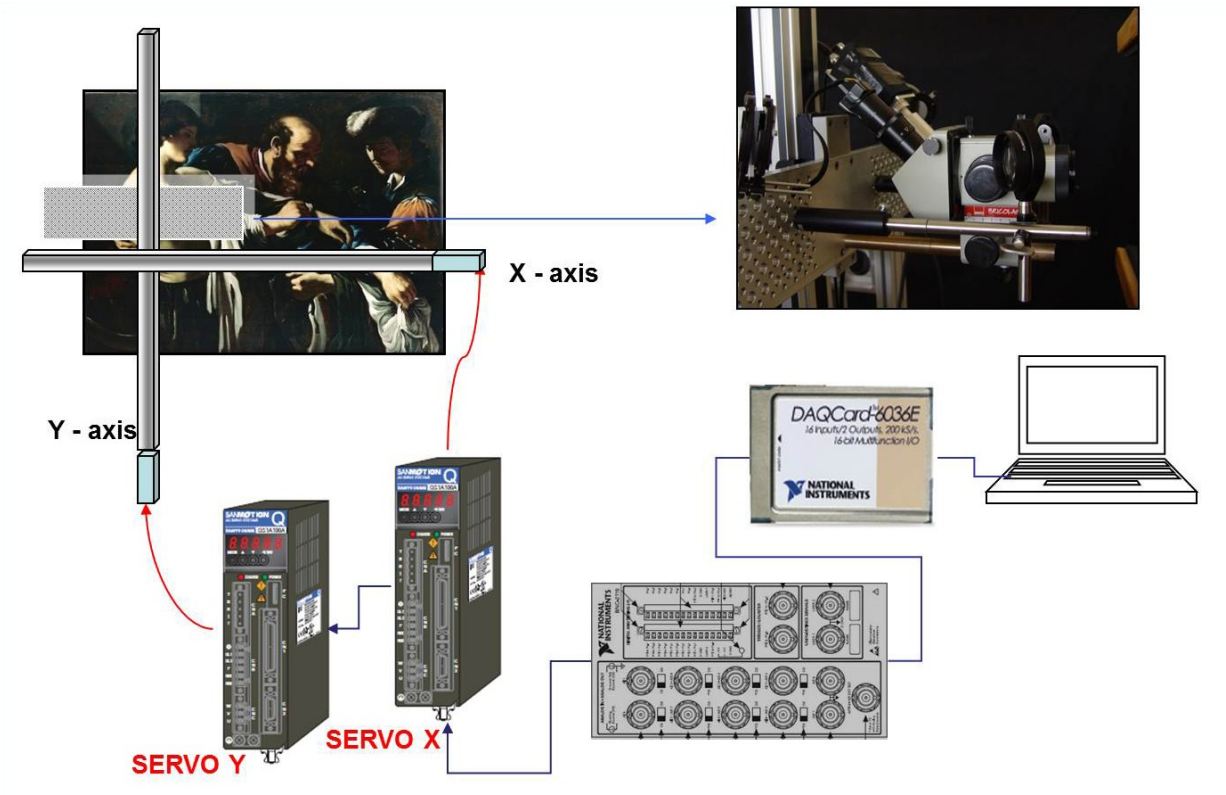

Fig. 198 Summary diagram showing the components of the scanning system (Peccenini, 2012).

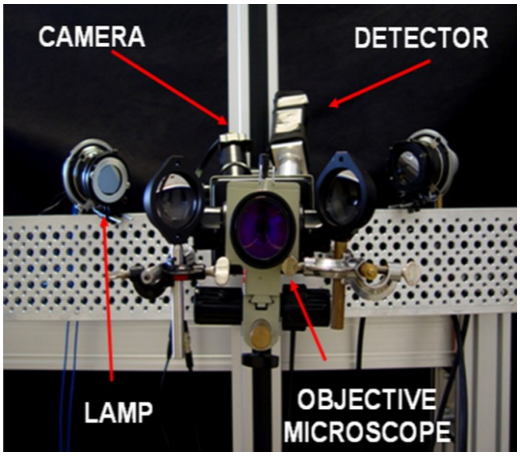

Fig. 199 Diagram showing the optical system (Peccenini, 2012).

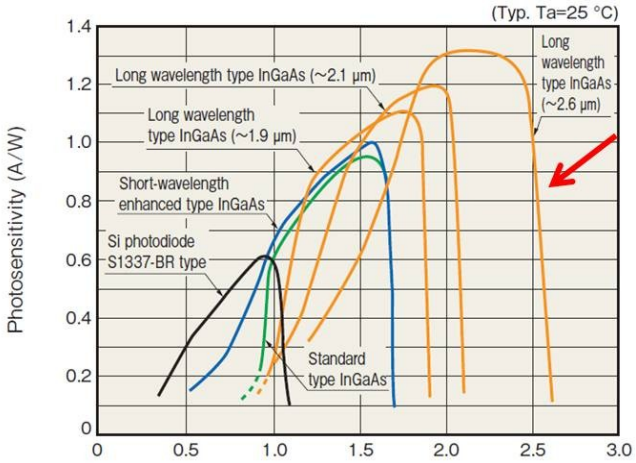

Fig. 200 Specification of InGaAs photodiode, and comparison among spectral responses of various InGaAs photodiodes, by Hamamatsu.
Red arrow indicates the response of K3413-08 model, employed in the scanning system (http://www.hamamatsu.com/resources/pdf/ssd/ingaas_kird0005e.pdf).

4.1.2 Digital radiography scanner

Digital radiography plays a fundamental role in scientific diagnostics of cultural heritage. As a matter of fact, it makes it possible to reveal the internal structure of a work of art, as well as some features regarding the execution technique and underpainting's information. However, since it is based on X-ray attenuation of materials, it cannot provide any analytical composition about materials. This possibility, otherwise, is offered by another punctual technique, which also employs X radiation: the X Ray fluorescence (XRF), presented below.

At the Larix Laboratory, a digital radiography facility, equipped with a motion system, has been implemented, allowing to scan paintings sized up to 1.5 × 2.5 m^2, thanks to the remote controlled translation (fig. 201).

Fig. 201 The X-ray scanner facility.

The source used is a rotating anode X-ray tube, with Mo anode, operated at a maximum kilovoltage of 49 kV.

Up to year 2012, the detector was a Flat-Panel (C7830DK, Hamamatsu) size 220.8 × 176 mm^2, which allowed an image acquisition with a spatial resolution of 10 lp/mm and an acquisition depth of 12 bit.

Nowadays, all sensor modules contain a two-dimensional CMOS (RadEye200) photodiode array. The detector module consists of a tiled array of two RadEye100 image sensors in a rugged stainless steel enclosure. Such a sensor features 2 million pixels, that is, a 1024x1000 pixel image area with 96 µm pixel size for a roughly 10x10 cm active area.

A scintillator screen, placed in direct contact with the photodiode array, converts incident x-ray photons into light, which in turn is detected by photodiodes.

A shielded cable connects the sensor head (fig. 202) to a separate camera electronics module. Here the analog video signal is processed, digitized to 12 bit resolution, and prepared for transmission to a PC via Gigabit Ethernet link.

The Remote RadEye X-ray camera delivers a typical dynamic range of 4000:1.

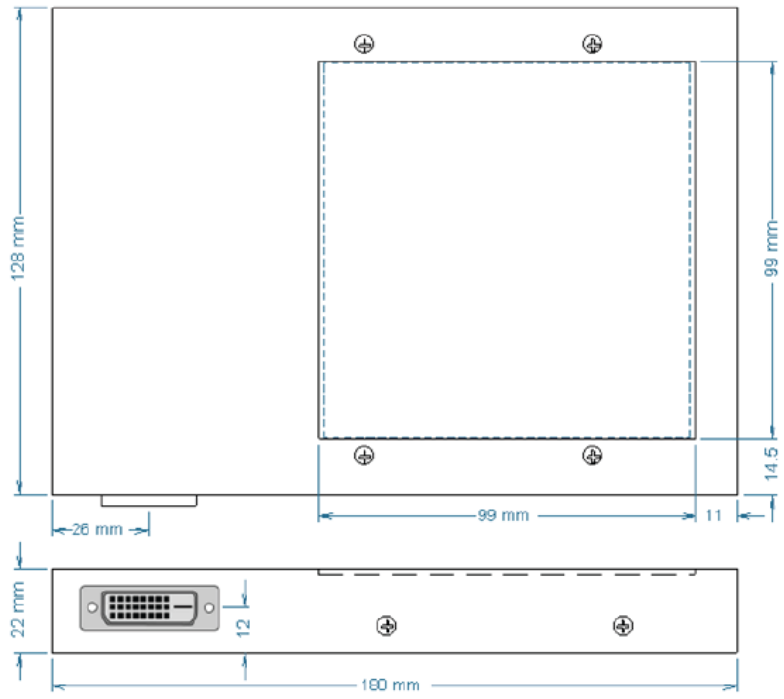

Fig. 202 Remote RadEye200 Sensor Head, showing sizes of the detector (http://www.teledynedalsa.com/imaging/products/x-ray/static-flat/remoteradeye/RM1244/).

4.1.3 K-edge differential radiography

A topographic map of a pigment on the whole surface of a painting can be obtained by means of K-edge technique, originally proposed by R. S. Lehmann for medical applications (Lehmann, 1981) and, in recent years, applied to Cultural Heritage (Albertin, 2008).

Such a technique takes advantage of the sharp rise of X-ray absorption coefficient of an element, that is, its K-edge discontinuity (fig. 203).

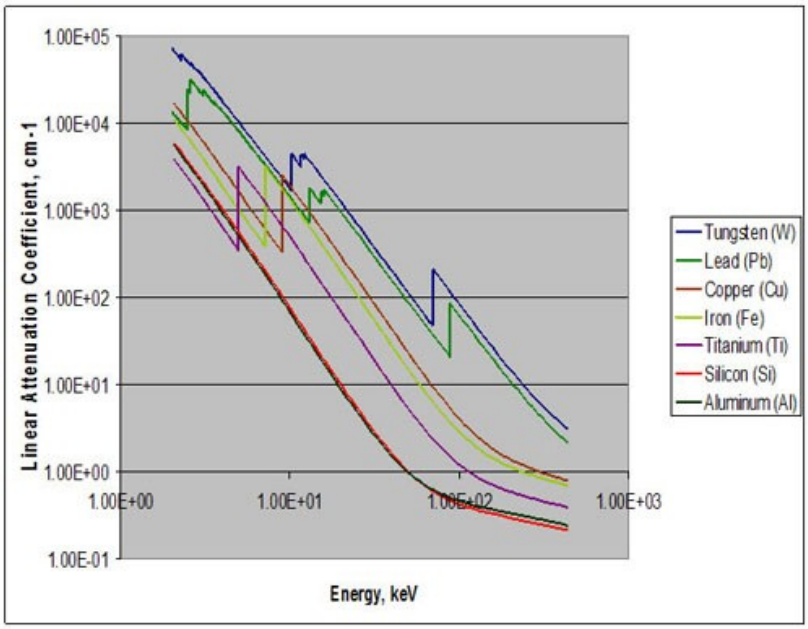

Fig. 203 K-edge radiography takes advantage of the sharp rise of X-ray absorption coefficient of the investigated element. In the diagram above, examples of some elements are shown (http://blog.sciencenet.cn/blog-870939-665414.html).

Two images obtained with monoenergetic X-rays, below and above the K-edge of a chemical element, are different for the higher absorption of that element above its edge.

Subtracting pixel-by-pixel those images, the presence of that element is easily recognizable, even if it is present in small amounts. So, Lehmann algorithm optimizes the image processing, giving mass density distribution (g/cm^2) of the target element.

Attenuation of monoenergetic X-rays of energy E, in a layer containing element *i*, is given by:

$$N(E) = N_0 (E) \exp \{ - [\mu/\rho (E)]_i (\rho \cdot t)_i \} \quad (a),$$

where:

N = transmitted photons number per unit of area, corresponding to image acquired for sample ,

N_0 = incident photons per unit of area, that correspond to white field image ,

μ/ρ (E) = mass attenuation coefficient ,

ρ_i = density of element *i* ,

t = thickness of the layer .

The Lehmann idea is that, provided the energy of X-rays is close to the K-edge of that element, the previous formula may be written considering only the element *i* and all other materials as a whole:

$$N(E_{\pm}) = N_0 (E_{\pm}) \exp \{ - [\mu/\rho (E_{\pm})]_i (\rho \cdot t)_i - [\mu/\rho (E_{\pm})]_{other} (\rho \cdot t)_{other} \} \quad (b)$$

This is a system of two equations and may be solved for two variables: $(\rho \cdot t)_i$ and $(\rho \cdot t)_{other}$:

$$(\rho \cdot t)_i = \{ [\mu/\rho (E_-)]_{other} \cdot \ln N_0/N (E_+) - [\mu/\rho (E_+)]_{other} \cdot \ln N_0/N (E_-) \} / K_0 \quad (c)$$

$$(\rho \cdot t)_{other} = \{ [\mu/\rho (E_-)]_i \cdot \ln N_0/N (E_+) - [\mu/\rho (E_+)]_i \cdot \ln N_0/N (E_-) \} / K_0 \quad (d)$$

$$K_0 = [\mu/\rho (E_-)]_{other} \cdot [\mu/\rho (E_+)]_i - [\mu/\rho (E_+)]_{other} \cdot [\mu/\rho (E_-)]_i \quad (e)$$

where:

(E_-) = energy (of monocromatic beam) lower than the K-edge ,

(E_+) = energy (of monocromatic beam) higher than the K-edge .

This is the solution called Lehmann algorithm. Two images can be obtained: the first one (c) is related to target element *i* (e.g., Cd), and the other one (d) concerns any other material represented in the layer.

The K-edge radiography facility installed at Larix Laboratory consists of a quasi-monochromatic beam, produced by Bragg diffraction of a mosaic graphite crystal (HOPG, Optigraph GmbH) with an area of 60 × 28 mm^2, 2 mm thick. Such a type of crystal allows a greater efficiency, taking from the monochromaticity of the beam (13 keV, 0:45 keV FWHM) (Baldelli, 2005).

Source and crystal are mounted on two motorized goniometers, allowing to vary the angle of incidence and, consequently, the energy of the output beam.

The differential system for radiography used an X-ray tube molybdenum anode, generating X-ray beams at high flux (up to 110 μA), in the range of 8-40 kV, according to the diagram shown in fig. 204.

The detector used for acquisitions, was a CCD (S7199, Hamamatsu), sized 150 x 6 mm^2, consisting of 3075 x 128 pixel pitch of 50 um, allowing to perform radiographies with a resolution of 10 lp / mm, and with a depth of 14 bits.

In figure 124, an example of K-edge differential radiography application on a painting, is shown.

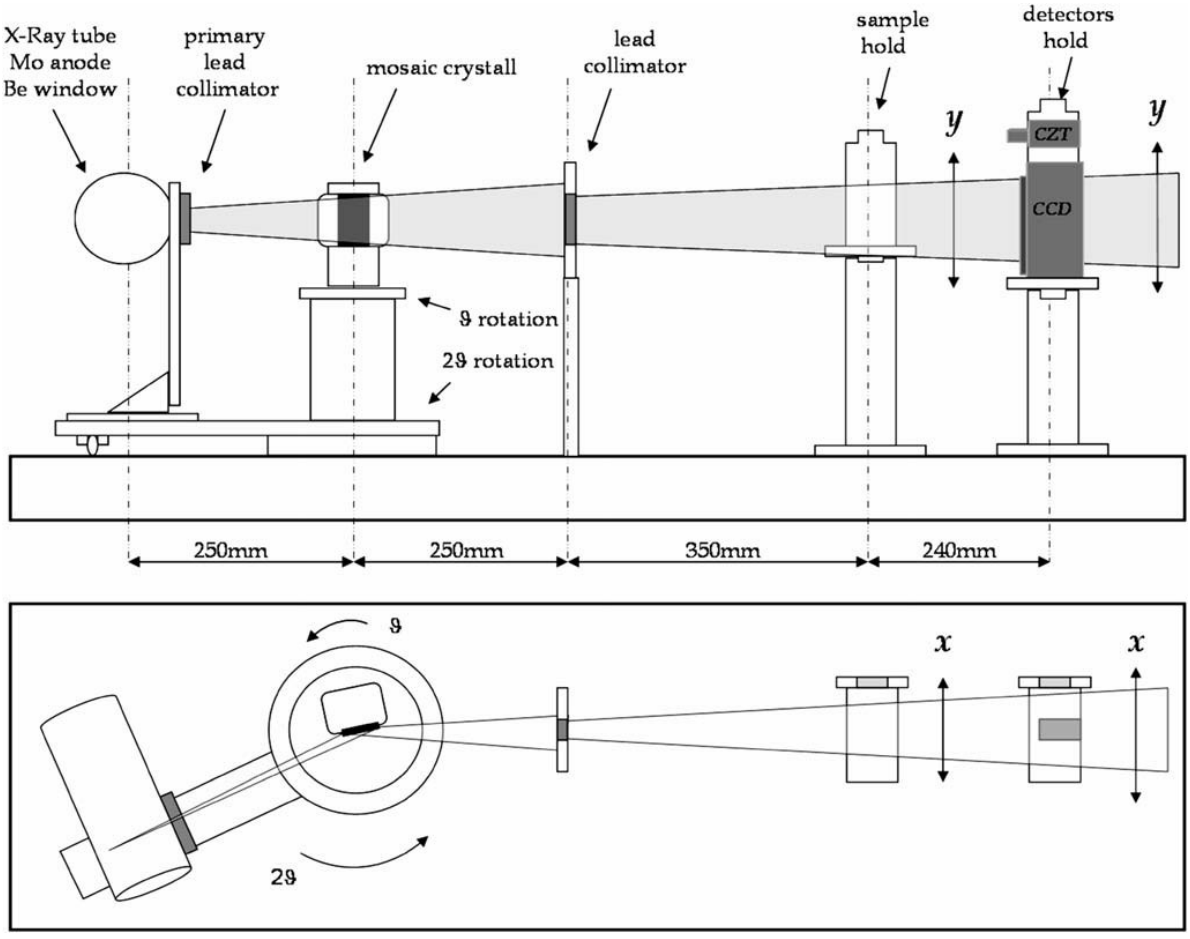

Fig. 204 The K-edge facility (Albertin, 2011 (b)).

4.1.4 Image spectroscopy

Image spectroscopy is a technique based on the digital acquisition of several images, at different wavelengths.

The device used for works presented here operates in the visible and near infrared spectral range (410 – 970 nm), and allows to obtain spectra reflectance factor of the surface, without a contact with it.

Portability and flexibility are important features of this device, allowing to perform *in situ* analysis of image spectroscopy.

The instrument used is a Pulnix TM-1325 *CL*© monochrome digital camera, equipped with a 1392 x 1040 pixel CCD (fig. 205a-b). A narrow band optical filter is placed in front of the camera, in order to spectrally select the light. Fifteen interferential filters, 10 nm FWHM bandwidth are used for multispectral imaging (fig. 206).

With such a device, spectral data are collected with a 40 nm sampling pitch, with exceptions for a better recognition of some pigments, as in the range between 670 and 750 nm.

Two 650 W halogen lamps are used so that light is collected in a 2x45°/0° geometrical configuration.

Seven Spectralon© diffuse reflectance standards (2%, 5%, 10%, 20%, 50%, 75%, 99%) by Labsfere Inc., are included in each framing, as references for reflectance determination (fig. 207).

Images obtained can be stored as 8-bit TIFF files (fig. 208), and each of them is averaged over 20 frames, in order to reduce incoherent noise. The same processing is reserved to the acquisition of white field images, these taken on a smooth cardboard, to correct the non-uniformity.

Images are captured and stored by a National Instrument NI PCI-1428 frame grabber, guided by dedicated software and developed in *Labview*© platform. The PCI card is hosted in a metal case and coupled, by means of a PCI-express card, to the PC.

Finally, image sequence processing is performed by Tele32 software, where calibration and correction operations of the images takes place by means of suitable algorithms, that finally enable to obtain spectra about radiation reflected from each zone (Pellicori, 2013).

The aim is to prevent possible discoloration of the painting, by identifying it earlier than the human eye. This objective, useful for each artefact, is particularly important for contemporary art, which is often made with innovative materials, whose durability is not known.

Fig. 205a Image spectroscopy device, equipped with Pulnix TM-1325 camera

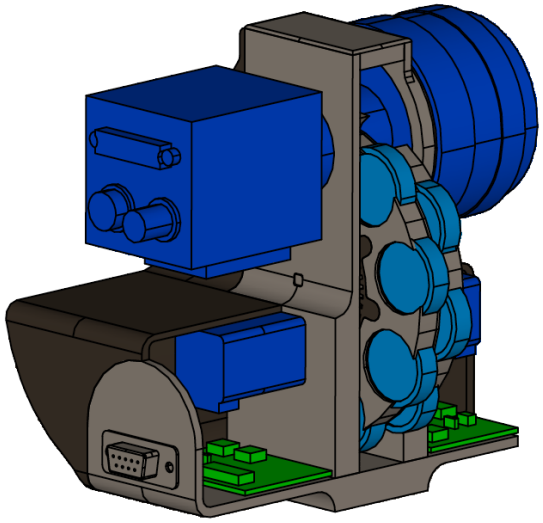

Fig. 205b Diagram showing the internal configuration of the device.
The two-wheel system, with eight places for the interferential filters, are shown.

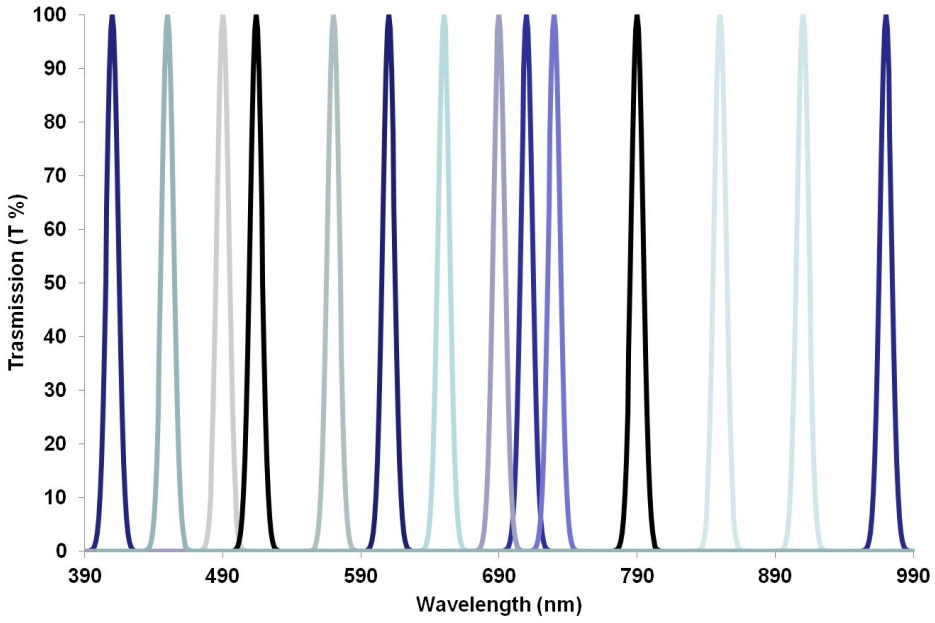

Fig. 206 The fifteen interferential filters, 10 nm FWHM bandwidth, used for multispectral imaging (Pellicori, 2013).

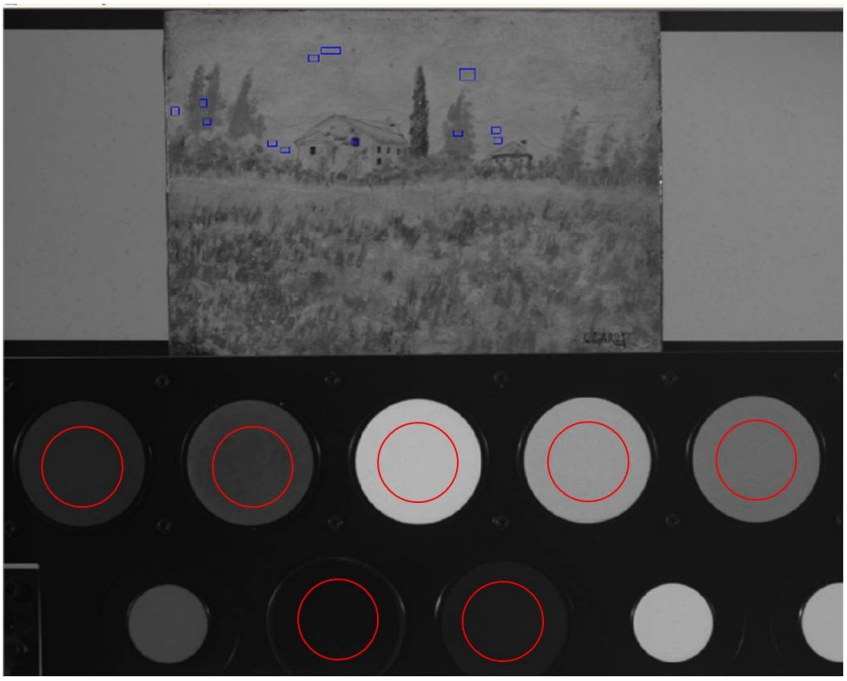

Fig. 207 Spectralon diffuse reflectance standards (2%, 5%, 10%, 20%, 50%, 75%, 99%), included in each framing, as references for reflectance determination (Pellicori 2013).

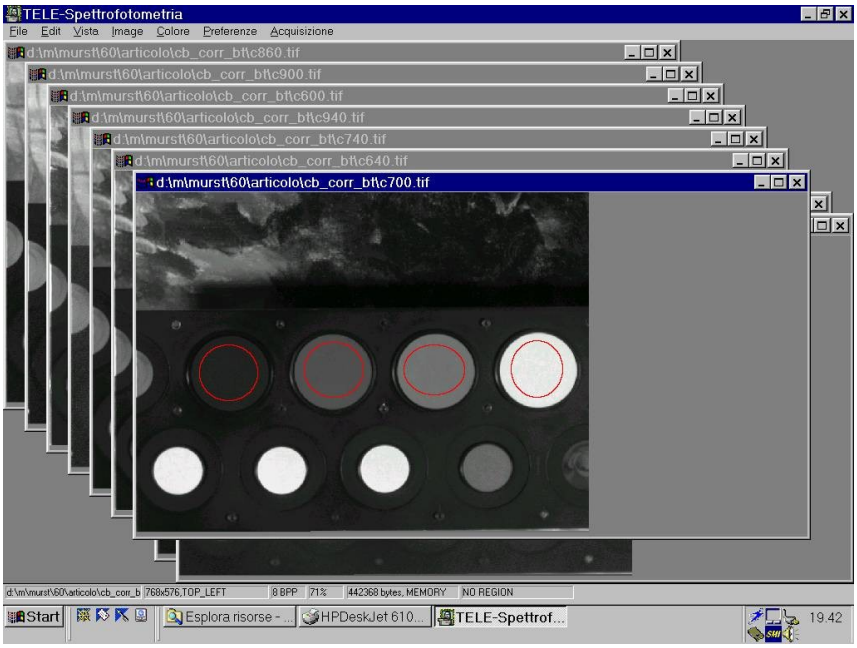

Fig. 208 Images obtained each 40 nm can be stored as 8-bit TIFF files.

To sum up, a sequence of multispectral images is acquired by means of the spectroscopy device. Subsequently, the spectral reflectance factor of every detail of the painting acquired in the photos, can be obtained from images. Repetition of measurements can be done over time, and a comparison of spectra obtained is then performed by means of multivariate analysis. Such a statistical method is useful in order to detect minimal systematic variations and, thus, to determine tendential alterations.

4.2 Commercial instruments

4.2.1 X Ray florescence (XRF)

Such a technique proved to be an advanced instrument for fast, accurate and non destructive analysis in the characterization of pictorial materials.

As a matter of fact, XRF (X Ray fluorescence) non invasively detects the constituent chemical elements of the examined area (points), through analysis of the characteristic X Ray fluorescence radiation emitted from elements, as a result of atomic excitation with appropriate energy.

The characteristic radiation emitted is thus revealed as a function of its energy (EDXRF, energy dispersive XRF) by a solid state detector (SSD), capable of detecting in a single measure, all detectable elements present in the analyzed area. In fact, the detector transforms the X-ray photons at different energy into electrical pulses of different amplitde. These are collected and analyzed, allowing to reconstruct and analyze the XRF spectrum of the sample.

The system used is a portable spectrometer Bruker ARTAX 200 Micro-EDXRF (figs. 209, 210) with the following characteristics: X-ray source with a Mo anode, tunable anode voltage from 0 to 50 kV; anodic current 0 up to 1500 μA (maximum power 50 W).

According to the particular type of artwork, it is possible to set up different measure options. In the works presented in here, the typical voltage setting is 50KV and the acquisition time ranges between 60 and 120 seconds. A Helium flux is enabled to recognize lighter elements (like *Potassium*, *Aluminum*, *Magnesium*), in the lower range (1 up to 10 KeV) of energy, lowering the absorption of air between target and detector.

Fig. 209 The XRF device.
Positioning of the instrument on a painting, on different areas to be investigated.

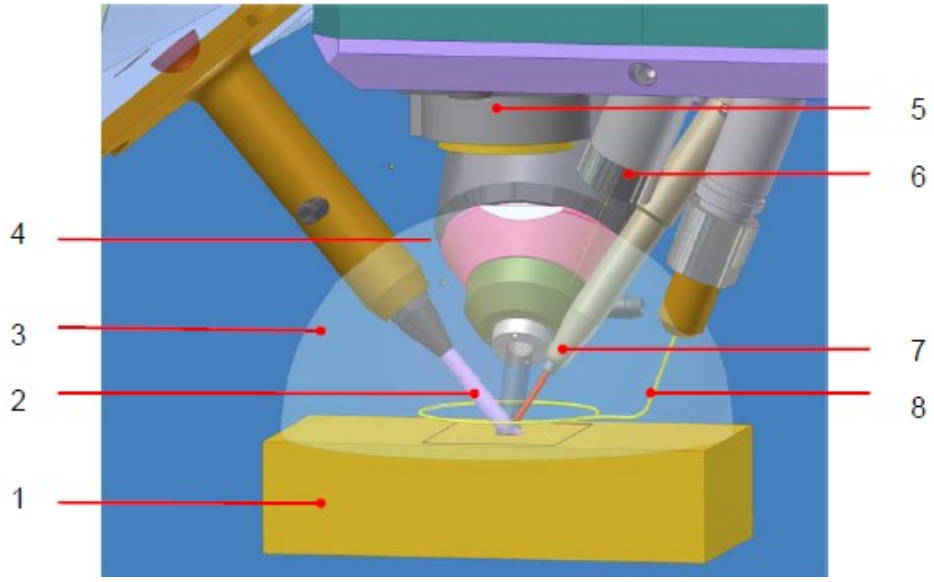

Fig. 210 Diagram showing the component parts of excitation and positioning (Artax manuals, Bruker).

1 Sample
2 X-ray excitation beam
3 X Ray fluorescence and scattered radiation
4 Radiation registered by detector
5 CCD camera
6 Sample lighting
7 Laser pointer for positioning
8 Collision sensor

Spectra obtained show the count rate of each element in the selected range, according to the characteristic energy of emitted X rays (fig. 211).

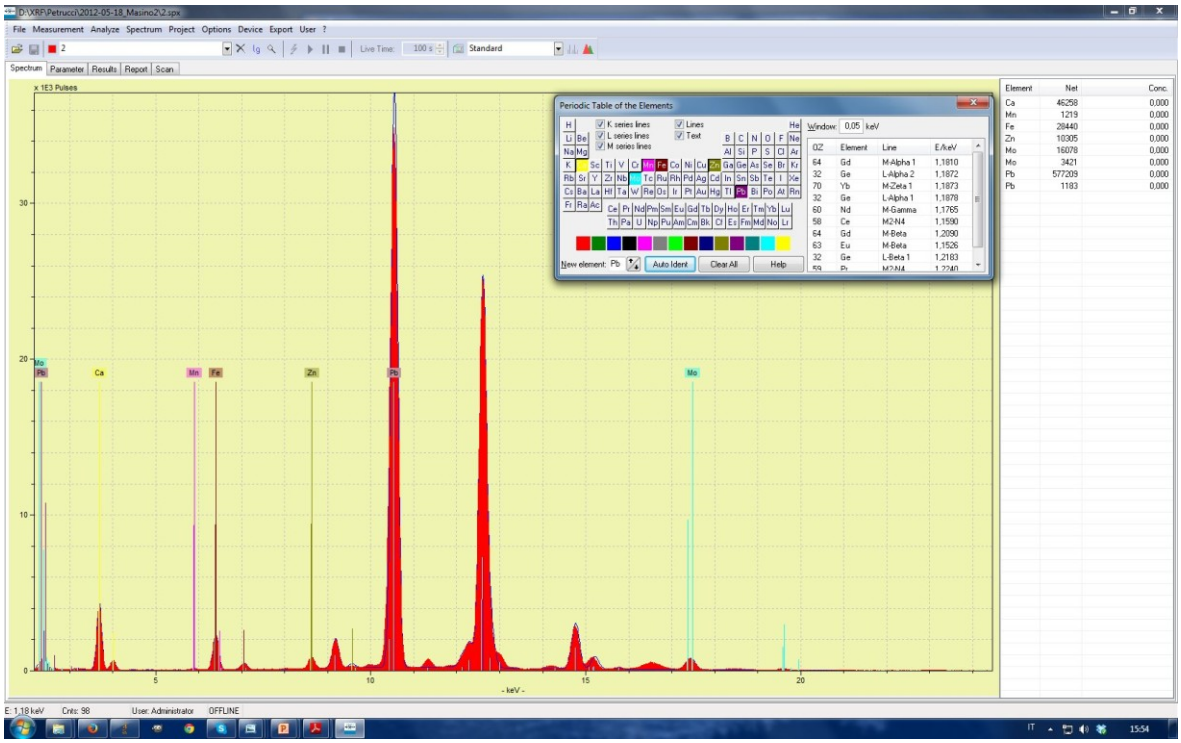

Fig. 211 Example of a XRF spectrum relating to an investigated point.

4.2.2 VIS Spectrophotometer

Reflectance spectroscopy is the optical investigation technique, based on measurement of the reflected light from a surface. The reflectance parameter is defined as the ratio of intensities between the incident ($\mathbf{I_0}$) and the reflected radiation ($\mathbf{I_R}$), at each wavelength:

$$\rho = I_R / I_0 .$$

Measurements reported here were carried out with a spectrophotometer Konica-Minolta mod. CM-2600d (fig. 212a-b).

It is a widely used instrument in the field of Cultural Heritage, for its ease of use, accuracy and repeatability of measurements. It has a d/8° measurement geometry, and allows to acquire reflectance spectra and colorimetric data in the range 360-740 nm, with a sampling interval of 10 nm. Measures can be acquired (with an instrumental error of 0.5%), both as total reflectance included specular component (SCI) and as diffuse reflectance excluding specular component (SCE).

Colorimetric data obtained from the reflectance values can be reported, in numerical form, as L*, a* and b* (Oleari, 1998).

The instrument internally consists of:

- Internal Light Source: 3 pulsed xenon flash lamps.
- Diffraction grating.
- Sensor: consists of silicon photodiodes, which collects the radiation dispersed by the grating.
- Integrating sphere: cavity internally treated with highly diffusive material, with the function of making the measurement independent of the geometry of illumination.

Each acquisition includes two sets of data: one, in total reflectance also includes the specular component (SCI), and the other, in diffuse reflectance, which excludes the specular component (SCE). This measurement mode, is obtained by the software, subtracting the spectrum of SCI data, the spectral measurements of the specular component (fig. 213a-b).

It is also possible to get measures excluding the portion of the ncdent ultraviolet spectral range 360-400nm, to avoid fluorescence effects.

The device has two different "masks" with two opening sizes, depending on the area to investigate, 3 or 8 mm in diameter. The acquisition of these measures is also remotely

possible. In this case, the instrument is managed by the computer, using the Spectra Magic® software.

The calibration of the instrument, preliminary to data collection, is made for both the white, and the black targets.

Fig. 212a Spectrophotometer mod. CM-2600d Konica-Minolta (http://www.konicaminolta.com/).

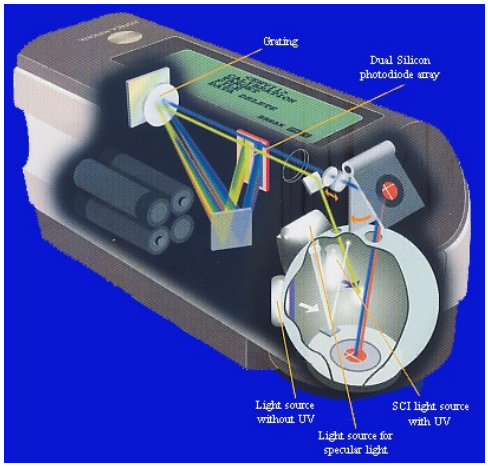

Fig. 212b Diagram of the internal constituent parts of the spectrophotometer (CM-2600d, Konica Minolta © 2001).

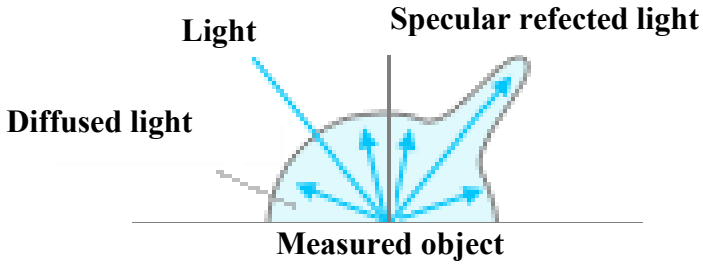

Fig. 213a Diagram showing both the specular and the diffused components of the reflected light.

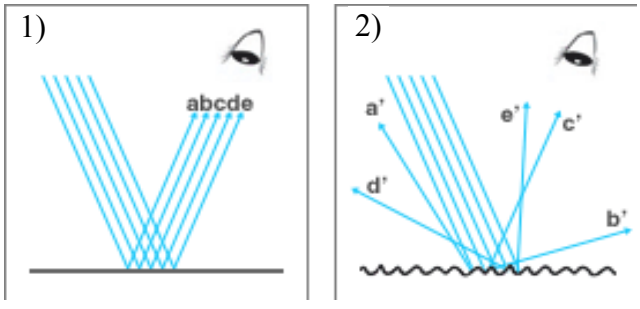

Fig. 213b SCI mode for total reflectance, data, including the specular component (1). SCE mode is used for diffuse reflectance, which excludes the specular component (2).

4.2.3 Wood lamp for ultraviolet fluorescence

Stimulation of visible light through ultraviolet excitation plays an important role among the diagnostic methods of investigation, and is widely used thanks to the immediacy of the response, the practicality and ease of use.

This technique allows to analyze the upper layers of a work of art, usually interested by the application of varnish, traditionally functional to protect the painting from external agents.

The work is placed under an ultraviolet light source (Wood lamp), which induces fluorescence - just observable in visible light - on painting materials (fig. 214).

Observation of ultraviolet fluorescence highlights the presence of the materials which is not clearly distinguishable in visible light, indicating non-homogeneous situations (accumulations in layers), not otherwise detectable.

Particularly, oldest varnishes usually produce a more intense fluorescence, on which subsequent restorations show up as dark areas.

Fig. 214 While performing ultraviolet florescence on Vedova's painting *Untitled*, with a Wood lamp, at *Casa Museo Remo Brindisi*.

4.2.4 Digital camera for infrared reflectography

As already mentioned before, infrared reflectography is an important technique for non-destructive examination of painted surfaces and, particularly, of preparatory drawings, *pentimenti*, writings and inscriptions, signatures and dates lying below the pictorial film.
This happens because of the lower diffusion suffered by near infrared radiation, whose wavelength is between 0.8 and 2 μm, in the paint layers, respect to visible light.

A Sony DSC-F717 digital camera (fig. 215) was used for the investigations, though in a limited infrared spectral range. It is a practical device to be used, allowing to acquire digital photos in both the near infrared and the visible range, simply by setting – or not – the "NightShot" mode.
This consists in the possibility of removing the internal filter, which normally cut off the infrared component of the incoming radiation, by a simple mechanical switch on the camera. In addiction, an appropriate filter (Schott glass filter RG-950) can be placed or removed over the lens.
In fig. 217a-b, a detail of a painting (fig. 216) is shown, comparing acquisitions obtained by both the Si CCD detector of the digital camera, and by the InGaAs detector, mounted on the scanning device (4.1.1). The greater penetration ensured by the InGaAs detector, makes more visible the strokes of the preparatory drawing.

Fig. 215 Sony photo camera (Cyber Shot F717) with Si CCD for IR reflectography and the IR filter (F.2 - 950 nm).

Fig. 216 G. Nardozzi, Flowers, 1889, oil on paper, private collection.

Fig. 217a-b Comparison of a detail. a) IR Reflectography acquired by Si CCD; b) IR Reflectography acquired by InGaAs detector (Peccenini, 2012).

Conclusions

Non invasive investigations proved to be useful by giving, for each artwork, different results, always aimed at better understanding the manufacturing of works of art.
On each different investigated work of art, different "knowledge questions" moved the investigations, that were differently applied and integrated, to better respond to various issues.
A further confirmation that, while working with non invasive techniques, an interdisciplinary approach, based on the complementarities of data obtained, must be adopted.

There are many aspects that may be drawn by the experiences described in this thesis. Among these, one regards the type of work of art and, in particular, the support. So, lightweight supports such as paper, for example, are well suited to be observed under the microscope, returning spectacular images when illuminated with raking light.
Anyhow, a normal diagnostic procedure always starts from the observation, of both the whole and the details, of the work to be studied. To a first photographic documentation, in raking and reflected light, that is, visible light, the use of different radiations, from the least to the most penetrating, follows.
So, ultraviolet fluorescence is useful in detecting the upper layers, constituted by varnish and retouches, or simply in differentiating the superficial pictorial materials.
Infrared reflectography, both in narrow and in wide range, gives data about the evolution of the creative process and, eventually, some stylistic information about the artist's technique.
More in depth, radiographies performed on some artworks allowed to investigate about their internal structure and the relative history and conservative state.
Identification of materials was carried out thanks to punctual techniques such as XRF. Particularly, it allowed to recognize materials containing the heaviest elements of the periodic table, typically present in the inorganic pigments.
Such a sequence of techniques can generally be used as a standard protocol to study ancient works of art.

For contemporary artworks, instead, diagnostic techniques that could be successfully applied, proved to be less numerous. Always moving from the "knowledge questions", that

every artwork posed, a limited number of image techniques were useful, for different purposes. An important issue pertains the identification of the artistic technique and the reconstruction of the creative steps that led to the final result.
As an example, only combining images obtained by raking light, transillumination and ultraviolet fluorescence, it was possible to reconstruct the particular technique adopted by Giulio Turcato, in the realization of his polymateric painting.
The use of hands in applying pure colours, directly from the tube to the canvas, characterizes the painting by Patruno. Features that were well highlighted simply by means of raking light. Moreover, and just in this case, XRF was useful in detecting pure colours, used *as they were*, squeezed out from the tube.
Only thanks to the infrared reflectography, instead, it was possible to detect the preparatory drawing, under the painting *Ettore e Andromaca*, by De Chirico.

Another important issue pertained contemporary materials *as they are*, used both for the realization and the restoration of works of art. This last aspect becomes particularly important for contemporary artworks, on which aging *patinas* and blackening layers often develop with greater rapidity than in ancient works. In addition, exposure conditions for contemporary works of art may be less controlled than those adopted for ancient works, already recognized as cultural heritage.
Just to study more in depth this aspect, the behavior over time of different restoration materials, even in association, applied on test layers and subjected to natural and artificial aging, has been evaluated. Their optical characteristics were investigated by means of imaging techniques and image spectroscopy and, subsequently, statistically organized with mathematical methods, such as the multivariate analysis. It was thus possible to monitor them and, in some cases, the possible deterioration occurred and/or in progress.

A further, practical experience accompanied the main topic of scientific investigations applied on artworks and materials. Such an experience was aimed at the realization of a prototype of dome, to be associated to a microscope. At this early stage of the work, the final objective was to create a device in which constant conditions of illumination and observation were guaranteed. A realization that was especially addressed to prints and paper samples, as the experience took place at the Centre for Fine Print Research, Bristol.

Overall, both ancient and contemporary artworks were investigated, sharing the nature of unique artworks, setting diversified objectives and requiring thus particular techniques.

Pubblications

- Albertin, 2008
  F. Albertin, M. Gambaccini, F. Petrucci, M. Gargano, N. Ludwig, M. Milazzo, F. Pedrielli, S. Chiozzi, F. Evangelisti
  Nuove applicazioni della radiografia digitale alla diagnostica dei dipinti
  Elettroottica 2008, Milano, B3.3

- Albertin, 2011 (a)
  Albertin F., Boselli L., Peccenini E., Pellicori V., Petrucci F., Tisato F.
  Spettroscopia in riflettanza per il monitoraggio di materiali pittorici contemporanei
  Atti della VII Conferenza Nazionale del Gruppo del Colore SIOF, Ed. Maggioli, Rimini, 2011, 576-583

- Albertin, 2012 (a)
  Albertin F., Boselli L., Peccenini E., Pellicori V., Petrucci F., Tisato F.,
  Image diagnostics on some paintings of the Remo Brindisi Collection
  Proceedings of the Meeting Science for Contemporary art - Ferrara 2011, Ed. Patron, Bologna, 2012, 19-27

- Albertin, 2012 (b)
  Albertin F., Boselli L., Peccenini E., Pellicori V., Petrucci F., Tisato F.
  Image Spectroscopy for conservation and diagnostics of contemporary painting materials
  Proceedings of the Meeting Science for Contemporary art - Ferrara, Ed. Patron, Bologna, 2012, 93-102

- Albertin, 2012 (c)
  Albertin F., Boselli L., Labate M., Peccenini E., Pellicori V., Petrucci F., Tisato F.
  Caratterizzazione dei materiali di un dipinto mediante radiografia differenziale al K-edge e XRF
  Atti del VII Congresso Nazionale di Archeometria (A.I.Ar.) 2012 - Modena, Ed. Patron, Bologna, 2012, PIG-P-2

- Albertin, 2013
  F. Albertin, L. Boselli, S. Chiozzi, E. Peccenini, V. Pellicori, F. Petrucci, G. Poldi, F. Tisato
  La radiografia e le diagnostiche fisiche del dipinto Madonna con Bambino tra San Rocco e San Sebastiano di Giovanni da Mel
  Progetto Restauro, Il Prato Editore, Padova, 2013, 40-48

- Adrover Gracia, 2010
  Adrover Gracia I., Bevilacqua N., Borgioli L.
  I pigmenti nell'arte dalla preistoria alla rivoluzione industriale
  Collana I Talenti, Il Prato Editore, Padova, 2010

- Armanino, 2011
  Armanino C., Casale M., Casolino C., Forina M., Lanteri S., Olivieri P.
  Chemometrics with PARVUS
  School of Chemometrics 2011, Genova University, Genova, June 6th-9t^{th} 2011

- Baldelli, 2005
  Baldelli P., Gambaccini M., Gilardoni M. C., Taibi A., Tuffanelli A.
  A prototype of a quasi-monochromatic system for mammography applications
  Phys. Med. Biol. 50, 2005, 2225-2240

- Briganti, 1991
  Briganti G.
  De Pisis. Catalogo generale
  Electa Mondadori (collana I moderni e i contemporanei), Milano, 1991

- Chiantore, 2005
  Chiantore O., Rava A.
  Conservare l'arte contemporanea. Problemi, metodi, materiali, ricerche
  Electa Mondadori, Milano, 2005

- Frezzato, 2009
  Frezzato F.
  Il libro dell'arte di Cennino Cennini
  Ed. Neri Pozza, Vicenza, 2009

- Heck,1987
  Heck A., Murtagh F.
  Mutivariate Data Analysis
  Astrophysics and Space science library, D. Reidel Publishing Company, Great Britain, 1987

- Holakooei, 2014
  Holakooei P., Petrucci F., Tisato F., Vaccaro C.
  Haft rang or cuerda seca? Spectroscopic approaches to the study of overglaze polychrome tiles from seventeenth century Persia
  Journal of Archaeological Science, 41, 2014, 447-460;
  http://dx.doi.org/10.1016/j.jas.2013.09.011

- Lehmann, 1981
  Lehmann L.A., Álovarez R.E., Macovsky A., Brody W.R.
  Generalized image combinations in dual KVP digital radiography
  Med. Phys., 8(5), 1981, 659-667

- Maltese, 2005
  Maltese C.
  Le tecniche artistiche
  Ed. Mursia, Milano, 2005

- McCallion, 2014
  Hoskins S., McCallion P.
  Continuous tone printing in silicone from CNC milled matrices
  Proc. SPIE 9018, Measuring, Modeling, and Reproducing Material Appearance, 90180O (February 24, 2014); doi:10.1117/12.2043123; http://dx.doi.org/10.1117/12.2043123

- Moioli, 2002
  Moioli P., Seccaroni C.
  Fluorescenza X. Prontuario per l'analisi XRF portatile applicata a superfici policrome
  Collana Arte e Restauro, Nardini Editore, Firenze, 2002

- Oleari, 1998
  Oleari C., A cura di
  Misurare il colore. Spettrofotometria, fotometria e colorimetria. Fisiologia e percezione.
  Hoepli Ed., Milano, 1998

- Parraman, 2014 (a)
  Parraman C.
  The visual appearance and surface texture of materials according to the old masters
  Proc. SPIE 9018, Measuring, Modeling, and Reproducing Material Appearance, 90180H (February 24, 2014); doi:10.1117/12.2041216; http://dx.doi.org/10.1117/12.2041216

- Parraman, 2014 (b)
  Parraman C., Tisato F.
  An investigation into the micro surface of artworks using alternative lighting techniques
  Proc. SPIE 9018, Measuring, Modeling, and Reproducing Material Appearance, 901808 (February 24, 2014); doi:10.1117/12.2041209; http://dx.doi.org/10.1117/12.2041209

- Petrucci, 2004
  Petrucci F.
  Image spectroscopy for diagnostics and conservation of contemporary art
  Proceedings of the Internaytional School of Physics "Enrico Fermi", Course CLIV, Physics methods in Archaeometry, Società Italiana di Fisica, Bologna, 2004, 331-345

- Piraccini, 2005
  Piraccini O., A cura di
  Casa Museo Remo Brindisi. Una collezione d'artista
  Editrice Compositori, Bologna, 2005

- Poldi, 2006
  Poldi G., Villa G.C.F.
  Dalla conservazione alla storia dell'arte - Riflettografia e analisi non invasive per lo studio dei dipinti
  Edizioni della Nomale, Pisa, 2006

- Siqueiros, 1976
  Siqueiros D. A.
  Dipingere un Murale
  Fabbri Editore, Milano, 1976

Websites

- A 3D scan of Van Gogh to create the perfect replica
  http://www.whiteboardmag.com/3d-scan-van-gogh-perfect-replica-formart/

- http://en.wikipedia.org/wiki/Bidirectional_scattering_distribution_function

- http://www.konicaminolta.com/

- http://www.konicaminolta.com/instruments/knowledge/color/index.html

- http://blog.sciencenet.cn/blog-870939-665414.html

- http://www.teledynedalsa.com/imaging/products/x-ray/static-flat/remoteradeye/RM1244/

Theses

- Albertin, 2011 (b)
  Albertin F.
  K-edge radiography and applications to Cultural Heritage
  Tesi di Dottorato in Fisica, Anni Accademici 2009-2011

- D'Avossa, 2012
  D'Avossa E.
  "Donna in lettura sul letto ed anziano". Valutazione con metodi non invasivi dello stato di conservazione del dipinto
  Tesi di laurea triennale (Corso in Scienze e Tecnologie per l'ambiente, la natura e i Beni Culturali – Università di Ferrara), Anni Accademici 2011-2012

- Del Farra, 2013
  Del Farra A.
  Characterization of XVI Century Pigments from the Veneto Region through Micro-Invasive Analysis
  Tesi di laurea triennale (Corso di laurea in Scienze Chimiche – Università di Ferrara), Anni Accademici 2012-2013

- Farioli, 2012
  Farioli V.
  Desco da parto: tipologia di manufatti artistici del XV secolo e diagnostica di un caso esemplificativo
  Tesi di laurea in Scienze e Tecnologie per l'ambiente, la natura e i Beni Culturali – Università di Ferrara , Anni Accademici 2011-2012

- Holakooei, 2013
  Holakooei P.
  Technological study of the seventeenth century *haft rang* tiles in Iran with a comparative view to the *cuerda seca* tiles in Spain
  Tesi di Dottorato in Scienze e Tecnologie per l'Archeologia e i beni Culturali, Anni Accademici 2010-2012

- Labate, 2011
  Labate M.
  Valutazione delle proprietà ottiche di consolidanti per restauro conservativo tramite tecniche fisiche non invasive
  Tesi di laurea triennale (Corso in Tecnologie per i Beni Culturali – Università di Ferrara), Anni Accademici 2010-2011

- Pasetti, 2002
  Pasetti L.
  Studio di un sistema di acquisizione di immagini multi spettrali per la diagnostica di opere d'arte
  Tesi di laurea in Fisica, Anni Accademici 2001-2002

- Peccenini, 2012
  Peccenini E.
  *2013***A scanning device for wide band infrared reflectography**
  Tesi di Dottorato in Fisica, Anni Accademici 2009-2011

- Pellicori, 2013
  Pellicori V.
  Image spectroscopy for diagnostic and conservation of contemporary art materials
  Tesi di Dottorato in Fisica, Anni Accademici 2010-2012

- Petitta, 2012
  Petitta B.
  Relazione di laboratorio
  Laboratorio di Archeometria, Corso in Scienze e Tecnologie per l'ambiente, la natura e i Beni Culturali, Università di Ferrara, Anni Accademici 2011-2012

Aknowledgements

Firstly, I need to thank the Physics and Earth sciences department, University of Ferrara, in the persons of Mauro Gambaccini and Roberto Calabrese, past and present directors of the Department, for hosting me in these three years. Many thanks also go the INFN (National Institute for Nuclear Physics, Section of Ferrara) and to TekneHub (High Technology Network, Emilia Romagna) for giving me the possibility to use the equipment.

The numerous works undertaken and developed over these three years gave me the opportunity to meet many people. And to grow, because from each of them I've learnt something valuable.
My deep gratitude goes to Professor Ferruccio Petrucci, a constantly present reference point. For his way, always respectful and unexceptionable, to face each issue. For his availability and the lucidity to find out always reasonable solutions. I really hope I can continue to work together much longer.
I shared this experience with Lara Boselli, Fauzia Albertin, Eva Peccenini and Virginia Pellicori. From and with them, I realized even more, that different ways to approach things can lead to very good results, always improvable. Thank you girls.

I am deeply grateful to Carinna Parraman, for welcoming me with warmth and kindness, and for having followed me with dedication during the internship at the *Centre for Fine Print Research* in Bristol. And... for sharing the pictures of Gromits... I am also very thankful to Peter and Peter, Linsay, Katie, Melissa, Cecilia, Angie, Sarah and Sarah, Steven, David, Paul and Paul, Jesse, Joanna, Tom, Chris (who very kindly 3D printed the basis for the dome), and to Grace and Nick and all the others, for welcoming me so warmly.
In addition, I would like to thank in a very special way Victoria, Poppy and Ned, for making me feel at home. Thanks to all of these special persons I felt pampered.

I am also grateful to my other referees, Prof. Aurelio Climent Font (University autonoma Madrid), and Arch. Antonio Rava (Torino), for reading and giving their opinions on my thesis.

Thanks to Maria Labate, Parviz Holakooei, Veronica Farioli, Emanuela D'Avossa, for the great work they've done in preparing their Master and PhD theses, to which, if only for a small part, I participated. Part of these work is presented in this thesis.

A big thanks goes to Laura Ruffoni and all the staff of the *Casa Museo Remo Brindisi*, to the architects Michela Biancardi, Alessandro Massarente (University of Ferrara), to Dr. Gaia Cammarata, to the Municipality of Comacchio and all the other people involved in the projects. All of them share the efforts for the valorisation and the preservation of the Heritage in the *Casa Museo*.

... Last but not least, I know that my family is always here, even if somebody from afar...
I am deeply grateful to my parents, Laura and Gianluigi, because if I am what I am, that's also because of them. Thanks to my lovely and wise little sister Chiara, that I am very proud of.
To put into words how I feel right now is very difficult. But the special persons I've met in these three years made me stronger and more aware of myself. Each having their own way. Special persons, to me, are many...
Some of them are solar and laugh heartily, never make me feel alone, even if far away. Some of them teach me to fight for an objective, to complicate my life or, sometimes, to make it easier.
Somebody comes from India and is very wise, some of them are obstinate and put soul into everything they do.
They are simple and curious and hungry for new things, and they want to make better both the present and the future.
And someone, Enrico, the most special of all, has made and is making happen something very big and has simply changed my life...

Grazie!

... I Lestrigoni e i Ciclopi
o la furia di Nettuno non temere,
non sarà questo il genere di incontri
se il pensiero resta alto e un sentimento
fermo guida il tuo spirito e il tuo corpo.

... The Lestrygonians and the Cyclops,
the angry Poseidon, do not fear them:
You will never find such as these on your path,
if your thoughts remain lofty, if a fine
emotion touches your spirit and your body.

(K. Kavafis, Itaca)